

Gonadotropin regulation of granulosa cells through follicular development and ovulation

Ejimedo Madogwe

Department of Animal Science, McGill University, Montreal

February 2020

A thesis submitted to McGill University in partial fulfillment of the requirements of the degree
of

DOCTOR OF PHILOSOPHY

© Ejimedo Madogwe, 2020

TABLE OF CONTENTS

ABSTRACT	vii
RESUME	ix
ACKNOWLEDGEMENTS	xi
CONTRIBUTION TO KNOWLEDGE	xiii
CONTRIBUTION OF AUTHORS	xv
LIST OF FIGURES	xvii
LIST OF TABLES	xviii
LIST OF ABBREVIATIONS	xix
CHAPTER 1 INTRODUCTION	1
1.1 Introduction	1
CHAPTER 2	
REVIEW OF LITERATURE	3
2.1 Regulation of follicular development by FSH	3
2.1.1 Follicular development	3
2.1.2 Granulosa cell proliferation and apoptosis	4
2.1.3 Estrogen production	5
2.1.4 Modulation of FSH regulation by growth factors	5
2.1.5 Signaling pathways induced by FSH	7
2.2 Regulation of ovulation by LH	7
2.2.1 Oocyte maturation and meiotic resumption	8
2.2.2 Cumulus expansion and ECM modification	9
2.2.3 Follicular rupture and ECM modification	10

2.2.4 Luteinization and ECM modification	10
2.2.5 ERK1/2 signaling and RSK3	11
2.3 Regulation of the granulosa cell transcriptome by FSH	13
2.4 Regulation of the granulosa cell transcriptome by LH	17
2.5 Summary of global analysis of gonadotropin regulated transcriptome in granulosa cells	23
2.6 Role of histone modifications in regulation of gene expression	24
2.6.1 Epigenetics	24
2.6.2 Histone modifications	25
2.6.3 Epigenetic modifications in differentiating cells	26
2.6.4 Signaling pathways regulating histone modifications.....	28
2.6.5 Epigenetic modifications in granulosa cells	28
2.7 Rationale, hypothesis and objectives	32
2.7.1 Rationale	32
2.7.2 Hypothesis	33
2.7.3 Specific objectives	34

CHAPTER 3

Global analysis of FSH-regulated gene expression and histone modification 35

3.1 Abstract	37
3.2 Introduction	38
3.3 Materials and methods	40
3.3.1 Granulosa cell collection	40
3.3.2 RNA Extraction/RNA Sequencing	40

3.3.3 Chromatin Immunoprecipitation and Sequencing	40
3.3.4 RNA-Seq data analysis	41
3.3.5 ChIP-Seq data analysis.....	42
3.3.6 Differential Transcript analysis	42
3.3.7 Pathway analysis	42
3.3.8 ChIP-qPCR	43
3.3.9 RT-qPCR	43
3.4 Results	44
3.4.1 FSH-regulated granulosa cell transcriptome	44
3.4.2 Functional analysis of differentially expressed genes	44
3.4.3 Pathway analysis of differentially expressed genes.....	45
3.4.4 Regulation of H3K4me3 in granulosa cells	45
3.4.5 Relationship between H3K4me3 enrichment and gene expression	46
3.4.6 Confirmation of sequencing data using qPCR and ChIP-qPCR	47
3.4.7 Expression of histone modifying enzymes and H3K4me3 at promoters	47
3.4.8 Differential transcript regulation by FSH	47
3.5 Discussion	49
3.6 Declaration of interest, funding, contributions and acknowledgements	54
3.7 Figures	55
3.8 Tables	62
3.9 Bibliography	65
CONNECTING STATEMENT 1.....	70

CHAPTER 4

LH surge-regulated trimethylation of lysine 4 of histone 3 drives gene expression in mouse granulosa cells via ERK1/2 71

4.1 Abstract	72
4.2 Introduction	73
4.3 Materials and Methods	75
4.3.1 Granulosa cell collection.....	75
4.3.2 RNA purification and sequencing.....	75
4.3.3 RNA-Seq data analysis.....	76
4.3.4 Chromatin Immunoprecipitation and Sequencing.....	76
4.3.5 ChIP-Seq data analysis.....	77
4.3.6 Pathway analysis.....	78
4.3.7 RT-PCR	78
4.3.8 ChIP-qPCR	78
4.4 Results	80
4.4.1 LH-regulated granulosa cell transcriptome	80
4.4.2 Regulation of H3K4me3 in granulosa cells	80
4.4.3 Relationship between LH-regulated H3K4me3 enrichment and transcriptome	81
4.4.4 Effect of ERK1/2 inhibition on LH-regulated transcriptome	82
4.4.5 Role of ERK1/2 signaling in LH-regulated cellular pathways	82
4.4.6 Relationship between LH-regulated ERK1/2-dependent genes and H3K4me3	83
4.4.7 Confirmation of sequencing data using qPCR and ChIP-qPCR	84

4.4.8 Expression of H3K4me3 methylation and demethylation enzymes	85
4.5 Discussion	86
4.6 Funding, Contributions and Acknowledgements	91
4.7 Figures	92
4.8 Tables	101
4.9 Bibliography	107
CONNECTING STATEMENT 2.....	111
CHAPTER 5	
Sustained ERK1/2 signaling is necessary for follicular rupture during ovulation in mice	112
5.1 Abstract	113
5.2 Introduction	114
5.3 Materials and Methods	115
5.3.1 Animal model	115
5.3.2 Superovulation and sample collection	115
5.3.3 Inhibition of ERK1/2 activity.....	116
5.3.4 Assessment of ovulation rate, oocyte maturation and ovarian histology in vehicle and PD0325901 treated mice	116
5.3.5 Reproductive phenotyping of <i>RSK3</i> ^{-/-} mice	117
5.3.6 RT PCR	117
5.3.7 PCR arrays	118
5.3.8 Protein extraction and immunoblotting	119
5.3.9 Statistical Analysis	120

5.4 Results	120
5.4.1 PD0325901 treatment at 4h post-hCG inhibits ERK1/2 activity in granulosa cells	120
5.4.2 PD0325901 treatment at 4h post-hCG inhibits follicular rupture without altering oocyte maturation and luteinization	120
5.4.3 Expression profile of RSK isoforms in granulosa cells	121
5.4.4 Ovulation rate and fertility of <i>RSK3</i> ^{-/-} mice	122
5.4.5 PD0325901 treatment at 4h post-hCG results in aberrant expression of genes involved in tissue remodeling and leukocyte infiltration in ovulating follicles	123
5.5 Discussion	124
5.6 Acknowledgements	129
5.7 Figures	130
5.8. Table	136
5.9 Bibliography	137
CHAPTER 6	
General discussion and conclusions	140
Bibliography	144

ABSTRACT

Infertility affects couples worldwide. Infertility also affects animal production systems resulting in reduced efficiency and profitability. Fertility is the successful reproduction of a species and it is 50% dependent on efficient ovarian follicular growth and successful ovulation in the female, which are regulated by the pituitary hormones follicle stimulating hormone (FSH) and luteinizing hormone (LH), respectively. Many genes and pathways are involved in these events, including ERK1/2 (MAPK3/1) that acts on several targets including the RSK3. Furthermore, histone modifications such as trimethylation of H3K4, a histone mark associated with active transcription, are involved in gene expression. We hypothesized that FSH and LH regulate follicular development and ovulation by instigating specific gene expression programs through H3K4me3 and ERK1/2 pathway. In the first study, we show that FSH regulates follicular development through mechanisms that include changes in gene expression and H3K4me3 enrichment. We also show that pathways associated with steroidogenesis and TGFB signaling are enriched by FSH. In the second study, we explored the role of ERK1/2 in LH-dependent H3K4me3 regulation in genes involved in the ovulatory process. Pharmacological inhibition of ERK1/2 perturbs the LH-regulated events associated with ovulation; cumulus expansion, meiotic resumption and luteinization. By comparing the LH-regulated genes with the genes with significant H3K4me3 enrichment, we were able to find a subset of 1198 genes with changes in mRNA abundance as well as H3K4me3 enrichment. Further comparison of this subset with the ERK1/2 dependent genes revealed 609 ERK1/2 dependent genes that also showed changes in mRNA abundance and H3K4me3 enrichment demonstrating that ERK1/2 plays a significant role in histone methylation thereby regulating gene expression in granulosa cells. In the third study, we describe the unique effect of sustained ERK1/2 signaling on ovulation. Using pharmacological inhibition of ERK1/2

and mice null for RSK3, the main ERK1/2 signal mediator, we showed that sustained ERK1/2 production disrupts follicular rupture but does not appear to affect luteinization, cumulus expansion and meiotic maturation. We also provide molecular evidence of imbalance in the expression of genes involved in extracellular matrix degradation and leukocyte infiltration necessary for follicular rupture. Overall, these studies provide molecular evidence for the mechanisms by which FSH and LH regulate ovarian follicular development and ovulation.

Key words: Follicular development, Ovulation, H3K4me3, ERK1/2, granulosa cells

RÉSUMÉ

Les problèmes d'infertilité affectent les couples du monde entier. L'infertilité affecte également les systèmes de production animale, ce qui réduit l'efficacité et le profit final. La fertilité est le résultat d'une croissance folliculaire ovarienne efficace et d'une ovulation réussie, qui sont respectivement sous le contrôle de l'hormone folliculo-stimulante (FSH) et l'hormone lutéinisante (LH). De nombreux gènes et voies moléculaires sont impliqués dans ces événements, dont ERK1/2 qui agit sur plusieurs cibles, incluant RSK3. De plus, des modifications d'histones telles que la triméthylation de H3K4, une marque d'histone associée à une transcription active, sont impliquées dans l'expression des gènes. Notre hypothèse est que la FSH et la LH contrôlent le développement folliculaire et l'ovulation en provoquant des programmes d'expression génique spécifiques via H3K4me3 et la voie ERK1/2. Dans la première étude, nous avons montré que la FSH contrôle le développement folliculaire grâce aux mécanismes qui incluent des changements dans l'expression des gènes et l'enrichissement de H3K4me3. Nous montrons également que les voies associées à la stéroïdogenèse et à la signalisation TGF β sont enrichies par la FSH. Dans la deuxième étude, nous avons exploré le rôle de ERK1/2 dans la régulation de H3K4me3 dépendante de la LH dans les gènes impliqués dans le processus ovulatoire. L'inhibition pharmacologique de ERK1/2 perturbe les événements régulés par la LH associés à l'ovulation, L'expansion des COC, la reprise méiotique et la lutéinisation. En comparant les gènes régulés par la LH avec les gènes avec un enrichissement significatif H3K4me3, nous avons pu décrire un sous-ensemble de 1198 gènes avec des changements dans l'abondance d'ARNm ainsi que l'enrichissement de H3K4me3. Une comparaison supplémentaire de ce sous-ensemble avec les gènes dépendants de ERK1/2 a révélé 609 gènes dépendants de ERK1/2 qui ont également montré des changements dans l'abondance d'ARNm et l'enrichissement de H3K4me3 démontrant que ERK1/2 joue un rôle important dans la

méthylation des histones, régulant ainsi l'expression des gènes dans les cellules de la granulosa. Dans la troisième étude, nous avons décrit l'effet unique d'une signalisation ERK1/2 soutenue sur l'ovulation. En utilisant l'inhibition pharmacologique de ERK1/2 et des souris nulles pour RSK3, le principal médiateur du signal ERK1/2, nous avons montré qu'une production soutenue d'ERK1/2 perturbe la rupture folliculaire mais ne semble pas affecter la lutéinisation, l'expansion des cellules de cumulus et la maturation méiotique. Nous fournissons également des preuves moléculaires d'un déséquilibre dans l'expression des gènes impliqués dans la dégradation de la matrice extracellulaire et l'infiltration des leucocytes nécessaires à la rupture folliculaire. L'ensemble de nos études fournissent des preuves moléculaires des mécanismes par lesquels la FSH et la LH contrôlent le développement folliculaire ovarien et l'ovulation.

ACKNOWLEDGEMENTS

I would like to thank my supervisor, Dr. Raj Duggavathi, for his guidance over the years, and the many debates that helped shape my thinking and allowed me to grow into myself. I would also like to thank my advisory committee members, Dr. Vilceu Bordignon, Dr. Sergio Burgos and Dr. Jean-Benoit Charron for their invaluable suggestions that resulted in vast improvements in my research and for the thoughtful questions that enabled me to dig deeper and broaden my scope. Special thanks to Dr. Roger Cue for being an amazing coordinator through the years.

My lab mates Dayananda Siddappa, Ricardo Sanchez, Terry Sczerbaniuk, Yasmin Schuermann, Milena Taibi, Audrey St-Yves, Teshome Alemu and Jasmine Randhawa for all the assistance, lively discussions and for becoming the friends I so desperately needed to survive! Special thanks to Milena for keeping me sane. The friends who made it all worth it; Mariana, Luke, Karina, Werner, Naomi, Laura, Juliana Ferst, Paula, Vitor, Simone, Deepak, Aditya, Cynthia Kaneza, Afitafo Akande (much love!), Francisca Oburo, Abel, Ailen, Tony Osagie, Precious Ijirigho, Iesha (Yuan), Yiyi Zhang, Adiba Sherhaj and Cj. And Eweme, king among men.

I wish to express my thanks to Susan Gregus, Cinthya Horvath, Abida Subhan and Ann Gossage for all the times they assisted me with administrative matters and answered my numerous questions. And Diane Langan for all her help at SARU. I am also grateful to Dr. Nicholas Gevry and Dr. Stephanie Bianco who answered my follow up questions with infinite patience. Thanks also to Boris Mayer for walking me through the ChIP process and making it so much easier to understand, and to Dr J.B. Charron for the use of lab equipment. Gabriel, Jordan and Hardev who stayed behind when my experiments ran late.

I would like to express my gratitude to the department of Animal Science for the Graduate

Excellence Awards (GEF and GREAT) and to NSERC for the NSERC CREATE award. Many thanks to Professor Kimmins, Burgos and Bordignon labs for use of lab equipment and assistance from lab members. Thank you so much!

And to the ladies who have made this journey easier Gerry Chevalier, Nathalie Beaudry, Danielle Hodgson, Lindsay O'Connell, Tatiana Smetkina and Meghan Sweet. Thank you! Also, to the professors who have guided me over the years especially Professors Omoyakhi, Bamikole, Njoku, Ikhatua and Nwokoro.

I am most grateful to my family members; my siblings and their spouses Onajite (and Uncle Odems), Odafe (and Peace), Oresiri (and Irene), Omogho (and Ayo), Emojefe (and Yemi), and Akporode for their unconditional love and support over the years. I am thankful for my dad who worked so hard all his life to ensure that we all get a good education because that foundation enabled me to get to where I am today. And to my Mum, for all she has sacrificed over the years to keep us standing and for all she still does.

Finally, a big thank you to all my friends (in Nigeria, Canada and around the world) who have made this journey sweeter.

CONTRIBUTION TO KNOWLEDGE

Chapter 3

In the first study, we tested the role of follicle stimulating hormone, FSH, in follicular development. Using next generation sequencing (ChIP- and RNA- Seq), we showed the downstream targets of FSH action. We also showed how H3K4me3 interacts with FSH to induce follicular development in granulosa cells. Furthermore, we examined specific transcript isoforms that are regulated. Altogether, we present a veritable database of information that can be used as a basis for further analysis which could translate into clinical trials/research.

Chapter 4

In the second study, we examined the role of luteinizing hormone, LH, and ERK1/2 in ovulation. LH induces oocyte maturation and ovulation via regulation of numerous genes and pathways including the ERK1/2 pathway. Using next generation sequencing (ChIP- and RNA- Seq), we examined the interaction of LH and H3K4me3 in granulosa cells. Then we looked at the transcriptome profile of LH and ERK1/2 using a MEK inhibitor. These enabled us to identify LH regulated genes, as well as ERK1/2 regulated genes. Furthermore, we were able to extract ERK1/2 regulated genes that are also regulated by H3K4me3.

Chapter 5

In the third study, we investigated the role of sustained ERK1/2 in follicular rupture and luteinization. We also investigated RSK3, a mediator of the ERK1/2 signal. The previous study showed a role for ERK1/2 when inhibited prior to LH. We sought to examine the role of ERK1/2 when inhibited at 4h after LH. Furthermore, among the family of RSKs, RSK3 was observed to be

regulated by LH. Using pharmacological inhibition of ERK1/2, we found that follicular rupture, but not luteinization or meiotic maturation are affected. Moreover, mice null for RSK3 showed defects in genes involved in extracellular modeling.

Overall, these studies provide a database of valuable information regarding follicular development and ovulation. These results will serve as a basis to further explore specific genes and pathways involved in the events that lead up to ovulation and investigate the mechanisms of action of histones such as H3K4me3.

CONTRIBUTION OF AUTHORS

This thesis was prepared according to McGill University thesis preparation guidelines in a manuscript format. Three manuscripts are presented.

Authors of manuscript 1 (Chapter 3)

Ejimedo Madogwe, Deepak Tanwar, Milena Taibi, Yasmin Schuermann, Audrey St-Yves and Raj Duggavathi.

Ejimedo Madogwe designed and conducted experiments, analyzed data and wrote the manuscript. Milena Taibi and Audrey St-Yves assisted with granulosa cell collection and optimization of the ChIP protocol. Yasmin Schuermann assisted with Bioinformatics analyses. Conceptualization of experimental ideas and critical reviewing of the manuscript was done by Raj Duggavathi.

Authors of manuscript 2 (Chapter 4)

Ejimedo Madogwe, and Raj Duggavathi.

Ejimedo Madogwe designed and conducted all the experiments, analyzed the data and wrote the manuscript. Conceptualization of experimental ideas and critical reviewing of the manuscript was done by Raj Duggavathi.

Authors of manuscript 3 (Chapter 5)

Ejimedo Madogwe, Yasmin Schuermann, Dayananda Siddappa, Vilceu Bordignon, Philippe P. Roux and Raj Duggavathi.

Ejimedo Madogwe designed experiments, collected and processed samples, analyzed and interpreted data, prepared figures and wrote manuscript; Dayananda Siddappa and Yasmin Schuermann contributed to ideas, designed experiments, collected and processed samples, interpreted data and reviewed the manuscript; Philippe P. Roux performed reproductive phenotyping of RSK3 mice and reviewed the manuscript and Vilceu Bordignon performed

analyses of oocyte maturation, contributed to experimental design and reviewed the manuscript;
Raj Duggavathi conceived the study, designed experiments, analyzed and interpreted data, and
edited the manuscript.

LIST OF FIGURES

Chapter 1

Figure 1.1 Ovarian follicles at different stages of development 1

Chapter 3

Figure 3.7.1 Classification of genes 55

Figure 3.7.2 Peak features and heatmap 56

Figure 3.7.3 Interaction between ChIP-Seq and RNA-Seq data 57

Figure 3.7.4 H3K4me3 enrichment and mRNA abundance 58

Figure 3.7.5 RT-PCR and ChIP-qPCR graphs 59

Figure 3.7.6 mRNA abundance of H3K4me3 methylases and demethylases 60

Figure 3.7.7 Interaction between DEGs and DETs 61

Chapter 4

Figure 4.7.1 Functional categorization of 4873 LH DEGs using IPA 92

Figure 4.7.2 Genomic features and functional categorization 93

Figure 4.7.3 Interaction of ChIP- and RNA-Seq regulated genes 94

Figure 4.7.4 Representative IGV images 95

Figure 4.7.5 Functional categorization of 2504 ERK1/2 regulated genes using IPA 96

Figure 4.7.6 Interaction of ChIP- and RNA-Seq regulated genes with ERK1/2 regulated genes 97

Figure 4.7.7 RT-PCR and ChIP-qPCR graphs 98

Figure 4.7.8 Expression of H3K4me3 methylases and demethylases 100

Chapter 5

Figure 5.7.1 Inhibition of ERK1/2 at 4h post-hCG results in reduced ovulation rate 130

Figure 5.7.2 Inhibition of ERK1/2 at 4h post-hCG disrupts follicular rupture without affecting cumulus expansion, oocyte maturation and luteinization 131

Figure 5.7.3 RSK3 is dramatically induced by hCG treatment 132

Figure 5.7.4 Reproductive phenotype of *RSK3*^{-/-} mice 133

Figure 5.7.5 Inhibition of ERK1/2 at 4h post-hCG results in abnormal expression of genes associated with extracellular matrix degradation and leukocyte infiltration 134

Figure 5.7.6 Proposed mechanism for ERK1/2 regulation of follicular rupture 135

LIST OF TABLES

Chapter 3

Table 3.8.1 Primer Sequences used in ChIP-qPCR and RT-qPCR	62
Supplementary Table 3.8.1 Quality Control metrics for sequencing data	63
Supplementary Table 3.8.2 FSH-regulated transcripts	64

Chapter 4

Table 4.8.1 List of primer sequences	101
Table 4.8.2 KEGG pathways	102
Table 4.8.3 Pathways and Protein classes	103
Supplementary Table 4.8.1 Quality control metrics	104
Supplementary Table 4.8.2 Top functions	105
Supplementary Table 4.8.3 Top Upstream regulators	106

Chapter 5

Table 5.8.1 List of primer sequences used in RT-PCR	136
---	-----

LIST OF ABBREVIATIONS

Ac: Acetylation

Adams1: A disintegrin and metalloproteinase with thrombospondin like motifs

Ahr: Aryl hydrocarbon receptor

ANOVA: Analysis of Variance

Areg: Amphiregulin

CEBPB: CCAAT Enhancer binding protein B

cDNA: Complementary DNA

ChIP: Chromatin Immunoprecipitation

COC: Cumulus oocyte complex

Cox2: Cyclooxygenase-2

CREB: cAMP response element binding protein

DNA: Deoxyribonucleic acid

DNase: Deoxyribonuclease

eCG: equine chorionic gonadotropin

EGF: Epidermal growth factor

Egr1: Early growth regulatory factor 1

EGSEA: Ensemble of gene set enrichment analyses

Ereg: Epiregulin

ERK1/2: Extracellular signal-regulated kinases 1 and 2

FDR: False discovery rate

FSH: Follicle Stimulating hormone

Gapdh: Glyceraldehyde 3-Phosphate dehydrogenase

GnRH: Gonadotropin releasing hormone

HAT: Histone acetyl transferase

hCG: human chorionic gonadotropin

HDAC: Histone deacetylase complex

HSD3B: 3 β -hydroxysteroid dehydrogenase

IgG: Immunoglobulin G

IU: International Units

KEGG: Kyoto encyclopedia of genes and genomes

LH: Luteinizing hormone

Lhb: Luteinizing hormone beta

Mapk: Mitogen activated kinases

Me: Methylation

mRNA: Messenger RNA

Pgr: Progesterone receptor

PKA: Protein Kinase A

PKC: Protein Kinase C

PMSG: Pregnant mare serum gonadotropin

PRKO: Pgr Knockout

Ptgs2: Prostaglandin endoperoxide synthase 2

qPCR: Quantitative Polymerase Chain Reaction

RNA: Ribonucleic acid

RSK: p90 Ribosomal S6 Kinase

Star: Steroidogenic acute regulatory protein

VEGF: Vascular endothelial growth factor

CHAPTER 1

INTRODUCTION

1.1 Introduction

The primary functions of the ovary are to produce the female gametes (oocyte) and the steroid hormones, estrogen and progesterone. Each oocyte is harbored in a specialized structure called a follicle, which contains two types of somatic cells, granulosa and theca cells. These two somatic cells collaborate to produce the steroid hormone estrogen. Follicles and the contained oocytes develop so that a species-specific number of follicles ovulate once every reproductive cycle to release the fertilizable oocytes into the uterus. The remnant of the ovulated follicle transforms into a transient gland called the corpus luteum (plural: corpora lutea), which produces another steroid, progesterone that is necessary for maintenance of pregnancy (Murphy, 2000, Robker et al., 2000b, Skinner et al., 2008).

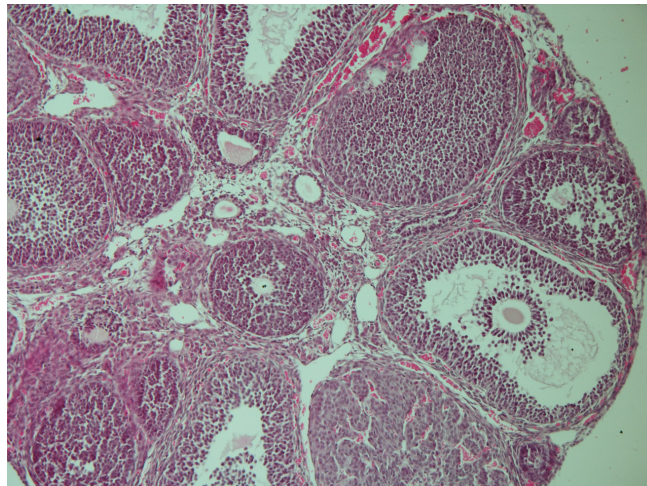


Figure 1.1 Ovarian follicles at different stages of development

At any given time, the ovary contains follicles at different stages of development (Figure 1.1). Primordial follicles are the smallest and most immature, with the oocyte surrounded by a single layer of flattened squamous cells. By yet to be deciphered mechanisms, a cohort of

primordial follicles are stimulated to begin growth. Follicles begin growth as the primary follicles, wherein the oocyte is surrounded by a single layer of cuboidal epithelium. The secondary follicle has two or more layers of cells surrounding the oocyte. An antral (or tertiary) follicle contains multiple layers of granulosa cells and is characterized by a fluid filled cavity called the antrum. When the antral follicle becomes the dominant preovulatory follicle, it ovulates in response to the preovulatory LH surge (Duggavathi and Murphy, 2009, Gilbert et al., 2011, Ginther et al., 1996). However, the processes of follicular development and ovulation involves an intricate system of signaling pathways and mechanisms that are not fully understood.

Epigenetics refers to the study of changes in gene expression that occur without alterations in the DNA sequence. These changes include chromatin remodeling, DNA methylation and post-translational modifications of histones. Epigenetic modifications are involved in mediating the interaction between an organism's genetics and its environment.

CHAPTER 2

REVIEW OF THE LITERATURE

2.1 Regulation of follicular development by FSH

Follicular development is regulated by two pituitary gonadotropic hormones, follicle stimulating hormone (FSH) and luteinizing hormone (LH) (Robker et al., 2000b, Bao and Garverick, 1998). FSH initiates three key events: proliferation of granulosa cells, estrogen synthesis and expression of LH receptor (*Lhcgr*) in granulosa cells. These events are critical for the development of the follicle to the preovulatory stage.

2.1.1 Follicular development

Follicular development begins when a cohort of follicles is recruited to grow and is characterized by an increase in the number of granulosa cells, increase in follicular diameter along with oocyte development. The initial recruitment of primordial follicles is gonadotropin independent as evidenced by the fact that follicular growth to secondary or early antral stages occurs unhindered in mice models lacking *Fshb*, *Fshr*, *Lhb* or *Lhcgr* (Zhang et al., 2001, Lei et al., 2001, Draincourt et al., 1987, Ma et al., 2004, Kumar et al., 1997). Follicular development beyond formation of the fluid-filled antrum depends on pituitary gonadotropins. A small but significant increase in FSH concentrations recruits a cohort of early antral follicles (about twenty-four follicles of 3 mm in diameter in cows) to grow further (Mihm and Austin, 2002, Ginther et al., 1996). It is well characterized in multiple species, including humans, that such FSH-induced follicular development occurs in waves, characterized by periodic recruitment of cohorts of small antral follicles. In mono-ovulatory species such as cows and humans, one follicle of such wave is selected as the dominant follicle and continues to grow whereas the rest of the follicles (subordinate

follicles) cease to grow and undergo atresia. Follicular atresia is characterized by a decrease in diameter and cellular apoptosis. The difference in follicular diameter between the dominant and subordinate follicles increases as the dominant follicle grows to reach a species-specific ovulatory diameter (Fortune et al., 2001).

Several studies during the last part of the 20th century have defined the hormonal milieu that favors the growth of the dominant follicle while suppressing the growth of the subordinate follicles (Xu et al., 2011, Yuan et al., 1998, Zielak-Steciwko and Evans, 2016). The FSH peak that initiated the follicular growth into a wave begins to decrease as the follicles grow. This is because of the inhibitory actions of the ovarian hormones namely estradiol and inhibins. Estradiol is mainly produced by the dominant follicle of the wave, whereas most secondary and early antral follicles secrete inhibins. While subordinate follicles fail, the dominant follicle survives the decreasing concentrations of FSH. This ability of the dominant follicle to thrive in the low FSH conditions has been attributed to its ability to utilize the available LH, as granulosa cells of the dominant follicle express LHCGR under the influence of FSH and estradiol (Xu et al., 1995, Fortune et al., 2001, Ginther et al., 1996, Bao et al., 1997). A study by the Youngquist group reported an increase in the expression of LHCGR between day 2 and 4 after the follicular wave emergence, when the dominant follicle begins to deviate from subordinate follicles in growth rate (Xu et al., 1995). Therefore, deciphering the mechanisms of FSH signaling is important to understand the molecular basis of follicular development to preovulatory stage.

2.1.2 Granulosa cell proliferation and apoptosis

As the follicle grows, several morphological and physiological changes occur in the follicular cells. Comparison of the dominant follicle to subordinate follicles have shown increases in the diameter, quantity of follicular fluid, granulosa cell numbers and higher concentrations of

estradiol in the follicular fluid (Ireland and Roche, 1983). Granulosa cells increase in number as the follicle grows and the formation of gap junctions between the granulosa cells and the oocyte provides essential nutritional and regulatory molecules to the oocyte that favor the acquisition of meiotic competence (Eppig et al., 1996). Moreover, granulosa cells also act through paracrine signaling to secrete factors that appear to be essential to the regulation of the development of the oocyte. This is evidenced by the lack of acquisition of meiotic competence when denuded oocytes are cultured in the absence of these cells, and the resumption of meiosis when granulosa cells are cultured with the denuded oocyte (Eppig et al., 1996, Herlands and Schultz, 1984). Notch signaling and Wnt/B-Catenin signaling (via *Foxo3a*) have been shown to regulate proliferation and apoptosis in developing follicles (Liu et al., 2019).

2.1.3 Estrogen production

FSH induces the production of estrogen by granulosa cells. One of the major features of the dominant follicle, apart from its bigger follicle diameter, is that it has a significantly higher concentration of estradiol than subordinate follicles. The acquisition of LHCGR by granulosa cells enables the dominant follicle to secrete an increasing quantity of estradiol in conjunction with the FSH induced production. In one study, it was proposed that the increase in estrogen levels in the dominant follicle favors the expression of genes associated with cell survival whereas the decrease in estrogen concentration in the subordinate follicle could be associated with a decrease in these genes and an increase in genes associated with apoptosis (Evans et al., 2004).

2.1.4 Modulation of FSH regulation by growth factors

Growth factors play a major role in follicular development as regulators of cell survival, proliferation and differentiation. They are peptide factors that function in an autocrine/paracrine/endocrine manner and include the epidermal growth factor (EGF), the insulin-

like growth factor (IGF), the fibroblast growth factor (FGF) and the transforming growth factor-beta (TGF- β) families. Each family is composed of a system of factors, receptors, binding proteins and binding-protein proteases (Monniaux et al., 1997).

As the dominant follicle develops, it acquires LHCGR on the granulosa cells (Xu et al., 1995, Fortune et al., 2001, Bao et al., 1997). FSH along with growth factors including the IGFs, EGFs and FGFs stimulate granulosa cell proliferation. IGF-I modulates FSH-regulated granulosa cell proliferation or differentiation depending on the stage of follicular development. IGFs stimulate granulosa cell proliferation in small but not large follicles and stimulate steroid production in granulosa cells of large but not small follicles in sheep (Monniaux et al., 1997).

Bone morphogenetic proteins (BMPs) along with growth differentiation factors (GDFs) are members of the TGF- β superfamily and have been reported to be essential for follicular development. The BMP family comprises twenty ligands and seven type I and II receptors (Gasperin et al., 2014). Transcripts of *BMPR1B* are upregulated in granulosa cells of subordinate follicles compared to dominant follicles and this upregulation in *BMPR1B* signaling supposedly leads to follicle regression and atresia (suppression of *BMPR1B* is important for dominant follicle development) (Gasperin et al., 2014).

The IGF system plays a major role in the selection of the dominant follicle. In the IGF system, there are two IGF ligands, IGF-I and IGF-II, two receptors, type I and II, six IGF binding proteins (IGFBP 1, 2, 3, 4, 5 and 6) and multiple proteases of IGFBPs. IGFBPs have an inhibitory effect, regulating the bioavailability of IGFs (Fortune et al., 2001). The effect of IGFs binding to their type I receptors has an inverse relationship to the concentration of IGFBPs. IGF-I mRNA abundance in granulosa cells and IGF-II mRNA abundance in theca cells, was found to be greater in the dominant follicle as compared to the subordinate follicle; whereas the concentration of

IGFBPs was lower in the follicular fluid of the dominant follicle (Yuan et al., 1998). It has been suggested that the decrease in mRNA abundance of IGF I and II in subordinate follicles and the increase in the gene expression of IGFBPs such as IGFBP-2 may lead to atresia in these follicles (Yuan et al., 1998, Monniaux et al., 1997). In line with this, IgfI knockout mice were found to be infertile, they failed to show behavioral signs of estrus and failed to ovulate even with administration of exogenous gonadotropins (Baker et al., 1996).

It has also been shown that IGF availability is increased due to the higher expression of IGF-binding protein proteases as the dominant follicle reaches preovulatory diameter (Rivera et al., 2001, Mihm et al., 2000). At about 1.5 days after the wave emergence, IGFBP-4 was significantly lower (15-fold) in the future dominant follicle when compared to the future largest subordinate follicle. The Ireland group suggest the use of IGFBP-4 levels as a reliable biochemical marker that can be used to identify the future dominant follicle; in fact, the follicle with lowest IGFBP-4 (and highest estradiol) concentrations always became the dominant follicle, and this was a more predictive feature of the dominant follicle than follicular diameter (Mihm et al., 2000).

2.1.6 Signaling pathways induced by FSH

There are several pathways involved in the regulation of cell death or survival including the PKA, PI3K-Akt, MAPK, mTOR, Wnt, TGF- β , and apoptosis pathways (Salilew-Wondim et al., 2014, Zielak-Steciwko et al., 2014, Evans et al., 2004, Hunzicker-Dunn and Maizels, 2006). The data on the roles of signaling pathways involved in FSH regulation of granulosa cells have mainly come from in vitro studies.

2.2 Regulation of ovulation by LH

The preovulatory LH surge terminates the FSH program and drives ovulation. The process of ovulation involves multiple processes including luteinization through terminal differentiation of

granulosa cells to luteal cells, cumulus cell expansion, oocyte meiotic resumption and follicle rupture (Duggavathi and Murphy, 2009, Richards et al., 2002b, Xu et al., 2011). Thus, the follicle's transition from estradiol production to progesterone production is accompanied by profound changes in follicular function (Shimada and Yamashita, 2011). Vascular permeability is increased through vasodilation, which favors downstream inflammatory responses (Liu et al., 2017). The follicle ruptures to release the oocyte and the follicular remnants are transformed into the corpus luteum (Conneely, 2010). Any dysregulation in these processes could result in abnormal outcomes including ovulation failure as evidenced by a corpus luteum still containing the trapped oocyte (Robker et al., 2000b).

2.2.1 Oocyte maturation and meiotic resumption

As the follicle grows to the preovulatory diameter, the oocyte increases in diameter (in mice, from ~20um to ~80um) and also goes through physiological changes to acquire meiotic and embryo developmental competence (Eppig et al., 1996, Herlands and Schultz, 1984). Gap junctions that connect the oocyte to the cumulus cells provide a means for small molecules with nutritional and regulatory functions, that are important for growth and development, to gain access to the oocyte (Eppig et al., 1996, Herlands and Schultz, 1984). Connexin 37 (a gap junction protein; GJA4) is the major connexin in oocyte-granulosa cell junctions and mice null for *Gja4* gene were shown to be infertile and lacked recognizable gap junctions in addition to abnormal follicular development (Simon et al., 1997). Furthermore, cAMP of cumulus cell origin was identified as the regulatory signal that maintains oocytes in meiotic arrest as evidenced by the resumption of meiosis that occurs when cAMP levels drop in the oocyte (Granot and Dekel, 1998). On the other hand, in the atretic subordinate follicles, oocytes undergo degeneration accompanied by loss of junctional contact between the cumulus cells and the oocyte (Assey et al., 1994).

In the dominant follicle, the oocyte undergoes changes that enable it to achieve competence to undergo final maturation, fertilization and early embryonic development. Two processes, nuclear and cytoplasmic maturation, have to occur for successful fertilization and development. Whereas nuclear maturation prepares the oocyte for progression of meiosis, cytoplasmic maturation prepares the oocyte for fertilization, activation and pre-implantation development (Eppig et al., 1996).

Prior to ovulation, the oocyte in the dominant follicle resumes meiosis and proceeds to metaphase II (Eppig et al., 1996). The release of the oocyte is perpetuated by the LH surge and it has been shown that the surge also disrupts the gap junctions (Gja4) between the cumulus cells and oocytes. This closure of passage of nutrients and small molecules from cumulus cells results in decreased cAMP concentration in the oocyte (Norris et al., 2008, Schultz et al., 1983). The drop in cAMP occurs around the time when the oocyte resumes meiosis (Schultz et al., 1983, Granot and Dekel, 1998). LH induces multiple signaling pathways including the ERK1/2 pathway, which is important for regulation of oocyte maturation and ovulation. In fact, mice null for *Erk1/2* in granulosa cells were infertile with no mature oocytes as evidenced by lack of germinal vesicle breakdown (Fan et al., 2009b).

2.2.2 Cumulus expansion and ECM modification

The LH surge also induces cumulus expansion and the associated extracellular modifications, wherein the secretion of hyaluronic acid by the cumulus cells of the ovulating follicle results in an increase in the space between the cells, a process known as cumulus expansion (Eppig et al., 1996). An extracellular matrix surrounds the mature oocyte and the surrounding cumulus cells, a process that is vital for ovulation and fertilization (Zhang et al., 2014, Brown et al., 2010, Duffy et al., 2019). LH induces the expression of genes that are involved in cumulus

expansion such as *Ptgs2*, *Tnfaip6*, *Has2*, *Ptx3* and *Pgr*. *Adamts1* knockout mice exhibited abnormal cumulus oocyte complex (COC) morphology as characterized by disorganized cumulus cell structures within the matrix (Brown et al., 2010). Also, ERK1/2 signal is important for cumulus expansion as the COC failed to expand in ERK1/2 granulosa cell KO mice (Fan et al., 2009b).

2.2.3 Follicular rupture and ECM modification

The extracellular matrix is uniquely remodeled in preparation for follicular rupture such that remodeling to degrade ECM, remove vascular supply and apoptotic removal of ovarian surface epithelium occurs at a specific region of the follicular wall. Proteases such as the families of matrix metalloproteinase (MMP) and ADAMTS (a disintegrin and metalloproteinase with thrombospondin-like motifs) are required for ECM modification and hence follicular rupture (Liu et al., 2017, Robker et al., 2000a, Brown et al., 2010, Lussier et al., 2017, Duffy et al., 2019). *ADAMTS1* and *Ctsl* have been reported to be downstream effectors of progesterone receptor action and have been proposed to be essential for follicular rupture (Robker et al., 2000a). *ADAMTS1* knockout mice had a decrease in ovulation rate (77%), decreased fertility (63%), lower cleavage of versican in the COC (75%) and abnormal follicle morphology, including a lack of invaginating regions (Brown et al., 2010). Follicular rupture failed to occur in the ERK1/2 granulosa-specific KO mice implicating ERK1/2 signaling in events leading up to follicular rupture (Fan et al., 2009b).

2.2.4 Luteinization and ECM modification (angiogenesis)

Following the rupture of the follicle to release the oocyte, granulosa cells terminally differentiate into luteal cells (Nimz et al., 2010, Richards, 1994). This process, which results in the formation of the corpus luteum is known as luteinization. It is an irreversible change and results in

increased progesterone production in preparation for and maintenance of pregnancy. At this point, most of the genes that were induced by LH (and FSH) show a decrease in expression (Richards, 1994).

Once again, the process of luteal formation requires ECM remodeling in such a way that the breakdown of the basement membrane, mesenchymal transition of granulosa cells, mobilization of theca cells and leukocytes among granulosa cells, and vascular invasion occur throughout the follicular wall except for the region involving follicular rupture. The LH surge also triggers the invasion of blood vessels, with the avascular granulosa cell compartment becoming highly vascularized in the ovulatory follicle with the development of a network of capillaries in the theca cells (Simon et al., 1997, Brown et al., 2010, Fraser and Duncan, 2005, Duffy et al., 2019). The vascular endothelial growth factor (VEGF) family has been reported to be essential for angiogenesis in the ovary, with inhibition of VEGF-A resulting in the suppression of angiogenesis (Fraser and Duncan, 2005). The basal wall of the thecal/vascular regions become invaginated due to rapid angiogenesis and versican is cleaved at the boundary between the granulosa and theca cells (Brown et al., 2010). Angiogenesis is greater in the corpus luteum with one study reporting more than 85% increase in circulation to the corpus luteum in human ovaries (Fraser and Duncan, 2005).

2.2.5 ERK1/2 signaling and RSK3

ERK1/2 has been shown to be necessary for ovulation (Fan et al., 2009b, Schuermann et al., 2018, Siddappa et al., 2015). It has been reported that ERK1/2 has over 160 known substrates in the cytoplasm and nucleus (Yoon and Seger, 2006), including p90 ribosomal S6 kinases (RSKs). RSKs belongs to the family of serine/threonine kinases and has several phosphorylation sites (Anjum and Blenis, 2008b). Four isoforms of the RSK family are encoded by the genes

Rps6ka1 (RSK1), *Rps6ka3* (RSK2), *Rps6ka2* (RSK3) and *Rps6ka6* (RSK4) and these genes have been implicated in several processes including transcription regulation and cell growth and survival (Anjum and Blenis, 2008b, Dumont et al., 2005). Expression of *RSK1-3* has been shown in the lung, heart, kidney, placenta, oocyte, cumulus and granulosa cells and RSK4 is expressed at a much lower level than all other RSKs in most cell types (Zhao et al., 1995, Zeniou et al., 2002, Dalbiès-Tran and Mermillod, 2003, Roux and Blenis, 2004, Adriaenssens et al., 2010, Anjum and Blenis, 2008a, Dümmler et al., 2005). The importance of the RSK proteins in the ovary is evidenced by the fact that *RPS6KA2* expression in human cumulus cells was shown to be associated with higher quality of embryos (Adriaenssens et al., 2010).

Overall, the gonadotropins FSH and LH regulate a myriad of biochemical, functional and morphological changes in granulosa cells. Gonadotropins bring about these stages of differentiation in granulosa cells through stage specific gene expression program. There have been numerous studies since the turn of the 21st century that have used real-time PCR to identify a small set of genes that are induced by FSH or LH in granulosa cells. While they have been successful in demonstrating the regulation of individual genes, they do not reveal the transcriptome level regulation by gonadotropins. Global level transcriptional mechanisms may be missed when focusing only on evidence from individual genes. Transcriptomics approaches such as microarrays and RNA-seq analyses are needed to view gonadotropin effects on the transcriptome of granulosa cells during follicular development, ovulation and corpus luteum development. Unlike a targeted gene approach, macro-analysis at omics scale enables discovery of gene groups that are expressed together potentially due to common underlying mechanisms. It will also enable bioinformatics analysis to generate novel hypotheses testing as a means to uncover novel regulatory mechanisms

of the biological processes. There have been a few studies in the recent past that have employed such a global approach, and these are summarized below.

2.3 Regulation of the granulosa cell transcriptome by FSH

As FSH activates multiple signaling pathways, it is expected to regulate several genes in granulosa cells. Though mice have been used as a model for transcriptomic studies due to the availability of an annotated genome, there are no known studies in this species, to the best of our knowledge, evaluating regulation of the granulosa cell transcriptome by FSH. However, there are multiple studies using bovine ovarian dynamics that have profiled the granulosa cell transcriptome during FSH regulated follicular growth (Evans et al., 2004, Fortune et al., 2001, Salilew-Wondim et al., 2014, Skinner et al., 2008, Zielak-Steciwko et al., 2014, Lussier et al., 2017).

The estrous cycle in cattle has two or three follicular waves. In each wave, FSH induces the growth of a cohort of follicles. One of these is selected as the dominant follicle and the other subordinate follicles undergo atresia. The granulosa cells of the dominant follicle acquire LH receptors so that they are responsive to the eventual LH surge (Gilbert et al., 2011, Bao and Garverick, 1998, Ginther, 2000). The dominant follicle regresses if the animal is in the luteal phase of the estrous cycle but ovulation occurs if luteolysis is induced during the growth phase of the dominant follicle (Fortune et al., 2001).

The earliest study (Evans et al., 2004) sought to identify the genes involved in apoptosis during follicular development in the bovine by comparing the dominant versus the subordinate follicles collected on days 2.5-3.5 of the synchronized estrous cycle. They used a labeled cDNA microarray containing 1,400 genes including a subset of 53 genes known to be involved in apoptosis pathways. The granulosa cells from subordinate follicles were found to be positively associated with genes involved in cell death and apoptosis. They reported increased mRNA abundance of β -glycan,

TNF α , *DRAK2*, *CAD* and *COX1* in granulosa cells of subordinate follicles. The authors concluded that inhibin binds to β -glycan and suppresses estradiol production which in turn results in lower intrafollicular estradiol concentrations and hence, a decrease in the expression of survival genes. Consequently, there is increased expression of genes involved in apoptosis and cell death.

A study by the Nilsson group (Skinner et al., 2008) compared the transcriptomes of granulosa cells of small (<5mm), medium (5-10mm) and large (>10mm) follicles collected from heifer ovaries at a slaughterhouse. The size categories of small, medium and large follicles represent follicles at the beginning, midpoint and end of FSH regulated follicular development. Microarray analysis detected 13,835 genes in granulosa cells with 334 being unique to small, 243 to medium and 815 to large follicle granulosa cells. They reported 7,810 transcripts that were common to all three follicle sizes. When a cut-off of greater than 1.5 (> 1.5) fold change was applied, 446 genes were found to be regulated between small vs medium, medium vs large and small vs large follicles (Skinner et al., 2008). The major categories of genes regulated across all follicular categories included signaling pathways, immune response, metabolism and transcription. The major cellular pathways regulated across all follicular categories included cell-to-cell adhesion, actin cytoskeleton, PPAR signaling, cytokine receptor interaction and MAPK signaling pathways. The authors focused on TGF- β signaling pathway as many studies have shown that multiple TGF family growth factors regulate ovarian functions. Pathway analysis using “Pathway Assist” software showed that expression of several TGF family cytokines (*GMFG*, *SDF1*, *SPPI*, *NOTCH1*, *VEGF*, *TGFB1*, *CCL2*, *CCL5*) increased with follicular development. Similarly, receptors of ligands *SDF1*, *CCL5* and *TGFB1* (*CXCR4*, *CCR1* and *TGFBRI*, respectively) were also upregulated in granulosa cells as the follicles grew.

In another study (Zielak-Steciwko et al., 2014), the Evans group sought to outline the microRNAs involved in bovine follicular development. MicroRNAs are small non-coding RNAs that alter gene expression by repressing translation or degrading mRNA and have recently been shown to be involved in regulation of gene expression in the ovary (reviewed in (Baley and Li, 2012)). They collected granulosa cell samples from dominant and subordinate follicles (~11 and 9 mm in diameter, respectively) of the first wave of the synchronized estrous cycle (day 2.5-3.5 after estrus). Unlike the previous study (Skinner et al., 2008), this study involved monitoring of the growth of the follicles being sampled. The microarray contained 1,488 bovine and human miRNAs, and with higher stringency false discovery rate (FDR) ($P < 0.01$) they identified higher abundance of 17 miRNAs and lower abundance of 32 miRNAs in granulosa cells of dominant follicles compared to subordinate follicles (Zielak-Steciwko et al., 2014). The higher levels of miR-18a-5p and lower levels of miR-582-5p in granulosa cells of dominant follicles were confirmed by qPCR. Pathway analysis of the miRNAs with greater expression in granulosa cells of dominant than subordinate follicles was carried out and the predicted target-pathways were gap junction, focal adhesion, Wnt signaling, PI3K-Akt signaling, MAPK signaling, regulation of actin cytoskeleton and chemokine signaling pathways. These pathways were similar to those identified as pathways targeted by FSH-regulated genes (Skinner et al., 2008). Interestingly, miR-582-5p, the miRNA with higher expression in granulosa cells of subordinate follicles was identified to target several genes of PI3K-Akt signaling pathway including the MCL1 (Myeloid cell leukemia sequence 1), which is involved in cell survival. The authors propose that subordinate follicles undergo atresia due to increased expression of miR582-5p, which reduces the translation of a survival gene MCL1 in granulosa cells.

Another study (Salilew-Wondim et al., 2014) used microarray analysis to profile the expression pattern of microRNAs in granulosa cells of subordinate and dominant follicles on day 3 and 7 of the synchronized estrous cycle. Similar to the study by Skinner *et al* (2008), this study also has the limitation of a lack of monitoring of follicular growth. Moreover, the grouping of follicles into dominant and subordinate categories was not consistent. Differential expression analysis detected 16 miRNAs, with 14 (including miR-449a, miR-449c, miR212, miR-222, mir-2-3p and miR-155) upregulated and 2 (miR-183 and miR-34c) downregulated in granulosa cells of subordinate follicles compared to those from dominant follicles at day 3. Predicted target genes were assessed and the enriched signaling pathways for those genes include Wnt, TGF- β , apoptosis and nerve growth factor. For follicles on day 7, there were 108 differentially expressed miRNAs, with 51 upregulated and 57 downregulated in subordinate follicles compared to dominant follicles. Pathway analysis of their predicted target genes revealed an enrichment in the Wnt signaling pathway, GnRH signaling pathway, MAPK signaling, oocyte meiosis, TGF- β , and focal adhesion (Salilew-Wondim et al., 2014).

Overall, there has been only one study profiling transcript profiles of granulosa cells of small, medium and large antral follicles. As the samples for microarray were obtained from an abattoir, they may represent follicles growing under the influence of FSH. However, because follicle development was not monitored in that study, the results cannot be directly attributed to FSH action. Nonetheless, some studies that profiled miRNA did monitor follicle development. Taking the data of mRNA and miRNA profiles together, it can be summarized that FSH regulates genes involved in proliferation, apoptosis, signaling pathways and cell-to-cell adhesion.

2.4 Regulation of granulosa cell transcriptome by LH

There have been studies demonstrating LH-regulated changes in the granulosa cell transcriptome in multiple species. Below are the studies that determined the changes in the transcriptome after the preovulatory LH surge in granulosa cells of the bovine, mouse, human and monkey.

Christenson *et al.* (2013) collected granulosa from dominant bovine follicles before and 21h after LH surge to investigate LH regulated genes and pathways. Microarray analysis showed that the LH surge altered the expression of 25% of genes expressed in granulosa cells and 2% of genes expressed in theca cells out of the 11,548 total genes that are expressed in the periovulatory follicle. The authors differentiated granulosa cells into antral and membrane-associated but there were only three genes (one before and two after the LH surge) that were differentially expressed between antral and mural granulosa cells. However, if LH-regulated fold changes were considered, 29 transcripts showed differential LH-regulation in antral granulosa cells compared to mural granulosa cells. Gene set enrichment analysis using IPA revealed that LH regulated transcripts for granulosa cells were enriched for functions such as cell cycle, cellular movement, DNA replication; while theca cells showed enrichment for lipid metabolism, cell death and survival and reproductive system development and function (Christenson *et al.*, 2013).

McRae *et al* (2005) investigated the LH-regulated changes in gene expression in murine granulosa cells. Granulosa cells were collected from mice prior to (48h PMSG, also 0h hCG) and 12h after hCG treatment (in mice, ovulation occurs 13-16h after hCG treatment). Gene expression patterns were analyzed using SAGE (serial analysis of gene expression). They reported 5,689 transcripts common to both time points, 1,806 transcripts unique to 0h hCG library and 2,382 transcripts unique to the 12h hCG library. They found 715 transcripts that were significantly

different in the 12h hCG group versus the 0h hCG, with 499 being significantly upregulated while 216 were significantly downregulated by hCG ($P < 0.05$). Selected transcripts were validated using RT-PCR. *Cyp19a1* and *Fshr* were downregulated by LH, whereas *Star*, *Timp1*, *Ctsl*, *Adamts1* and *Ereg* were upregulated (McRae et al., 2005). It is important to note that SAGE is not as sensitive as microarray/RNA-seq analyses and this study was limited by oocyte contamination as evidenced by oocyte-specific genes among the list of transcripts present in granulosa cells at both time-points studied. Nonetheless, this technique is sensitive enough to detect the abundant genes that were markedly regulated by LH.

A study by Rao *et al* (Rao et al., 2011) reported LH-regulated changes in gene expression in the preovulatory follicle of the buffalo cow using microarray. The water buffalo and domestic cattle, both belonging to Bovidae family, are closely related. Granulosa cell samples were collected before, and at 1, 10 and 22h post peak LH surge. Using microarray, they determined that within 1h of the peak LH surge, 450 genes were differentially expressed (222 genes upregulated, and 228 genes downregulated) with a fold change greater than or equal to 2. By 22 h, 111 genes were shown to be differentially expressed (31 of these genes were upregulated and 80 genes were downregulated) relative to before the LH surge. Furthermore, they observed that many of the genes that were regulated at 1h post LH surge had an opposite regulation by 22h post LH surge. Further analysis of the top 15 differentially expressed genes at 1h and 22h post peak LH surge revealed that the upregulated genes at 1h were enriched for cellular signaling and matrix modulators while the top downregulated genes were related to cell cycle regulation and apoptosis. At 22h, the top upregulated genes were associated with proteins involved in the transition of granulosa cells to luteal tissue while the top downregulated genes were related to processes involved in coagulation system, steroidogenesis, Wnt and IGF signaling. They observed that many genes were

downregulated and reasoned that LH appears to be important for switching off the expression of genes involved in metabolism and proliferation (Rao et al., 2011).

Gilbert *et al.* (2011) used a genome wide bovine oligo array to study the effect of the LH surge on the gene expression profile of granulosa cells. They chose 3 different time points corresponding to distinct stages in the ovulatory process; 2h prior to the LH surge, 6h after the LH surge (early response) and 22h after the LH surge (late response). Granulosa cell samples were collected from cows following an ovarian stimulation protocol involving GnRH treatment, which induces an endogenous LH surge within 2h. The microarray revealed more than 8000 positive signals, 7084 of which were shared between the three time-points as well as some other transcripts which were unique to one of the three stages. The PCA analysis showed that at a minimum fold change of 1.5, there were 1788 transcripts (57%; 1007 upregulated and 781 downregulated) regulated between -2h LH and 22h LH. They observed that 1358 (43%) of the transcripts were LH dependent, with 39% being regulated by 6h LH (673 upregulated and 555 downregulated) and 4% by 22h LH (56 upregulated and 74 downregulated). A list of differentially expressed transcripts was generated from the microarray and included genes known to be involved in folliculogenesis such as *TIMP1*, *TIMP2*, *TNFAIP6*, *INHBA* and *FST*. These were also confirmed by qPCR validation. Gene ontology and pathway analysis using DAVID and IPA software revealed specific profiles of biological functions and molecular processes unique to each time point. The -2h LH group revealed processes involved in cell proliferation, while the 6h LH group showed enrichment of processes associated with response to chemical stimulus, extracellular matrix, lipid synthesis and blood vessel development. The 22h LH group had an enrichment of terms associated with intracellular transport, protein localization and protein folding (Gilbert et al., 2011).

Xu *et al* (2011) investigated the transcriptome of the ovulatory follicle in the rhesus monkey. Samples were collected at 0h, 12h, 24h and 36h post hCG treatment from the ovary bearing the large dominant follicle. In primates, ovulation occurs within 36h of the LH surge (Wissing *et al.*, 2014, Xu *et al.*, 2011). First, they showed that samples from within each time point clustered uniquely, however, there seemed to be more similarity between the 24h and 36h post hCG groups. Though the RNA used for microarray analysis was isolated from granulosa and theca cells along with oocytes, most of the transcripts found to be regulated should be of granulosa cell origin due to proportional majority. Gene ontology analysis revealed 54 significant categories with 5 major themes that were associated with cholesterol regulation, steroid synthesis, growth factors, immune function and prostaglandin regulation. (Xu *et al.*, 2011).

Wissing *et al* (2014) investigated the transcriptome of granulosa cells before and after ovulation in women. Granulosa cell samples were collected before hCG treatment and 36h after hCG treatment (from the same woman in the same cycle). Microarray analysis revealed 1186 genes (572 upregulated and 614 downregulated) that were differentially expressed in the granulosa cell samples before and after hCG treatment (Fold change > 2, P < 0.0001, FDR < 0.012). Gene function enrichment analysis of the differentially expressed genes revealed that inflammation- and coagulation-related genes were upregulated whereas cell cycle-related genes were downregulated after hCG treatment (Wissing *et al.*, 2014). Looking at the follicular fluid before and after hCG treatment, they found that estrogen concentration decreased significantly and CYP19A1 expression also decreased. Progesterone concentration increased as did StAR expression after hCG treatment. Testosterone levels remained unchanged before and after hCG treatment. FSHR and LHCGR expression decreased after hCG treatment. Summarily, genes related to cell cycle regulation (such as CDKN1A and CDC20) were downregulated, whereas genes related to

inflammation, angiogenesis and coagulation (such as PTGS2 and CD24) were upregulated after hCG treatment. Genes related to extracellular matrix remodeling (such as HAS2 and ADAMTS9) were highly upregulated as well as EGF-like ligands (AREG and EREG). The transcription factors, EGR1, EGR2, Jun and c-FOS were also highly upregulated by hCG treatment while FOXL2 was downregulated (Wissing et al., 2014).

A recent study (Liu et al., 2017) used zebrafish as a model and hypothesized that ‘ovulation is controlled by conserved genes and signaling pathways in vertebrates’. They reasoned that this will enable them to identify genes that are uniquely involved in ovulation. This study included wild type and Pgr-KO zebrafish with the Pgr-KO group serving as a reference due to the established anovulatory phenotype of these in previous studies done in mice. In this study, ‘follicular cells’ refers to granulosa and theca cells as it was deemed impractical to separate these cells because of small cell size and indistinguishable physical properties. These samples were then used for RNA-sequencing (single end reads, 50bp). They reported 3,567 (> 10%) genes that were differentially expressed in the WT compared to the Pgr-KO (fold change ≥ 2 and FDR adjusted pvalue ≤ 0.05). They retained 2,888 genes (1230 upregulated and 1658 downregulated in WT vs Pgr-KO) that have mouse orthologs to investigate conserved genes. Biological processes such as angiogenesis, cell migration, apoptosis, response to growth factor and inflammatory response were enriched in the WT. Signaling pathways enriched in WT were Ras, PI3K-Akt, and Foxo; while Pgr-KO had pathways related to cell cycle such as mitochondrial transition and DNA strand elongation (Liu et al., 2017). Interestingly, they compared their data with human and mouse transcriptomic datasets from EMBL and GEO databases, respectively. The criteria were set as absolute $\log_2\text{foldchange} > 1$ and $\text{FDR} < 0.05$. Analysis revealed 283 upregulated and 378 downregulated genes to be evolutionarily conserved as evidenced by their presence in both the

zebrafish and mammalian (human and/or mouse) samples. The upregulated genes appeared to fall into specific groups such as genes related to inflammatory response or apoptosis, vascularization, cell matrix adhesion and extracellular matrix modelling. Downregulated genes were mostly those related to cell cycle. Even though 77% of the DEGs in zebrafish did not show a significant difference in mammalian samples, this study found common genes – *Ptgs2*, *Runx1*, *Adamts9*, *Tnfrsf6*, *Timp2*, *Ptx3*, and *Esr2* – across three species. The authors rightly proposed that these are evolutionarily conserved genes (Liu et al., 2017).

Feidler *et al* (2008) sought to investigate the involvement of miRNAs in the posttranscriptional regulation of mural granulosa cells in the periovulatory follicles of mice. In the first part of their microarray analysis, they found 196 and 206 detectable miRNAs present at 0h and 4h hCG respectively, in two of three samples and 13 miRNA transcripts to be differentially expressed between these two time-points ($p < 0.05$). *Mir132* (fold change 16.9) and *Mir212* (fold change 21.7) were found to be significantly upregulated at 4h hCG and these were validated using qPCR (Fiedler et al., 2008). In the next part of this study, they collected granulosa cells at 0h, 1h, 2h, 4h, 6h, 8h and 12h post hCG treatment. Analysis using qPCR revealed a significant upregulation of *Mir132* (17-fold) and *Mir212* (34-fold) between 2 and 12h post hCG treatment compared to 0h hCG. Importantly, the primary microRNA (Pri-miRNA; *Mir132/212_pri*; the single transcript that yields both miRNAs) transcript showed an increase in expression 1h prior to the detection of the mature forms. This indicates that changes in the primary transcript preceded the changes in the mature forms of *Mir132* and *Mir212*. Further *in vivo* studies are required to elucidate the role of these two miRNAs in granulosa cells during ovulation.

Taking these studies from multiple species together, it can be concluded that the preovulatory LH surge positively regulates the genes involved in steroidogenesis, inflammation,

angiogenesis, cellular movement and tissue remodeling while negatively regulating the genes involved in cell cycle.

2.5 Summary of global analysis of gonadotropin regulated transcriptome in granulosa cells

Overall, there have been several studies employing microarray analysis to investigate the regulation of the granulosa cell transcriptome by FSH and LH. All of these transcriptome data are publicly available and are suitable for meta-analysis to determine a more concrete set of genes regulated by the gonadotropins. With that possibility, gonadotropin regulation of the transcriptome needs to be probed further. What are the mechanisms of regulation of transcription in granulosa cells? What epigenetic mechanisms are critical for gonadotropin induced gene expression? Which transcription factors drive granulosa cell transcriptome? It is possible to address these questions because of tremendous improvements in next generation sequencing, bioinformatics tools and improved annotation of genomes of multiple species.

There are several studies including Zhao *et al* (Zhao et al., 2014) that have compared microarray analysis against RNA-seq analysis. All of them have found that whereas most of the differentially regulated genes are identified by both transcriptome profiling techniques, RNA-seq technology has been adjudged as a more sensitive, reproducible and reliable method. Microarray technology has the inherent background hybridization issues that reduce the accuracy of transcript abundance measurements. Importantly, probes differ considerably in hybridization efficiency and transcripts can be measured only for the genes for which probes are designed. Because of differences in hybridization strength, cross-hybridization, and other experimental variables, microarrays provide a noisy output signal. RNA-Seq does not rely on pre-designed probes. Thus, RNA-Seq can detect novel transcripts and isoforms, map exon/intron boundaries, discover

sequence variations and reveal splice variants. RNA-Seq is more sensitive in detecting genes with very low expression and more accurate in detecting expression of extremely abundant genes.

2.6 Role of histone modifications in regulation of gene expression

2.6.1 Epigenetics

Histones are proteins that package DNA into structural units called nucleosomes that enable the compaction of DNA. There are 4 core histones H2A, H2B, H3 and H4 that form an octamer around which 146 base pairs of DNA winds. These core histones make up the nucleosome which in turn determines chromatin accessibility (Luger et al., 1997). Chromatin can therefore exist in an open conformation referred to as euchromatin, or in a closed conformation referred to as heterochromatin (Venkatesh and Workman, 2015).

Another epigenetic modification that can alter gene expression is DNA methylation. DNA methylation typically occurs in CpG islands and is catalyzed by enzymes known as DNA methyltransferases (Dnmts) and involves the transfer of a methyl group to cytosine (C5) by S-adenyl methionine (SAM). DNA methylation alters chromatin structure, thereby preventing the binding of transcription factors (Moore et al., 2013). This results in repression of gene expression (Lee et al., 2013). DNA methylation has been reported to be necessary for several mechanisms that require a stable form of silencing such as X chromosome inactivation and genomic imprinting and is proposed to be involved in crosstalk with histone modifications and microRNAs (Moore et al., 2013).

Histone variants are distinguished from canonical core histones mainly by the fact that they are expressed, unlike core histones, outside of synthesis (S) phase and incorporated into chromatin in a DNA replication-independent manner (Li et al., 2007). Histone variants have homologies to

canonical core histones but are generally not as ubiquitous. They represent yet another mechanism for nucleosomes to differ from one another without covalent modification of core subunits (Craig, 2005). Histone variants play critical roles in chromatin structure and function such as activation of transcription, DNA repair, X chromosome inactivation and heterochromatin formation. Among the core histones, H2A has the largest number of variants, including H2A.Z, MacroH2A, H2A-Bbd, H2AvD, and H2A.X (Redon *et al.*, 2002). The addition of variants can change the physicochemical properties of the nucleosome (Billon and Cote, 2013).

Recent advances in next generation sequencing (NGS) technology has resulted in several techniques/assays that enable DNA-protein interactions to be captured both *in vivo* and *in vitro* and analyzed. Methods such as chromatin immunoprecipitation followed by massively parallel sequencing (ChIP-Seq) allow DNA-protein interactions to be profiled on a genome-wide basis (Robertson *et al.*, 2007).

2.6.2 Histone modifications

Transcriptional regulation of gene expression is promoted or repressed by the alteration of chromatin accessibility and histone modifications (Kuo and Allis, 1998). These reversible post translational modifications (PTMs), which include acetylation, methylation and phosphorylation occur on the amino-terminal ends of the histones (histone tails) (Hiroi *et al.*, 2004, Fischle *et al.*, 2003). The mechanism of regulation has been attributed to a ‘histone code’ which occurs over and above the genetic (DNA) code (Jenuwein and Allis, 2001). There are enzymes known as writers which add histone modification marks and erasers which remove these modification marks. Readers are effector proteins that translate the code and bind to DNA thereby regulating transcription (Venkatesh and Workman, 2015, Moore *et al.*, 2013).

This additional level of regulation increases the complexity and diversity of gene expression. The complexity is further increased by the different variants of each histone that are also involved in regulation of gene expression/transcription. These variants can replace core histones and usually differ from the core histones by changes in just a few amino acids or possession of larger domains but these slight alterations may result in different outcomes including regulation of transcription (Venkatesh and Workman, 2015).

Histone acetylation is predominantly associated with active transcription and involves the transfer of an acetyl group from acetyl coenzyme A, a process which is catalyzed by histone acetyltransferases and reversed by histone deacetylases (Kuo and Allis, 1998). The methylation of lysines at histone tails is usually carried out by enzymes that contain SET (Su (var), Enhancer of Zeste, and Trithorax) domains such as SUV39H1 which methylate H3K9 specifically and the MLL/SET1 methyltransferase family which forms a complex and is associated with methylation of H3K4 (Santos-Rosa et al., 2002, Takahashi et al., 2011). Histone methylation can be linked to activation or repression of genes depending on which lysine is involved, the degree of methylation (mono-, di- or trimethylation) and the target histone (Mozzetta et al., 2015). H3K4me3 is associated with euchromatin and active gene expression (Santos-Rosa et al., 2002). H3K9me3 on the other hand is associated with heterochromatin and thus repression (Peters et al., 2002, Ugarte et al., 2015)

2.6.3 Epigenetic modifications in differentiating cells

In embryonic stem cells (ESCs), bivalent chromatin domains (H3K4me3 and H3K27me3) maintain active developmental genes at low levels “while keeping them poised for activation” (Bernstein et al., 2006). Matsamura *et al.* (2015) identified a pairing of H3K4me3 and H3K9me3

that appears to maintain adipocytes in a poised state until differentiation is required. They proposed that the methyltransferase SETDB1 is recruited to sites immediately downstream of H3K4me3 marked transcription start sites where it methylates H3K9 establishing the bivalent domain. These bivalent domains were found at the promoter regions of two important transcription factors, CCAAT/enhancer-binding protein alpha (C/EBP α) and Peroxisome proliferator-activated receptor gamma (PPAR γ), which are essential for differentiation of adipocytes (Matsumura et al., 2015).

Another study (Zubek et al., 2016) looking at domain length reported the association of CHD1 with H3K4me3. CHD1 is a chromatin remodeling protein that is required for preinitiation complex assembly, that is, initiation of transcription and thus gene expression. Hence, it is important for the expression of developmental genes. The authors observed a relationship between elongated CHD1 binding and longer H3K27ac and H3K4me3 domains and suggested a possible contribution to increased gene expression (Zubek et al., 2016).

A study by Ugarte *et al.* (2015) found that pluripotent mouse ESCs appear to contain significantly more euchromatin than multipotent hematopoietic stem cells (HSCs) which in turn contain more euchromatin than mature hematopoietic cells. Specifically, 79% in ESCs, 55% in HSCs and 34% in mature myeloid cells. These observations indicate that chromatin tends to become less accessible as cells undergo differentiation. They also showed that the global levels of DNA methylation and individual histone modifications do not appear to change significantly in either ESCs or HSCs even though chromatin is in a more open conformation on a global level in these cells. Thus, these epigenetic modifications occur at certain regions on regulatory genes and are likely not a result of a change in a single epigenetic modification. Taking it a step further, they considered H3K9me3, a mark associated with heterochromatin and found that ESCs had the least amount of heterochromatin, followed by HSCs and then mature cells (Ugarte et al., 2015).

Furthermore, they inhibited the histone methyltransferase G9A which catalyzes mono- and dimethylation of H3K9. Inhibition of heterochromatin formation delayed HSC differentiation as shown by impaired silencing of some genes associated with differentiation and impaired migration capacity, leading the authors to conclude that efficient differentiation of stem cells is dependent on proper transitioning from euchromatin to heterochromatin (Ugarte et al., 2015).

2.6.4 Signaling pathways regulating histone modifications

Tee *et al.* (2014) reported a role for ERK1/2 signaling in the regulation of chromatin accessibility at developmental genes in mouse ESCs. Inhibition of ERK1/2 resulted in an increase in nucleosome occupancy and a decrease in occupancy of the Polycomb repressive complex 2 (PRC2) and RNA Polymerase II (RNAPOLII) at the promoter regions of Erk2-PRC2-targeted developmental genes. PRC2 reportedly recruits H3K27me3 and the authors observed a decrease in H3K27me3 at the promoters of numerous developmentally regulated genes after ERK1/2 inhibition. A possible role for ERK1/2 in the regulation of nucleosome occupancy was suggested based on the observation that Erk2 binding appeared to correspond to regions of histone eviction whereas loss of Erk2 favored increased nucleosome density (Tee et al., 2014).

2.6.5 Epigenetic modifications in granulosa cells

Our understanding of the role of epigenetic modifications in the regulation of gene expression is evolving. The relationship between epigenetic modifications and ovulation is currently being investigated by several groups.

Lee *et al.* (2013) investigated some of these changes in granulosa cells prior to ovulation in the rat and reported a significant increase in histone H4 acetylation at the proximal promoter of the *Star* gene at 4h post-hCG, which then decreased to basal levels at 12 hours post-hCG. H3K4me3 (a mark associated with active genes) was also reported to have gradually increased in

the proximal promoter after hCG injection and was significantly higher at 12 hours compared to 0 hours. H3K9me3 and H3K27me3 are marks associated with repression and their levels were shown to have decreased and were both significantly lower at 12 hours compared to 0 hours. They compared these results to the results from RLC-16 cells, which are rat liver cells that do not express *Star*. The authors suggest that histone acetylation of the *Star* proximal promoter is involved in *Star* gene expression by increasing the binding activity of CEBPB through the change in chromatin structure of the *Star* promoter (Lee et al., 2013). They also found that levels of H3 and H4 acetylation and H3K4me3 in the *Cyp19a1* promoter region significantly decreased at 12 hours after hCG injection compared to 0 hours. H3K27me3 was significantly higher at 12 hours compared to 0 hours post-hCG. Analysis of the chromatin structure in the *Star* and *Cyp19a1* promoters revealed that the relative percentage of chromatin protection against DNase 1 digestion decreased in the *Star* proximal promoter after hCG and was significant at 4 hours and 12 hours compared to 0 hours suggesting that the chromatin structure becomes more relaxed after hCG injection. In contrast, the relative percentage of chromatin protection in the *Cyp19a1* promoter region increased after hCG injection, and there was a significant difference at 12 hours compared with 0 hours suggesting that the chromatin structure becomes condensed after hCG injection (Lee et al., 2013).

Summarily, levels of histone modifications (Histone H4 acetylation, H3K4me3, H3K9me3 and H3K27me3) were altered and chromatin was remodeled at the promoter regions of *Star* and *Cyp19a1*, leading to an increase in gene expression of *Star* and repression of *Cyp19a1* (Lee et al., 2013).

In a separate study from the same laboratory, they identified five genes (HDAC4, HDAC10, EZH2, SETDB2 and CIITA) as histone modifying enzymes that were altered in the

granulosa cells of LH treated rats. *HDAC4*, *HDAC10*, *EZH2* and *SETDB2* mRNA levels decreased while *CIITA* mRNA levels decreased at 4 or 12 h post hCG. These enzymes function as histone acetylation or histone methylation enzymes (Maekawa et al., 2016). The authors proceeded to tie these results together by suggesting that after the ovulatory LH surge, EZH2 recruitment is decreased in the promoter region of *Star* but is increased at the *Cyp19a1* promoter. EZH2 reportedly induces H3K27me₃, a mark associated with repression (Maekawa et al., 2016).

In another study, LH regulated downregulation of *CYP19A1*, *HSD3B1* and *CYP17A1* was associated with chromatin remodeling at the promoter regions of these genes in bovine follicles (Nimz et al., 2010). Transcript analyses of the three genes were performed on the granulosa cells and theca cells of large dominant follicles before and after LH. The relative transcript abundance of CYP19A1 appeared to be higher in granulosa cells and was significantly downregulated by LH whereas CYP17A1 relative transcript abundance was found to be higher in theca cells than in granulosa cells although it was significantly downregulated by LH. HSD3B1 transcript abundance was similar between granulosa cells and theca cells but significant reduction after LH was found only in theca cells. Results from the CHART-PCR (Chromatin accessibility followed by real-time PCR) analysis revealed that chromatin was significantly more protected in bovine granulosa cells after the LH surge in CYP19A1 and HSD3B1. However, for CYP17A1, there was a significant increase in relative chromatin protection only in theca cells (from less than 40% before LH to about 60% after LH) although granulosa cells maintained high values (~60%). The relative protection values for CYP19A1 in granulosa cells were the highest with an increase of approximately 50% (from less than 20% before LH to more than 70% post LH) (Nimz et al., 2010).

In an article by Zhang *et al.* (2014) using mouse granulosa cells, they reported LH-induced changes in histone modifications such as acetylation of histone H2BK5ac and H3K9ac at the

promoter region of LH target genes, which in turn resulted in an increase in gene expression of these genes. They attributed the increased acetylation to the histone acetyltransferase CBP/P300 working in conjunction with CITED4 (coactivator family) and a possible mechanism of action is an increase in chromatin accessibility which in turn favors DNA-binding proteins. Looking at the expression of some LH target genes such as *Areg*, *Ereg*, *Btc*, *Pgr*, *Ptgs2*, *Tnfaip6*, *Sult1* and *Ptx3*, they found that these genes were upregulated by forskolin/PMA within 4h of treatment. However, by 20h, expression levels had returned to basal levels. Furthermore, when treated with trichostatin A (TSA), a histone deacetylase (HDAC) inhibitor, some of the LH target genes (*Areg*, *Pgr*, *Btc*, *Ptx3* and *Tnfaip6*) remained high up to 24h after forskolin/PMA treatment. The authors suggested that after ovulation, HDAC may be an important regulator in the regulation of gene silencing. Moreover, when the granulosa cells were treated with a CBP inhibitor (C646), the increase in acetylation of H2BK5ac and H3K9ac was abrogated. TSA treatment had the opposite effect, that is, an increase in acetylation levels of H2BK5ac and H3K9ac (Zhang et al., 2014). However, these data are limited by the fact that histone modifications were analyzed by Western blotting and not by ChIP, which enables site specific analysis.

Aryl hydrocarbon receptor (*Ahr*) appears to be involved in the regulation of follicular development and ovulation in mice. Teino *et al* (2014) sought to investigate the mechanism by which this gene is regulated in the ovary. Mice were treated with eCG (PMSG – an FSH analog) and then hCG (LH analog). Relative mRNA abundance and protein level analyses showed that *Ahr* is induced by eCG but downregulated by hCG. Next, they looked at the possible involvement of histone acetylation by treating granulosa cells with TSA, a HDAC inhibitor, and found that TSA prevented the downregulation of *Ahr* by hCG. Based on these results, they asked if this downregulation by hCG was because of a decrease in chromatin accessibility at the *Ahr* promoter.

Indeed, CHART-PCR revealed increased nucleosome protection in the hCG treated granulosa cells leading the authors to conclude that hCG induced downregulation of Ahr was as a result of “structural remodeling of the Ahr promoter chromatin” (Teino et al., 2014).

Mehta *et al.* (2015) investigated gene expression in granulosa cells of the buffalo. The authors sought to prevent the inhibition of CYP19A1 and 17 β -estradiol (E2) in buffalo granulosa cells which is induced by LPS and contributes to infertility postpartum in dairy animals due to uterine infections. CYP19A1 is induced by FSH and is a rate limiting enzyme in the synthesis of estradiol which as stated earlier is a key event in FSH-induced follicular development. They pre-treated granulosa cells for 2 hours with TSA, a HDAC inhibitor, and found that granulosa cells that received this treatment before the 24 hours LPS treatment showed a significant increase in global H3 acetylation (K9/14) levels as opposed to granulosa cells that received 24 hours LPS alone which showed a significant global decrease in H3 acetylation (K9/14) levels compared to controls. Furthermore, CYP19A1 and E2 were significantly downregulated in LPS-treated granulosa cells whereas in LPS-treated granulosa cells that were TSA pre-treated, CYP19A1 and E2 levels showed a significant increase that was comparable to control levels. Taken together, the authors concluded that “TSA pretreatment reversed the inhibitory effect of LPS on CYP19A1 expression and E2 production” through chromatin remodeling at the CYP19A1 proximal promoter II where it had the effect of increasing acetylation of H3 (K9/14) by preventing LPS mediated H3 deacetylation (Mehta et al., 2015).

2.7 Rationale, Hypothesis and Objectives

2.7.1 Rationale

Decades of research, both *in vivo* and *in vitro*, into the mechanisms involved in follicular development and ovulation have revealed intricate pathways and a variety of genes that are

temporally and spatially regulated to ensure successful release of a fertilizable and developmentally competent oocyte (Bianco et al., 2019, Cacioppo et al., 2017, Christenson et al., 2013, Espey and Richards, 2002, Herlands and Schultz, 1984, Robker et al., 2000b, Schultz et al., 1983, Assey et al., 1994). It is well established that FSH primarily regulates follicular growth and LH is the primary instigator of the ovulatory process. Both of these gonadotropins achieve these processes through specific gene expression programs in ovarian follicular cells. The discovery that gene regulation can occur without changes in the DNA, a term referred to as epigenetics, has changed the landscape of scientific research (Kuo and Allis, 1998, Lee et al., 2013, Li et al., 2007, Marmorstein and Trievel, 2009). Our understanding of protein-DNA interactions and how they regulate gene expression is constantly being updated.

Epigenetic modifications such as chromatin accessibility and histone modifications have been shown to be among the mechanisms involved in regulation of granulosa cell genes. These modifications regulate gene expression and they do not appear to be altered on a global scale, but rather in a tissue-specific manner and at defined regions of specific genes (Nimz et al., 2010, Ugarte et al., 2015).

However, there are still large knowledge gaps regarding the pathways that regulate these epigenetic modifications and how they contribute to the regulation of ovarian function. Investigating these processes remains a key challenge but will broaden our understanding of the mechanisms of ovulation and enable us to treat or reverse infertility both in humans and livestock.

2.7.2 Hypothesis

Our general hypothesis was that the gonadotropins, FSH and LH, induce alterations in histone modifications in granulosa cells during follicular development and ovulation. We had the following specific hypotheses:

Hypothesis 1: Changes in gene expression induced by FSH to regulate follicular development involves H3K4me3 enrichment in granulosa cells;

Hypothesis 2: LH regulates ovulatory genes through H3K4me3 and ERK1/2 modulates the H3K4me3 deposition at LH-regulated genes;

Hypothesis 3: Sustained ERK1/2 production beyond immediate early hours of LH surge is important for ovulation in mice.

2.7.3 Objectives

Our overall objective was to investigate the role of FSH and LH in the regulation of gene expression through the actions of H3K4me3 and the ERK1/2 signaling pathway using a murine model. Our specific objectives for each study were:

- 1) To ascertain how FSH regulates follicular development in granulosa cells (Chapter 3)
- 2) To analyze the changes in the global transcriptome and H3K4me3 in LH-regulated granulosa cells and examine the role of ERK1/2 on H3K4me3 action (Chapter 4)
- 3) To decipher the roles of sustained ERK1/2 signaling during ovulation (Chapter 5)

CHAPTER 3

Under Review by the peer reviewed journal 'Molecular Reproduction and Development'

MRD-19-0346

Global analysis of FSH-regulated gene expression and histone modification

Authors

Ejimedo Madogwe¹, Deepak K. Tanwar^{1,2}, Milena Taibi¹, Yasmin Schuermann¹, Audrey St-Yves¹
and Raj Duggavathi^{1*}

Affiliations

¹Department of Animal Science, McGill University, 21111, Lakeshore Road, Sainte-Anne-de-Bellevue, QC H9X 3V9.

² Current address: Laboratory of Neuroepigenetics, Medical Faculty of the University of Zürich and Department of Health Sciences and Technology of the Swiss Federal Institute of Technology, Statistical Bioinformatics Group, Swiss Institute of Bioinformatics, CH-8057 Zürich, Switzerland

Short title

FSH-regulated gene expression in granulosa cells

Correspondence

[*raj.duggavathi@mcgill.ca](mailto:raj.duggavathi@mcgill.ca); Department of Animal Science, McGill University, 21111 Rue Lakeshore, Sainte-Anne-de-Bellevue, QC H9X3V9

Key words (4)

Follicle stimulating hormone (FSH), Granulosa cells, Transcriptional regulation, H3K4me3

3.1 Abstract

Follicle stimulating hormone (FSH) regulates ovarian follicular development through a specific gene expression program. We analyzed FSH-regulated transcriptome and histone modification in granulosa cells during follicular development. We used super-stimulated immature mice and collected granulosa cells prior to and 48h after stimulation with equine chorionic gonadotropin (eCG). We profiled the transcriptome using RNA-sequencing (N=3/time-point) and genome wide trimethylation of lysine 4 of histone H3 (H3K4me3; an active transcription marker) using chromatin immunoprecipitation and sequencing (ChIP-Seq; N=2/time-point). Across the mouse genome, 14,583 genes had an associated H3K4me3 peak and 63-66% of these peaks were observed within ≤ 1 kb promoter region. There were 72 genes with differential H3K4me3 modification at 48h-eCG (absolute log fold change > 1 ; FDR < 0.05) relative to 0h-eCG. Transcriptome data analysis showed 1463 differentially expressed genes at 48h-eCG (absolute log fold change > 1 ; FDR < 0.05). Among the 20 genes with differential expression and altered H3K4me3 modification, *Lhcgr* had higher H3K4me3 abundance and expression, while *Nrip2* had lower H3K4me3 abundance and expression. Using ChIP-qPCR, we showed that FSH regulated expression of *Lhcgr*, *Cyp19a1*, *Nppc* and *Nrip2* through regulation of H3K4me3 at their respective promoters. Transcript isoform analysis using Kallisto-Sleuth tool revealed 875 differentially expressed transcripts at 48h-eCG ($b > 1$; FDR < 0.05). Pathway analysis of RNA-seq data demonstrated that TGF β signaling and steroidogenic pathways were regulated at 48h-eCG. Thus, FSH regulates gene expression in granulosa cells through multiple mechanisms namely altered H3K4me3 modification and inducing specific transcripts. These data form the basis for further studies investigating how these specific mechanisms regulate granulosa cell functions.

3.2 Introduction

Follicle-stimulating hormone (FSH) initiates three key events within ovarian follicles: proliferation of granulosa cells, estrogen synthesis and expression of luteinizing hormone (LH) receptor (*Lhcgr*) in granulosa cells (Duggavathi and Murphy, 2009, Hillier, 1994, Richards, 1979, Richards, 2001, George et al., 2011). These events are critical for the development of the follicle to preovulatory stage and oocyte maturation. The initial recruitment of primordial follicles is gonadotropin independent as evidenced by unhindered follicular growth to secondary or early antral stages in mice models lacking *Fshb*, *Fshr*, *Lhb* or *Lhcgr* (Zhang et al., 2001, Lei et al., 2001, Draincourt et al., 1987, Ma et al., 2004, Kumar et al., 1997). These studies have also shown that follicular development beyond formation of the fluid-filled antrum depends on pituitary gonadotropins.

It is well established in multiple species, including humans, that FSH-induced follicular development occurs in waves, characterized by periodic recruitment of cohorts of small antral follicles to grow further (Mihm and Austin, 2002, Ginther et al., 1996). In mono-ovulatory species such as cows and humans, one follicle of each wave is selected as the dominant follicle that reaches ovulatory size, whereas the rest of the follicles (subordinate follicles) cease to grow and undergo atresia. Several studies during the last part of the 20th century have defined the hormonal milieu that favors the growth of the dominant follicle. The ability of the dominant follicle to thrive in the low FSH conditions has been attributed to its ability to utilize the available LH, as granulosa cells of the dominant follicle express LHCGR under the influence of FSH and estradiol (Xu et al., 1995, Fortune et al., 2001, Ginther et al., 1996, Bao et al., 1997).

As the follicle grows, several morphological and humoral changes occur in the follicular cells. Comparison of the dominant follicle to subordinate follicles, mainly in cattle, have shown

increases in diameter, quantity of follicular fluid, granulosa cell numbers and higher concentrations of estradiol in the follicular fluid (Ireland and Roche, 1983). Targeted gene expression analyses mainly in rodent models have shown that FSH regulates follicular development through a specific gene-expression program involving aromatase (*Cyp19a1*), inhibin alpha (*Inha*), estrogen receptor beta (*Esr2*), the liver receptor homolog-1 (*Nr5a2*) and aryl hydrocarbon receptor (*Ahr*) (Richards, 1994, Evans et al., 2004, Teino et al., 2014, Fan et al., 2009a).

Epigenetic modifications such as post-translational modification of histones add another layer of complexity to the regulation of gene expression. Histone methylation, regulated by methyltransferases, is associated with active or repressed gene expression and this is dependent on the type of histone and the location of the modified amino acid residue. One of the best studied histone modifications is trimethylation of lysine 4 of histone 3 (H3K4me3), which is associated with active gene expression (Mozzetta et al., 2015, Lee et al., 2013, Gu and Lee, 2013) and this modification is mainly found in the promoter regions of induced genes (Santos-Rosa et al., 2002).

Therefore, we hypothesized that FSH regulates follicular development through changes in the gene expression through altered H3K4me3. Our objective was to profile gene expression by RNA-sequencing and histone modification through chromatin immunoprecipitation, followed by sequencing. Here we have used bioinformatics tools to uncover the FSH-regulated gene expression in mouse granulosa cells.

3.3 Materials and methods

3.3.1 Granulosa cell collection

Immature (post-natal 21-23 days) C57BL/6NCrl female mice (Charles River) were housed in standard plastic rodent cages and maintained on a 12-h light and 12-h dark cycle with feed and water provided *ad libitum* (Rodent Diet; Harlan Teklad, Canada). All animal experiments were approved by the Animal Care and Use Committee of McGill University. Immature mice were injected intraperitoneally with 5 IU eCG (Folligon, Merck) to stimulate follicle development. Granulosa cells were collected prior to and 48h after treatment (Duggavathi et al., 2008a, Dupuis et al., 2014).

3.3.2 RNA Extraction/RNA Sequencing

Total RNA was extracted from granulosa cells collected prior to eCG treatment (0h eCG) and 48h after eCG treatment (48h eCG) using the Direct-Zol RNA MiniPrep Isolation Kit (Zymo Research, Cedarlane Laboratories) as per the manufacturer's protocol. RNA was quantified using the Nanodrop 2000 spectrophotometer (ThermoFisher Scientific). Samples were sent to the functional genomics platform (McGill University and Genome Quebec Innovation Centre) for library preparation using 250ng of mRNA. Only RNA samples with an RNA integrity number (RIN) of 8.2 and above were used. The libraries were sequenced using the Illumina HiSeq 4000 PE 100. The RNA-Seq data will be available from the GEO data repository (GSE140371). RNA-Seq quality metrics are presented in Supplementary Table 1A.

3.3.3 Chromatin Immunoprecipitation and sequencing

Chromatin immunoprecipitation was carried out using granulosa cells collected prior to eCG treatment (0h eCG) and 48h after eCG treatment (48h eCG) from 2 groups of 4 pooled mice (n = 2 biological replicates). This protocol was adapted from previous reports (Svotelis et al., 2009,

Haring et al., 2007, Hisano et al., 2013a, Kuo and Allis, 1999, Bianco et al., 2014a). Briefly, pelleted granulosa cells were crosslinked with 1 percent formaldehyde in PBS for 15 minutes at room temperature. Cells were lysed and sonicated (Q55 Sonicator, Fisher Scientific USA) to obtain chromatin fragments of 200-500bp. Ten percent of the sonicated chromatin was removed as input and 5 percent to evaluate sonication efficiency. The rest of the chromatin was immunoprecipitated at 4°C overnight with either H3K4me3 antibody (Abcam; ab8580) or Rabbit IgG (Abcam; ab171870). The next day, magnetic beads (Protein A Dynabeads; Life technologies) were added to the reaction and incubated with rotation at 4°C for 4 hours. DNA-protein complexes were eluted after several washes and crosslinks reversed by incubating overnight at 65° C. After treatment with RNase A and proteinase K, DNA was then purified using the Qiagen PCR Purification kit (Qiagen) and quantified using the Nanodrop 2000 spectrophotometer (Thermofisher Scientific). Samples were sent to the functional Genomics platform McGill University and Genome Quebec Innovation Centre for library preparation and sequencing using the Illumina HiSeq 2000 SR 50. The ChIP-Seq data will be available from the GEO data repository (GSE140371). ChIP-Seq quality metrics are presented in Supplementary Table 1B.

Bioinformatics

3.3.4 RNA-Seq data analysis

Sequenced reads were assessed for quality using FastQC; v 0.11.5 (Andrews, 2014). The STAR program, a splice aware aligner, was used for read alignment (Dobin et al., 2013) and uniquely mapped reads were 87-90 percent. The read counts were then uploaded to Network Analyst (Xia et al., 2015) for analysis of differential expression.

3.3.5 ChIP-Seq data analysis

Sequenced reads were assessed for quality using FastQC; v 0.11.5 (Andrews, 2014) and adapters trimmed using Trimmomatic; v 0.36 (Bolger, 2014). Subsequently, sequences were mapped to the mouse genome (mm10) using Bowtie2; v 2.2.9 (Langmead and Salzberg, 2012) and peak calling was performed using MACS2; v 2.1.1 (Zhang et al., 2008) and a matrix of counts (enrichment) was obtained (Hisano et al., 2013b) that was then used to analyse differential enrichment of H3K4me3 using Network Analyst, a tool designed to enable statistical and visual analyses of gene expression data (Xia et al., 2015, Xia et al., 2013). Peaks were also annotated using ChIPseeker; v 1.18.0 (Yu et al., 2015) and peak data visualized using the integrative genomics viewer (IGV) (Robinson et al., 2011).

3.3.6 Differential Transcript Analysis

We used the Kallisto-Sleuth pipeline to analyse transcripts. The Kallisto program was used to run the first part of the analysis which involves quantification of transcript abundance (Bray et al., 2016). Differential analysis was done using the R package, Sleuth (solive) (Pimentel et al., 2017). Differential transcripts were identified using the Wald test in Sleuth and the b-value for further filtering.

3.3.7 Pathway Analysis

EGSEA (Alhamdoosh et al., 2017) and Network Analyst (Xia et al., 2015) were used for Kyoto Encyclopedia of Genes and Genomes (KEGG) pathway analysis, as well as enrichment analysis of biological processes using the list of FSH-regulated genes (DEGs; n = 1463).

The list of FSH-regulated genes (DEGs; n = 1463) was also uploaded and used for data analysis and interpretation using various functions in the Ingenuity pathway analysis (IPA; Ingenuity Systems Inc., Redwood City, CA) tool.

3.3.8 ChIP-qPCR

Chromatin immunoprecipitation was carried out as previously described using H3K4me3 and IgG antibodies (Abcam). A ten percent aliquot was taken from each sample after sonication but prior to incubation with the respective antibodies to serve as input for the qPCR reaction. Integrated DNA technologies (IDT) designed primers in the peak regions of the promoter identified for *Lhcgr*, *Cyp19a1*, *Nppc* and *Nrip2*. The purified DNA was then used in the qPCR reaction (ChIP-qPCR) with the CFX394 Real time PCR system (BioRad). Amplicon abundance was expressed as the percent of immunoprecipitated DNA relative to the input DNA. The sequences of the primer sets used are listed in Table 1A.

3.3.9 RT-PCR

For validation of RNA-Seq results and characterization of the histone modifying enzymes, total RNA was extracted (Qiagen microRNA kit; Qiagen, Toronto, CA) from granulosa cells collected at 0h eCG and 48h eCG. The purity and quantity of each sample was measured using the Nanodrop 2000 (ThermoScientific). We synthesized cDNA from 250ng of total RNA using the iScript cDNA Synthesis kit (BioRad) according to the manufacturer's instructions. All primers were purchased from Integrated DNA technologies (IDT, USA). We analyzed mRNA expression by quantitative real time PCR (RT-PCR) using the CFX384 (BioRad). Expression data for each gene of interest was normalized to mean expression levels of four reference genes *Gapdh*, *B2m*, *L19* and *Sdha*. The sequences of the primer sets used are listed in Table 1B.

3.4 Results

3.4.1 FSH-regulated granulosa cell transcriptome

First, we sought to investigate the regulation of gene expression by FSH at the level of the transcriptome. The quality assessment of sequenced reads of granulosa cells collected before (0h eCG) and after eCG treatment (48h eCG) showed that uniquely mapped reads accounted for 87-90 percent of the total reads (Supplementary Table 1A). Differential gene expression analysis using edgeR revealed 1463 differentially expressed genes (DEGs) between 48h eCG and 0h eCG ($\text{abs}[\log\text{FC}] > 1$ and $\text{FDR} < 0.05$). Of these, 755 genes were found to be upregulated, whereas 708 genes were downregulated. Well known FSH-regulated genes among these DEGs include *Fshr*, *Lhcgr*, *Cyp19a1*, natriuretic peptide precursor type C (*Nppc*), pregnancy associated plasma protein (*Pappa*) and low density lipoprotein receptor (*Ldlr*) (Kumar et al., 1997, Richards, 1979, Richards, 2001, Zielak-Steciwko and Evans, 2016, Irving-Rodgers et al., 2009, Gebremedhn et al., 2015, Parakh et al., 2006, George et al., 2011, Hunzicker-Dunn and Maizels, 2006).

3.4.2 Functional analysis of differentially expressed genes

Ingenuity pathway analysis to find functional categories among differentially regulated genes using the core analysis function showed that majority of the differentially regulated genes were located in the cytoplasm and plasma membrane, as well as the extracellular space and nucleus (Figure 1A). The top ten functional categories of these genes included enzymes, transporters, transcription regulators, peptidases, kinases, ion channels, G-protein coupled receptors, transmembrane receptors, growth factors and cytokines (Figure 1B and C). Among these, “enzymes” was the biggest class followed by ion channels/transporters. Some of the differentially regulated enzymes were *Cyp19a1* and *Lss*. Of interest were the genes among growth factors (*Inhba*

and *Nog*) and transcription regulators (*Nupr1* and *Nrip2*). The differentially regulated non-coding RNA genes included *Mir409* and *Snord37*.

Further, the upstream regulator analysis in IPA identified chorionic gonadotropin (CG), transforming growth factor beta 1 (TGFB1), tumor necrosis factor (TNF), estrogen receptor 2 (ESR2) and beta-estradiol among the top upstream regulators. Of these, CG, TGFB1, ESR2 and beta-estradiol were identified to be positively regulated by eCG treatment ($p < 0.05$).

3.4.3 Pathway analysis of differentially expressed genes

We used Ensemble of Gene Set Enrichment Analyses (EGSEA) (Alhamdoosh et al., 2017) and Network analyst (Xia et al., 2014) tools to uncover Kyoto Encyclopedia of Genes and Genomes (KEGG) pathways differentially regulated by eCG treatment. The common enriched KEGG pathways identified by both tools were Steroid biosynthesis, Fat digestion and absorption, Terpenoid backbone synthesis, and TGF-beta signaling pathways (AdjP < 0.05) (Figure 1D).

3.4.4 Regulation of H3K4me3 in granulosa cells

Post-translational modification of histones is a very important mechanism by which gene expression is regulated. Therefore, we evaluated FSH-regulated changes in H3K4me3 in granulosa cells. Overall alignment rate of reads to the mouse reference genome (mm10) was above 97 percent for all samples with unique reads corresponding to about 70 percent of the total reads (Supplementary Table 1B).

We first examined the nature of the genomic addresses with H3K4me3 peaks. About 61-67% of the peaks were located in the promoter region within 1 kilobase ($\leq 1\text{kb}$) from the transcription start site (TSS), the remainder being distributed over other gene features including the 3' untranslated region (UTR), 5' UTR, exons, introns and distal intergenic regions (Figure 2A).

Upon differential analysis using edgeR and applying a filter of absolute log fold change > 1 and $FDR < 0.05$, we found that 72 genes had differential H3K4me3 enrichment at 48h compared to 0h eCG (Figure 2B). Of these, 24 genes, including *Lhcgr*, had peaks upregulated and 48 genes, including *Nrip2*, had peaks downregulated by eCG treatment. We did not perform functional analysis of these 72 genes as this number is too small for any meaningful functional categorization.

3.4.5 Relationship between H3K4me3 enrichment and gene expression

We explored if there were any changes in H3K4me3 enrichment associated with the genes that were differentially expressed in response to eCG treatment. Among the 1463 differentially expressed genes in RNA-Seq dataset and 72 genes with differential H3K4me3 enrichment in ChIP-Seq dataset, 20 genes were common to both datasets (Figure 3A). Of these, 14 genes showed higher expression with upregulated H3K4me3 enrichment and 6 genes showed lower expression with downregulated H3K4me3 enrichment (Figure 3B). *Lhcgr* expression was higher (3.73 logFC, $FDR < 0.05$) in association with higher H3K4me3 enrichment (1.79 logFC, $FDR < 0.05$) in its promoter region. On the other hand, *Nrip2* was downregulated (-1.68 logFC, $FDR < 0.05$) with a lower H3K4me3 enrichment (-1.24 logFC, $FDR < 0.05$) in its promoter (Figure 4A).

There were 52 genes with differential H3K4me3 enrichment that were not differentially expressed at 48h eCG. Conversely, 1443 differentially expressed genes did not have differential H3K4me3 enrichment at 48h eCG. Among them, expression of *Fshr* (1.32 logFC, $FDR < 0.05$) and *Cyp19a1* (1.98 logFC, $FDR < 0.05$) was higher at 48h eCG without any changes in H3K4me3 enrichment (Figure 4B). Especially for *Cyp19a1*, it was surprising to see that despite an apparent increase in H3K4me3 enrichment (Figure 4B, IGV panel), the differences were not statistically significant.

3.4.6 Confirmation of sequencing data using qPCR and ChIP-qPCR

We then sought to confirm the relationship between the expression of genes and the H3K4me3 enrichment at their promoters using qPCR and ChIP-qPCR, respectively. Using qPCR, we were able to show that there was higher mRNA abundance of *Fshr*, *Ahr*, *Nppc* ($p < 0.05$) while mRNA abundance of *Nrip2* showed a tendency to be lower at 48h eCG compared to 0h eCG ($p = 0.06$; Figure 5A). Using ChIP-qPCR, we found higher H3K4me3 enrichment at the promoter regions of *Lhcgr*, *Nppc* and *Cyp19a1* ($p < 0.05$), while H3K4me3 enrichment at the promoter region of *Nrip2* was lower at 48h eCG compared to 0h eCG ($p < 0.05$; Figure 5B).

3.4.7 Expression of histone modifying enzymes and H3K4me3 at their promoters

None of the genes coding for histone methyltransferases and demethylases were among the differentially regulated genes in both RNA-Seq and ChIP-Seq datasets. However, we found that promoters of all these genes, except *Ash11* had H3K4me3 enrichment. We then sought to confirm RNA-seq data for these genes. Except for *Kmt2e* (*Mll5*; $p < 0.05$), there were no differences in the mRNA abundance of genes coding for the histone methyltransferases *Kmt2a* (*Mll1*), *Kmt2c* (*Mll3*), *Ash11* (*Kmt2h*) and *Setd1b* (*Kmt2g*) between 0h and 48h eCG ($p > 0.05$; Figure 6). Also, none of the histone demethylases *Kdm1a* (*Lsd1*), *Kdm1b* (*Lsd2*), *Kdm5a* (*Jarid1a*), *Kdm5b* (*Jarid1b*) and *Kdm5c* (*Jarid1c*) showed differences in mRNA abundance between granulosa cells collected at 0h and 48h eCG ($p > 0.05$; Figure 6).

3.4.8 Differential transcript regulation by FSH

It has been estimated that the primary mRNA of approximately 95% of multiexon genes undergo alternative splicing and that there are about 100,000 intermediate- to high-abundance alternative splicing events in major human tissues (Pan et al., 2008). Therefore, we sought to understand FSH-regulated gene expression at the transcript level using a recently developed Kallisto-Sleuth pipeline (Bray et al., 2016, Pimentel et al., 2017). Applying a more stringent cut-

off using the bias estimator, also known as beta value (Hamilton et al., 2018), we identified 875 differentially expressed transcripts (DETs) from 740 genes ($abs [b] > 1$ and $FDR < 0.05$). Of these, 628 DETs from 515 genes were upregulated and 247 DETs from 227 genes were downregulated. Comparing these 740 genes having DETs identified using the Kallisto-Sleuth pipeline to the 1463 DEGs identified in the gene-level analysis pipeline (above), we found 453 common genes (Figure 7A). Of these, there were 379 FSH-induced genes, with specific transcripts, including *Fshr*, *Lhcgr*, *Cyp19a1*, *Cyp11a1*, *Star*, *Ahr*, *Pappa*, *Ldlr* and *Nppc* (Figure 7B). The identity of specific transcripts of these FSH-regulated genes are presented in Supplementary Table 2.

3.5 Discussion

Follicle stimulating hormone is widely used in assisted reproductive technologies such as controlled ovarian stimulation which aims at producing multiple follicles in order to increase the chances of a successful pregnancy. An optimal dose has to be administered to each patient as too high a dose may lead to overstimulation, multiple pregnancies and severe side-effects like ovarian hyperstimulation syndrome, whereas too low a dose may lead to poor ovarian response and/or failed conception (Raju et al., 2013). Despite numerous studies investigating a small group of FSH-regulated genes in granulosa cells, there are only a few studies profiling FSH-regulated genes at transcriptome level. Also deciphering the mechanisms of FSH signaling is important to understand the molecular basis of follicular development to preovulatory stage and develop therapeutic tools to manage infertility. In this study, we have combined RNA-Sequencing and ChIP-Sequencing technologies to study FSH-regulated gene expression in mouse granulosa cells.

Given the high percentage of unique reads in both RNA- and ChIP-Seq data that were aligned to the mouse genome, it was encouraging for us to undertake further bioinformatics analyses. The 1463 DEGs observed in our study appear to be a reasonable number, given that other studies in mouse granulosa cells have found between 1000 to 2000 DEGs during LH-induced ovulation (Meinsohn et al., 2018, Binder et al., 2013, Fan et al., 2009b). However, our numbers are higher than the 708 genes observed in bovine granulosa cells treated with FSH *in vitro* (Nivet et al., 2018). This difference in the number of DEGs could be attributed to differences in the timeline (48h in our study vs 4h in the bovine study), source of granulosa cells for transcriptome analysis (*in vivo* vs *in vitro*), hormone used to stimulate (eCG vs recombinant human FSH) in addition to species differences (mouse vs cow). In our study, the 755 upregulated genes included well-known FSH-induced genes such as *Fshr*, *Lhcgr*, *Cyp19a1*, *Nppc*, *Pappa* and *Ldlr* (Kumar et

al., 1997, Richards, 1979, Richards, 2001, Zielak-Steciwko and Evans, 2016, Irving-Rodgers et al., 2009, Gebremedhn et al., 2015, Parakh et al., 2006, George et al., 2011, Hunzicker-Dunn and Maizels, 2006).

Categorization of the DEGs based on cellular localization showed that the regulated genes were more or less uniformly distributed in different cell compartments including the extracellular matrix. This observation indicates that FSH regulates multiple aspects of granulosa cell differentiation including fatty acid metabolism and steroid biosynthesis as evidenced by differentially regulated cellular pathways. Our study also showed that FSH appears to promote granulosa cell differentiation through paracrine and juxtacrine signaling; growth factors were one of the class of genes represented among DEGs. This inference is further supported by the fact that TGF β 1, TNF and estradiol were the FSH-induced upstream regulators as identified by multiple bioinformatic tools. Indeed, the FSH-regulated granulosa cell differentiation ought to involve a multitude of other local factors as most of the antral follicular growth happens when FSH levels are low. It is well established in bovine studies that granulosa cells of the dominant follicles dramatically enhance estradiol synthesis and begin to express LHCGR around the time of deviation (Xu et al., 1995), which occurs when the FSH levels in circulation reach nadir relative to the transient peak that induced that follicular wave (Ginther et al., 2003).

It has been shown that *Fshr* expression increases in the granulosa cells as follicles switch from being gonadotropin independent to being gonadotropin dependent and this usually occurs in the late preantral stage of follicular development leading to antrum formation (Verbraak et al., 2011, George et al., 2011). Despite what appears to be an increase in H3K4me3 enrichment at the promoter region, the ChIP-Seq analysis did not reveal any significant difference based on the cut-off values. However, *Fshr* expression increased over two-fold in the RNA-Seq data and this

increase was also confirmed by RT-qPCR. This indicates that *Fshr* gene was already in “transcription mode” by the time we collected granulosa cells (the eCG0h granulosa cells were collected from small antral follicles). Indeed, FSHR expression has been shown in granulosa cells of follicles at as early as primary stage (Findlay and Drummond, 1999). On the other hand, *Lhcgr* was regulated at mRNA level and its increased expression was associated with increased H3K4me3 enrichment at the promoter as per ChIP-seq data. This increased enrichment of H3K4me3 was confirmed by ChIP-qPCR, thereby demonstrating that eCG treatment increased *Lhcgr* mRNA levels by enhancing the H3K4me3 enrichment at its promoter.

However, some of the important genes known to play a role in granulosa cells during follicular development were regulated at mRNA level, but the H3K4me3 at their promoter was not regulated by eCG treatment, as per ChIP-seq data. For example, ChIP-seq data analysis showed that H3K4me3 was not altered at the promoter regions of *Cyp19a1* and *Nppc*, the two very important genes in granulosa cells. Based on the importance of these genes, we sought to examine H3K4me3 levels at their promoters using ChIP-qPCR technique. The fact that this targeted technique, in contrast to the robust ChIP-seq technology, showed a clear regulation of H3K4me3 levels at their promoters by FSH points more to technical aspect of this study than the underlying biological principle. The lack of regulation in ChIP-seq data could be related to higher background noise in sequenced reads, which itself could be due to the depth of sequencing and the number of biological replicates. This study should be used as a point of reference to have higher than 2 biological replicates and higher than the 30 million reads per sample when studying H3K4me3 in ovarian granulosa cells. Most importantly, our ChIP-seq data allowed us to identify the genomic addresses of H3K4me3 peaks in the promoter regions of the genes of interest and probe their regulation using targeted approaches like ChIP-qPCR. In that sense, our ChIP-seq data set that is

publicly available (submission to GEO is in progress) will be useful to other researchers in aiding them to identify the exact genomic address of H3K4me3 enrichment at the promoters of any genes of interest and examine their regulation in ovarian granulosa cells.

The key feature of the large antral follicle is the synthesis of steroids. As mentioned above, eCG treatment induced *Cyp19a1*, which is known to increase in response to FSH and is a rate limiting enzyme for estrogen synthesis in granulosa cells of multiple species (Hillier, 1994, Verbraak et al., 2011, Stocco, 2008, Parakh et al., 2006). We also found that eCG induced *Cyp11a1*, which catalyzes the conversion of cholesterol to pregnenolone (Wigglesworth et al., 2015, Segers et al., 2012). It was shown, using microarray analysis, in cultured bovine granulosa cells that FSH induced both *CYP19A1* and *CYP11A1* at 4h after treatment (Nivet et al., 2018). We also found an increase in Lanosterol synthase (*Lss*) at 48h eCG (2.5-fold). *Lss* functions as a catalyst in cholesterol biosynthesis and is induced by FSH (Segers et al., 2012, Fan et al., 2009a). The promoter of *Lss*, like *Fshr* also had H3K4me3 enrichment although this was not significantly regulated by FSH.

One of the novel genes we found to be regulated by FSH in this study was nuclear receptor interacting protein 2 (*Nrip2*). The promoter of *Nrip2* had reduced H3K4me3 enrichment in response to eCG treatment, which was also associated with lower mRNA levels in the RNA-Seq data. These observations were confirmed by ChIP-qPCR and qPCR, respectively. Nuclear receptors are transcription factors that regulate transcriptional activation. NRIP2 (also known as NIX1) downregulates transcriptional activation by nuclear receptors such as NR1F2 (Greiner et al., 2000). NRIP2 has been shown to regulate cell renewal in cancer cells by activating the Wnt pathway (Wen et al., 2017). Thus, the role of *Nrip2* in granulosa cells needs further research.

With the confirmation that FSH regulates granulosa cell gene expression, at least in part, through H3K4me3 at their respective promoters, the obvious question is whether or not there is a change in the expression levels of genes involved in H3K4 methylation. Though none of these histone methylation genes were among the differentially regulated genes in both RNA- and ChIP-seq dataset, we found a significant increase only in *Kmt2e* expression, by qPCR. Although the mechanism of action is still poorly understood, it does not seem to have histone methyltransferase activity like the other members of the mixed lineage leukemia (MLL) family, but plays a unique role in the regulation of gene expression (Zhang et al., 2017, Cheng et al., 2008). While several histone modifying enzymes have been identified, their regulation and signaling mechanisms are still under investigation. Each enzyme requires specific substrates and other cofactors such as transcription factors and coactivator complexes in order to exert its regulatory effect on the target histone (Marmorstein and Trievel, 2009). Therefore, FSH appears to regulate the functions of H3K4 methylation enzymes (not their expression) by mechanisms including, but not limited to, regulation of expression of transcription factors or other protein modifying enzymes.

In summary, here we have identified several FSH-regulated genes that provide a basis for further exploration. Overall, the results provide evidence that FSH regulates expression of the important granulosa cell genes, such as *Lhcgr*, by altering H3K4me3 at their promoters. By extension, it is possible that FSH could be involved in other modifications of histones in granulosa cells during follicular development.

3.6 Declaration of interest, Funding, Contributions and Acknowledgements

Conflict of interest statement

The authors declare that there is no conflict of interest that could be perceived as prejudicing the impartiality of the research reported

Funding

This work was supported by the National Science Research Council (NSERC) grant (RGPIN-2019-06667) - RD; NSERC-CREATE and Graduate Excellence Fellowship – EM

Author contribution

E.M. contributed to ideas, designed experiments, collected and processed samples, analyzed and interpreted data, prepared figures and wrote manuscript; D.K.T. took part in data assembly and analyses; M.T. took part in planning experiments and collecting samples; Y.S. took part in collecting samples and data analyses; A.S. took part in planning experiments and processing samples; R.D. conceived the study, designed experiments, analyzed data, and edited the manuscript.

Acknowledgements

The authors would like to thank Dr Vilceu Bordignon, Dr Jean-Benoit Charron and Dr Sarah Kimmins for use of facilities. In addition, we would like to thank Dayananda Siddappa, Boris Mayer and Keith Siklenka for their invaluable assistance.

3.7 FIGURES

Figure 3.7.1 Classification of RNA-Seq DEGs. (A) Functional classification of genes: Location; (B) Functional classification of genes: Type; (C) Number of genes in each category. (D) Pathways enriched by the 1463 DEGs as shown by EGSEA.

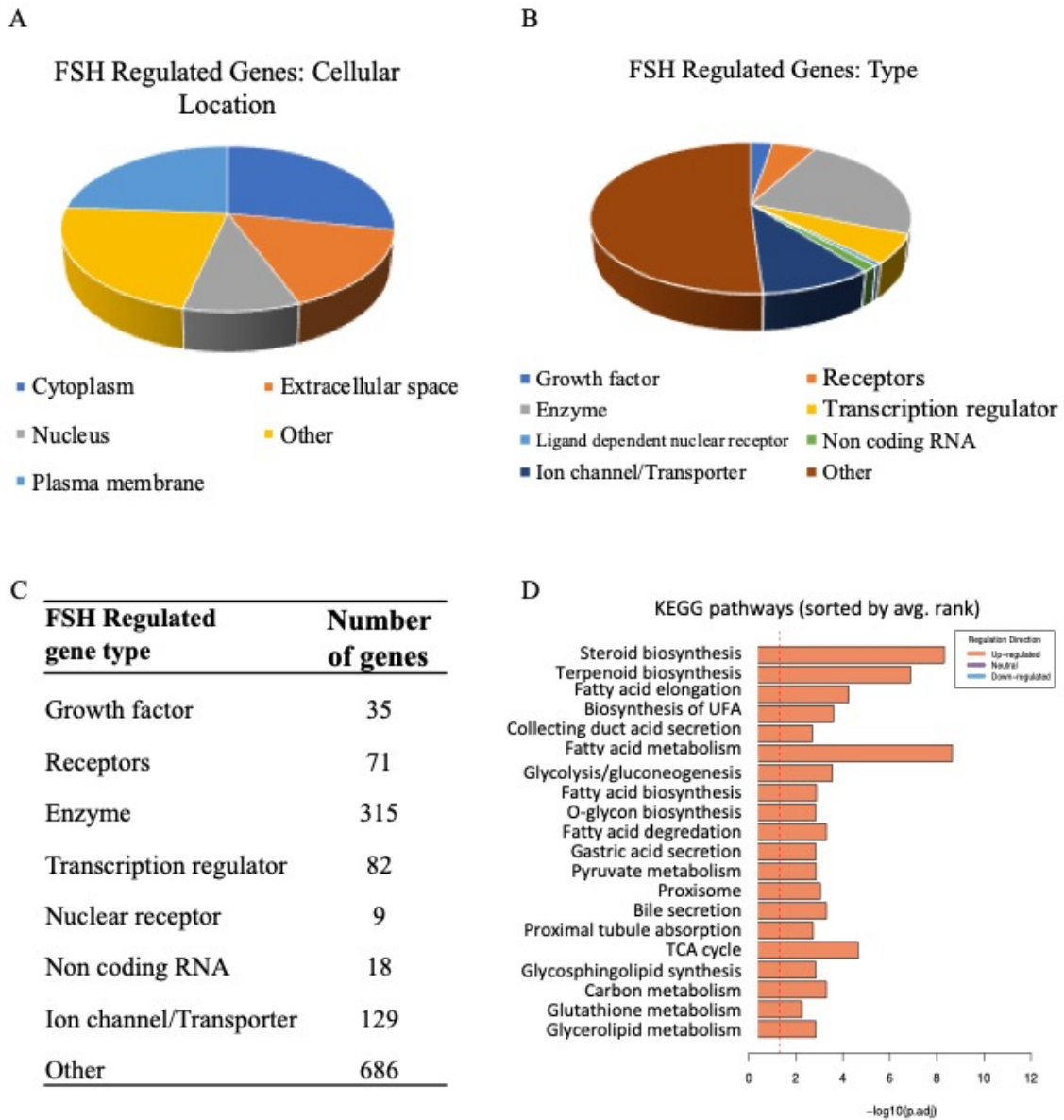


Figure 3.7.2 Peak features and heatmap. (A) Features of H3K4me3 peaks. The ChIPseeker package was used for the annotation of peaks as identified by MACS2 to the different genomic features. (B) Heatmap of the 72 ChIP-Seq genes that showed significant differential abundance. Network Analyst

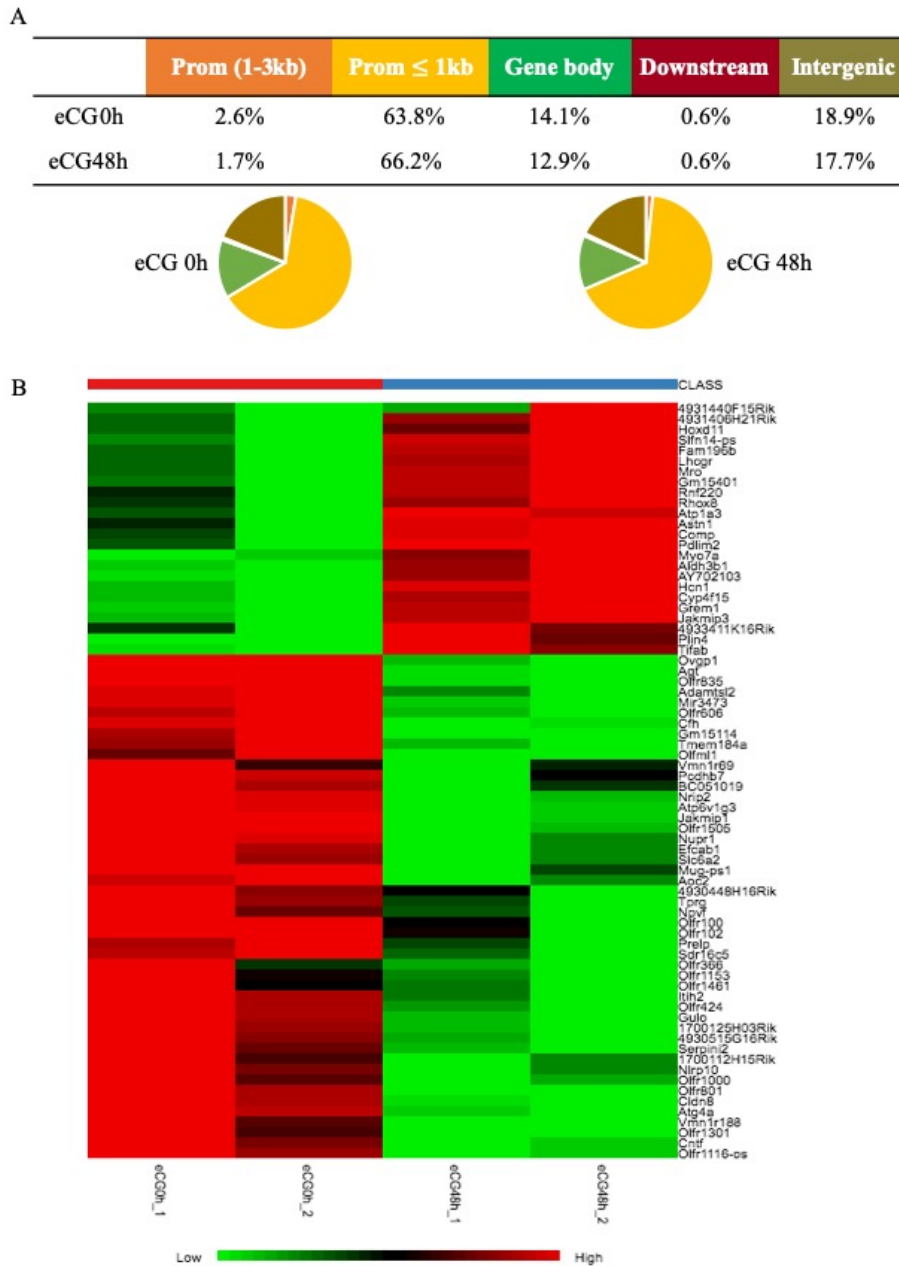


Figure 3.7.3 Interaction between ChIP-Seq and RNA-Seq data. (A) Venn diagram indicating the interaction between the ChIP-Seq data and the RNA-Seq data. (B) Bar chart showing the 20 genes that are regulated by differential H3K4me3 abundance as well as differential gene expression.

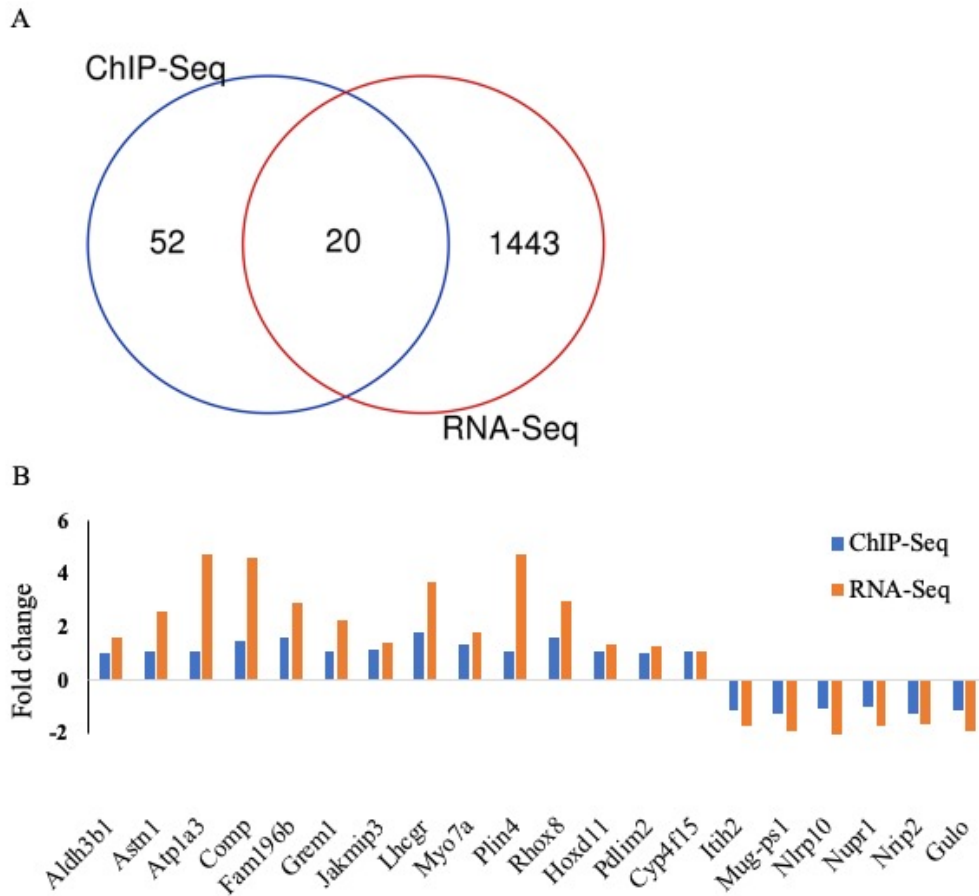


Figure 3.7.4 H3K4me3 enrichment and mRNA abundance. Images from integrative genomics viewer (IGV) and Network analyst showing H3K4me3 enrichment in the promoter regions and mRNA abundance of (A) *Lhcgr* and *Nrip2*, from 20 genes with differential H3K4me3 enrichment as well as differential gene expression in the ChIP- and RNA-Seq data ($\text{abs}[\log\text{FC}] > 1$ and $\text{FDR} < 0.05$) (B) *Cyp19a1* and *Fshr*, from 1443 genes with differential gene expression in the RNA-Seq data ($\text{abs}[\log\text{FC}] > 1$ and $\text{FDR} < 0.05$) but no significant differential H3K4me3 enrichment in the ChIP-Seq data.

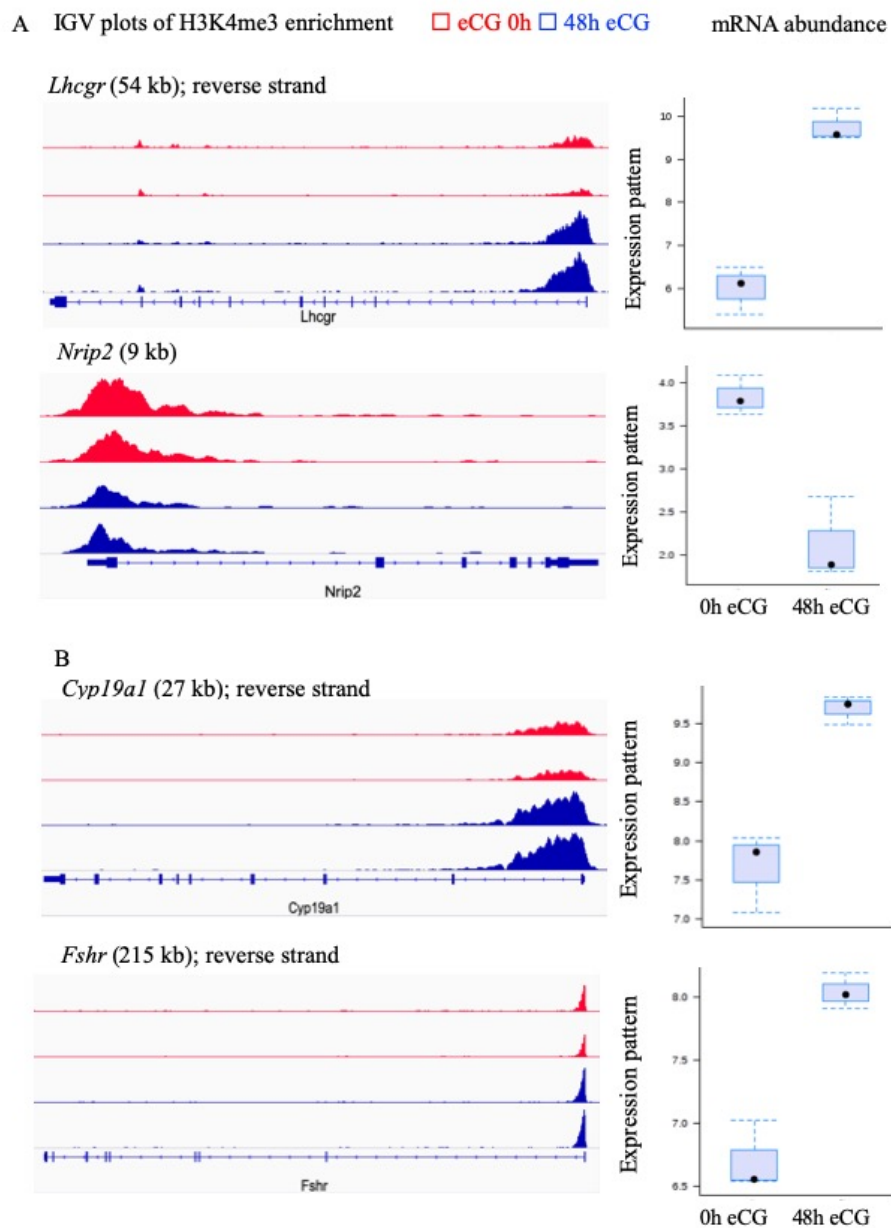
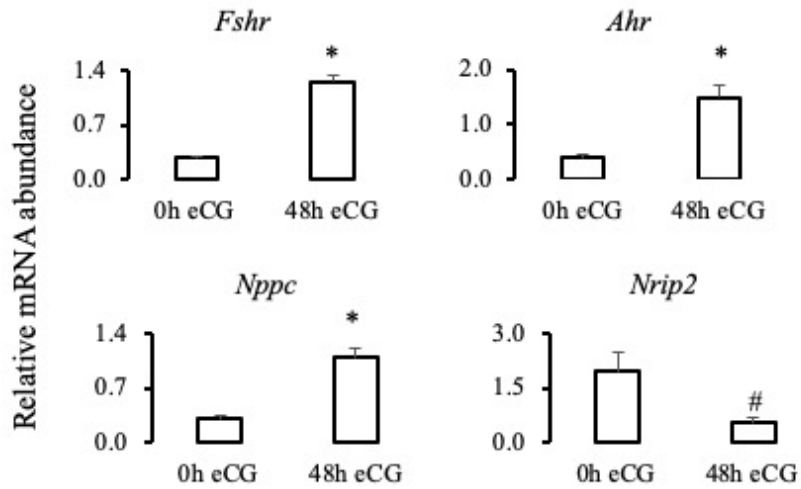


Figure 3.7.5 RT-PCR and ChIP-qPCR graphs. (A) Graphs of mRNA abundance from RT-qPCR of *Fshr*, *Ahr*, *Nppc* and *Nrip2*. * indicates significant difference ($p < 0.05$). # indicates a trend ($p=0.06$). (B) Graphs indicating percent input from ChIP-qPCR of the promoter regions of *Lhcgr*, *Cyp19a1*, *Nppc* and *Nrip2*. * indicates significant difference ($p < 0.05$)

A



B

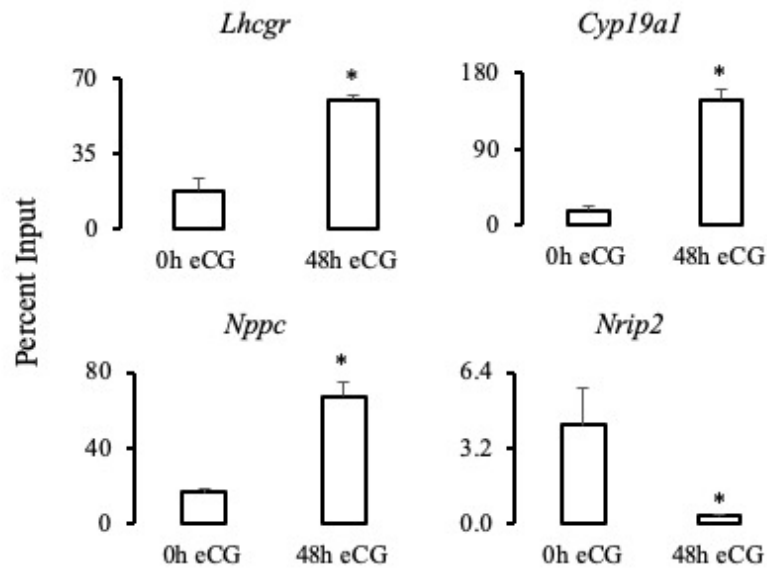


Figure 3.7.6 mRNA abundance of H3K4me3 methylases and demethylases. Graphs of mRNA abundance of the histone methylases *Kmt2a*, *Kmt2c*, *Kmt2e*, *Ash1l* and *Setd1b* and the histone demethylases *Kdm1a*, *Kdm1b*, *Kdm5a*, *Kdm5b* and *Kdm5c*. * indicates significant difference ($p < 0.05$)

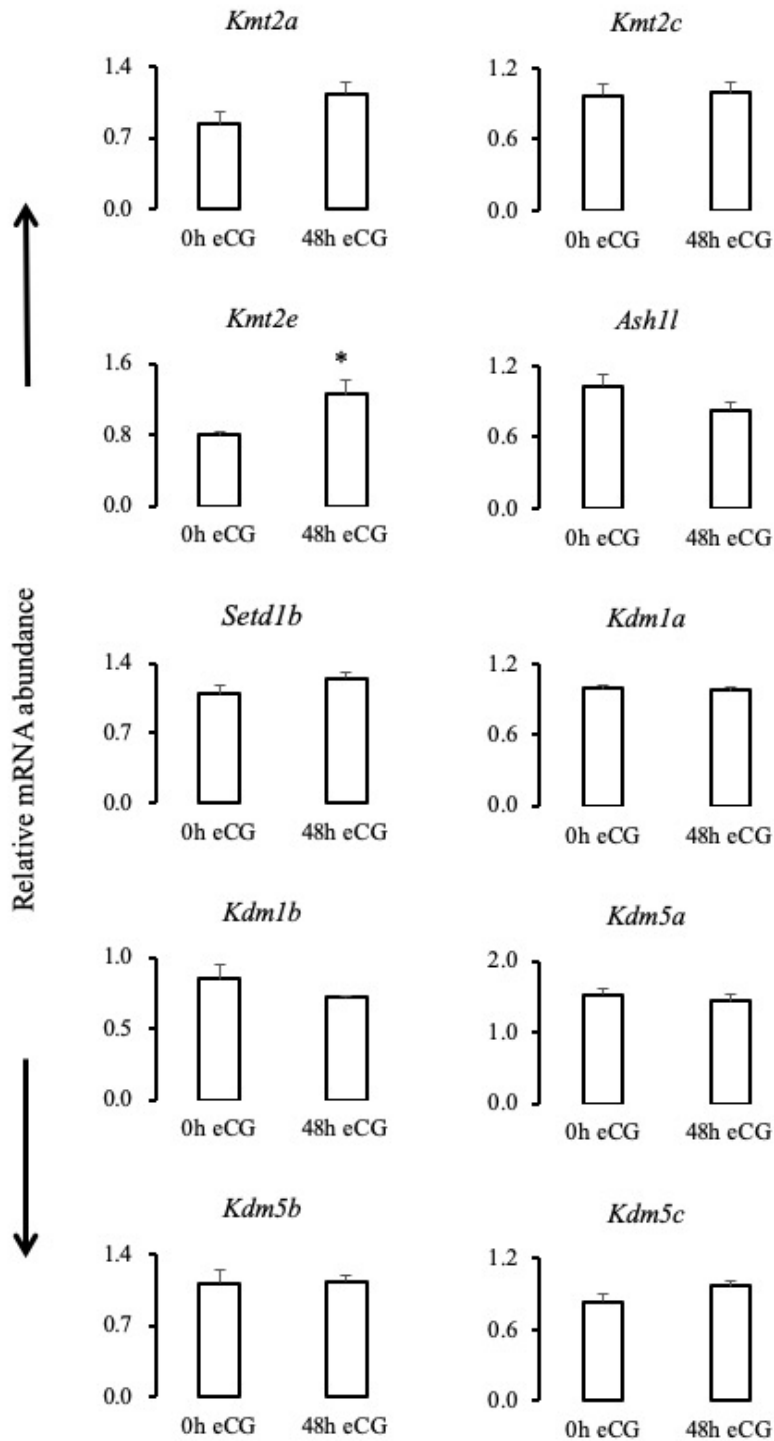
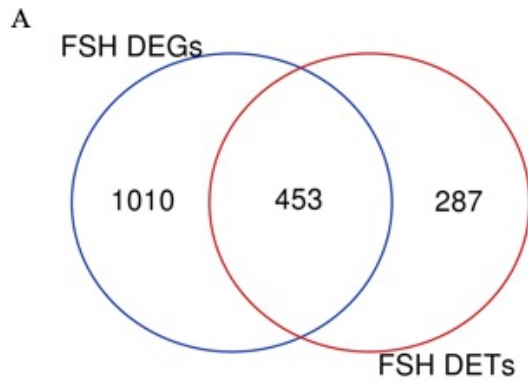


Figure 3.7.7 Interaction between DEGs and DETs. (A) Venn diagram indicating the interaction between the 1463 DEGs and 875 DETs in the RNA-Seq data. (B) 379 common FSH-induced genes and transcripts



B

379 Common FSH induced genes and transcripts

1110002J07Rik	Ahsg	Avpi1	Ces2g	Cyp26b1	Eng	Gale	Hlx	Lipg	Mvd	Parvb	Prkca	Scarb1	Suca	Tmem37	Wisp2
4930486L24Rik	Akr1b7	Bace2	Chat15	Cyp51	Enpp6	Galnt7	Hmgcr	Loxl1	Mvk	Pcdh1	Prlr	Scd1	Socs1	Tmem45a	Wnt10b
4930550L24Rik	Akr1c14	Bcl6b	Cish	Cypr1	Epdr1	Gda	Homer2	Loxl4	Myct1	Pcdh17	Procr	Sema3d	Sox30	Tmem86a	Xpupcp2
5330417C22Rik	Akr1c18	Bhmt	Cldn18	Dct2	Epha3	Gdnf	Hoxd11	Lrp11	Myo7a	Pcdh8	Ppfb2	Serpina3a	Sox8	Tmem88	Zpld1
6430548M08Rik	Alas2	Bpgm	Cldn5	Dcn	Ephb2	Ggt5	Hsd17b7	Lrrn1	Ncald	Peolce	Prr14	Serpina3n	Sparc	Tmprss13	
Ahcb1b	Aldh1a7	Bpifb6	Clic3	Dgat2	Ereg	Gimap4	Hsd3b1	Lrrn3	Ndufa4l2	Pesl9	Prss35	Serpini1	Spns2	Tmprss6	
Abcc2	Aldh3b1	Btn19	Cntn3	Dhcr24	Esam	Gimap5	Icam2	Lrrm1	Nos3	Pde11a	Psd	Sftp2	Sqle	Tnfrsf6	
Abcc9	Aldob	Bves	Col16a1	Dhcr7	Fads1	Gimap6	Ili1	Lsr	Nostrin	Pde4b	Ptgr	Sftp4	S8sia1	Tnfrsf9	
Acan	Alox12	Cabp1	Col18a1	Dll4	Fads2	Gja6	Igf3	Lss	Notch1	Pdgfr	Ptpnb	Sgk1	S8sia5	Tnxb	
Acat2	Angpt1	Caenala	Col6a5	Dmbt1	Fads3	Gldn	Igf3	Ltbp1	Notch3	Pdlim2	Qsox1	Shisa4	Star	Tom111	
Ace2	Ano3	Cadm3	Col8a1	Dock5	Fam162b	Gm2a	Inhba	Luzp2	Notch4	Pecam1	Rab27a	Shisa6	Sv2c	Trim10	
Acsf4	Apln	Calm1	Comp	Dpp1	Fam167b	Gpihbp1	Inhbb	Lypd6	Npb	Pex10	Ramp2	Slc12a7	Syp	Trpv4	
Acss2	Aplnr	Cur2	Corin	Dpp10	Fam198b	Gpr141	Inal6	Mapkapk3	Nppc	Pgr151	Rasip1	Slc12a8	Syt12	Tspan11	
Adam19	Apo1	Cd109	Cox4i2	Dcc2	Fbxl22	Gpr179	Isg20	Masp1	Nr0b2	Phospho1	Rem1	Slc16a2	Syt3	Tspan15	
Adam3	Apol6	Cd151	Cox7a1	Dusp1	Fdft1	Gpr39	Islr2	Me1	Nrap	Pik3c2g	Rhcg	Slc16a3	Tboxa2r	Tspo	
Adams1	Arap3	Cd34	Csrp2	Ebp	Fdps	Gprc6a	Igh3	Megf10	Nrcam	Pik3cg	Rhod	Slc24a4	Tgfb1	Tyh2	
Adhl	Areg	Cd47	Cst8	Ecm1	Fgfr4	Grem1	Ighb1	Megf9	Nsdhl	Pla1a	Rhox8	Slc26a7	Tie1	Ube2l6	
Adh7	Arhgef15	Cd55	Ctla2a	Eoscr	Flt1	Grem2	Jakmip3	Mfnp4	Nup62cl	Plin4	Rnd2	Slc29a4	Timp1	Ulbp1	
Adipor2	Asah2	Cd93	Ctrb1	Egfl7	Frdm5	Grim2b	Kcnj16	Mfng	Ogdhl	Plin5	Robo2	Slc47a1	Tinag1l	Unc13d	
Adora1	Aspn	Cdh13	Ctsh	Ehfn1	Fshr	Grp1	Kif26b	Mgat4c	Olfir1251	Pivap	Rsd2	Slc4a1	Tm4sf1	Usp5	
Adra1d	Astn1	Cdh15	Cxcl12	Elovl2	Fst	Gsg11	Lama4	Mgst2	Oxtr	Podnl1	Raux2	Slc5a4b	Tm7af2	Vcam1	
Adra2a	Atp12a	Cdh5	Cyp11a1	Elovl6	Fut8	Gata4	Ldh2	Mmel1	P2ry14	Ppp1r14a	S100a6	Slc6a12	Tmem141	Vcan	
Afap111	Atp1a3	Cela1	Cyp11b1	Emb	Gabra1	Gstm6	Ldlr	Mmm2	Pappa	Ppp1r3g	Sbn	Slc6a14	Tmem206	Vnn3	
Agnat2	Atp4b	Ces2a	Cyp19a1	Emcn	Gabbr2	Gstm7	Lgmn	Mrap	Paqr7	Pqlc3	Sc5d	Slc7a8	Tmem221	Vwa1	
Ahr	AU021092	Ces2e	Cyp21a1	Emp1	Gabbr3	Gypa	Lhcg	M64a4d	Paqr8	Prickle2	Scara5	Slitrk6	Tmem26	Wfs1	

3.8 TABLES

Table 3.8.1 Primer Sequences used in (A) ChIP-qPCR and (B) RT-qPCR

A

Gene name	Sequence (5' - 3')
Lhcgr-F	TCACACTCACAGACGTGATAAA
Lhcgr-R	CCTTAGCACAAACGGCTTTC
Cyp19a1-F	AGAAGAAGCACAGCTCACAAG
Cyp19a1-R	GGGAGCATCTAACACCCATTT
Nppc-F	AGAAGGGCTTGCCAAAGG
Nppc-R	GCGTCCGATGGTGTACTTA
Nrip2-F	CGCTGCTCTCGCCTATTATT
Nrip2-R	CCCTATAGCTTCTGCCTTTCTC

B

Gene symbol	Sequence (5' - 3')
mGapdh-F	AGGTCGGTGTGAACGGATTTG
mGapdh-R	TGTAGACCATGTAGTTGAGGTCA
mL19-F	ATGAGTATGCTCAGGCTACAGA
mL19-R	GCATTGGCGATTTTCATTGGTC
mB2m-F	TTCTGGTGCTTGTCTCACTGA
mB2m-R	CAGTATGTTCCGGCTCCCATT
mSdha-F	GGAACACTCCAAAAACAGACCT
mSdha-R	CCACCCTGGGTATTGAGTAGAA
mAhr-F	AGCCGGTGCAGAAAAACAGTAA
mAhr-R	AGGCGGTCTAACTCTGTGTTC
mFshr-F	GTGCTACCAAGCTTCGAGTCAT
mFshr-R	GTGCTACCAAGCTTCGAGTCAT
mNppc-F	CAGAAAAAGGGTGACAAGACTCC
mNppc-R	ATCCCAGACCGCTCATGGA
mNrip2-F	CAGCAGCGCCAACTCAAAC
mNrip2-R	GGCGTCTTTGGATCACACTGT
mKmt2a-F	ATGAGCAGTCTTAGGTTTTGGC
mKmt2a-R	CTCCCGCAGGTTTTTCGAG
mKmt2c-F	TGTCACAGTGTGGTCAATGTT
mKmt2c-R	GAGGGTCTAGGCAGTAGGTATG
mKmt2e-F	AGATGCACTTACAATCAAGAGGG
mKmt2e-R	AGGGCTGGTATAACCAATAGTCT
mSetd1b-F	TCCTCAAGCTCCGACAAGGAT
mSetd1b-R	CGTCGATGTCTGAATCAATCTGG
mAsh11-F	TTAGGATTGGGTTCTGATTCCGA
mAsh11-R	CGATTCCGCTTGCGAGGAT
mKdm1a-F	GTGGTGTTATGCTTTGACCGT
mKdm1a-R	GCTGCCAAAAATCCCTTTGAGA
mKdm1b-F	TACGAGTCCCAGAGTATTCGC
mKdm1b-R	GGATGAGGTTTCTCAAAGCCAG
mKdm5a-F	GCCCTTTGCGGAGAAAACG
mKdm5a-R	TGGACTCTAGGAGTGAAACGG
mKdm5b-F	CTGGGAAGAGTTCGCGGAC
mKdm5b-R	CGCGGGGTGAAATGAAGTTTAT
mKdm5c-F	GAGGCCAGACAAGAGTGAAA
mKdm5c-R	TTGGGAATCTTTAAGGATGAGCC

Supplementary Table 3.8.1 Quality control metrics

(A) Quality Control metrics for the RNA-Sequencing data (B) Quality Control metrics for the ChIP-Sequencing data

A

Sample		Number of Reads (Millions)	Aligned exactly one time (Millions)
0h eCG	1	21	19 (89.22%)
	2	26	23 (89.81%)
	3	25	22 (90.54%)
48h eCG	1	19	17 (88.48%)
	2	34	31 (90.75%)
	3	17	15 (87.94%)

B

Sample		Number of Reads (millions)	Overall Alignment rate	Aligned Exactly 1 time (millions)
0h eCG	1	34	97.21%	23 (68.04%)
	2	24	97.69%	17 (70.4%)
48h eCG	1	32	97.83%	24 (74.52%)
	2	34	97.95%	24 (69.39%)

Supplementary Table 3.8.2 FSH-regulated transcripts identified using the Kallisto-Sleuth pipeline

Gene ID	Gene Symbol	Transcript ID	b	pval	qval
ENSMUSG00000032937	Fshr	ENSMUST00000035701.4	1.07	7.67E-19	2.25E-16
ENSMUSG00000024107	Lhcgr	ENSMUST00000024916.5	2.75	1.58E-25	1.10E-22
ENSMUSG00000032274	Cyp19a1	ENSMUST00000034811.7	2.07	2.99E-04	4.80E-03
ENSMUSG00000032274	Cyp19a1	ENSMUST00000215736.1	1.44	5.74E-13	7.14E-11
ENSMUSG00000032323	Cyp11a1	ENSMUST00000034874.13	1.50	9.85E-12	9.69E-10
ENSMUSG00000019256	Ahr	ENSMUST00000116436.8	1.09	1.38E-25	9.81E-23
ENSMUSG00000028370	Pappa	ENSMUST00000084501.3	3.04	2.35E-42	5.97E-39
ENSMUSG00000032193	Ldlr	ENSMUST00000034713.8	1.31	1.04E-18	3.02E-16
ENSMUSG00000026241	Nppc	ENSMUST00000027449.5	1.23	2.29E-17	5.54E-15

3.9 BIBLIOGRAPHY

- Alhamdoosh, M., Law, C., Tian, L., Sheridan, J., Ng, M., & Ritchie, M. (2017). Easy and efficient ensemble gene set testing with EGSEA [version 1; referees: 1 approved, 3 approved with reservations]. *F1000Research*, 6(2010). doi:10.12688/f1000research.12544.1
- Andrews, S. (2014). *FastQC A Quality Control tool for High Throughput Sequence Data*.
- Bao, B., Garverick, H. A., Smith, G. W., Smith, M. F., Salfen, B. E., & Youngquist, R. S. (1997). Changes in messenger ribonucleic acid encoding luteinizing hormone receptor, cytochrome P450-side chain cleavage, and aromatase are associated with recruitment and selection of bovine ovarian follicles. *Biol Reprod*, 56(5), 1158-1168.
- Bianco, S., Brunelle, M., Jangal, M., Magnani, L., & Gevry, N. (2014). LRH-1 governs vital transcriptional programs in endocrine-sensitive and -resistant breast cancer cells. *Cancer Res*, 74(7), 2015-2025. doi:10.1158/0008-5472.can-13-2351
- Binder, A. K., Rodriguez, K. F., Hamilton, K. J., Stockton, P. S., Reed, C. E., & Korach, K. S. (2013). The absence of ER-beta results in altered gene expression in ovarian granulosa cells isolated from in vivo preovulatory follicles. *Endocrinology*, 154(6), 2174-2187. doi:10.1210/en.2012-2256
- Bolger, A. M., Lohse, M., & Usadel, B. (2014). Trimmomatic: A flexible trimmer for Illumina Sequence Data. *Bioinformatics*, btu170.
- Bray, N. L., Pimentel, H., Melsted, P., & Pachter, L. (2016). Near-optimal probabilistic RNA-seq quantification. *Nature Biotechnology*, 34, 525. doi:10.1038/nbt.3519
<https://www.nature.com/articles/nbt.3519#supplementary-information>
- Cao, F., Fang, Y., Tan, H. K., Goh, Y., Choy, J. Y. H., Koh, B. T. H., . . . Fullwood, M. J. (2017). Super-Enhancers and Broad H3K4me3 Domains Form Complex Gene Regulatory Circuits Involving Chromatin Interactions. *Sci Rep*, 7, 2186. doi:10.1038/s41598-017-02257-3
- Cheng, F., Liu, J., Zhou, S. H., Wang, X. N., Chew, J. F., & Deng, L. W. (2008). RNA interference against mixed lineage leukemia 5 resulted in cell cycle arrest. *Int J Biochem Cell Biol*, 40(11), 2472-2481. doi:10.1016/j.biocel.2008.04.012
- Dahl, J. A., Jung, I., Aanes, H., Greggains, G. D., Manaf, A., Lerdrup, M., . . . Klungland, A. (2016). Broad histone H3K4me3 domains in mouse oocytes modulate maternal-to-zygotic transition. *Nature*, 537(7621), 548-552. doi:10.1038/nature19360
<http://www.nature.com/nature/journal/v537/n7621/abs/nature19360.html#supplementary-information>
- Dobin, A., Davis, C. A., Schlesinger, F., Drenkow, J., Zaleski, C., Jha, S., . . . Gingeras, T. R. (2013). STAR: ultrafast universal RNA-seq aligner. *Bioinformatics*, 29(1), 15-21. doi:10.1093/bioinformatics/bts635
- Draincourt, M. A., Fry, R. C., Clarke, I. J., & Cahill, L. P. (1987). Follicular growth and regression during the 8 days after hypophysectomy in sheep. *J Reprod Fertil*, 79(2), 635-641.
- Duggavathi, R., & Murphy, B. D. (2009). Development. Ovulation signals. *Science*, 324(5929), 890-891. doi:10.1126/science.1174130
- Duggavathi, R., Volle, D., Matak, C., Antal, M., Messaddeq, N., Auwerx, J., . . . Schoonjans, K. (2008). Liver receptor homolog 1 is essential for ovulation. *Genes and Development*, 22, 1871-1876.
- Dupuis, L., Schuermann, Y., Cohen, T., Siddappa, D., Kalaiselvanraja, A., Pansera, M., . . . Duggavathi, R. (2014). Role of leptin receptors in granulosa cells during ovulation. *147(2)*, 221. doi:10.1530/rep-13-0356

- Evans, A. C. O., Ireland, J. L. H., Winn, M. E., Lonergan, P., Smith, G. W., Coussens, P. M., & Ireland, J. J. (2004). Identification of Genes Involved in Apoptosis and Dominant Follicle Development During Follicular Waves in Cattle. *Biology of reproduction*, *70*(5), 1475-1484. doi:10.1095/biolreprod.103.025114
- Fan, H.-Y., Gonzalez-Robayna, I., Hernandez-Gonzalez, I., Rudd, M. D., Liu, Z., Richards, J. S., & Zeleznik, A. J. (2009). FSH and FOXO1 Regulate Genes in the Sterol/Steroid and Lipid Biosynthetic Pathways in Granulosa Cells. *Molecular Endocrinology*, *23*(5), 649-661. doi:10.1210/me.2008-0412
- Fan, H. Y., Liu, Z., Shimada, M., Sterneck, E., Johnson, P. F., Hedrick, S. M., & Richards, J. S. (2009). MAPK3/1 (ERK1/2) in ovarian granulosa cells are essential for female fertility. *Science*, *324*(5929), 938-941. doi:10.1126/science.1171396
- Findlay, J. K., & Drummond, A. E. (1999). Regulation of the FSH Receptor in the Ovary. *Trends in Endocrinology & Metabolism*, *10*(5), 183-188. doi:10.1016/S1043-2760(98)00144-1
- Fortune, J. E., Rivera, G. M., Evans, A. C., & Turzillo, A. M. (2001). Differentiation of dominant versus subordinate follicles in cattle. *Biol Reprod*, *65*(3), 648-654.
- Gebremedhn, S., Salilew-Wondim, D., Ahmad, I., Sahadevan, S., Hossain, M. M., Hoelker, M., . . . Tesfaye, D. (2015). MicroRNA Expression Profile in Bovine Granulosa Cells of Preovulatory Dominant and Subordinate Follicles during the Late Follicular Phase of the Estrous Cycle. *PLoS One*, *10*(5), e0125912-e0125912. doi:10.1371/journal.pone.0125912
- George, J. W., Dille, E. A., & Heckert, L. L. (2011). Current concepts of follicle-stimulating hormone receptor gene regulation. *Biology of reproduction*, *84*(1), 7-17. doi:10.1095/biolreprod.110.085043
- Ginther, O. J., Beg, M. A., Donadeu, F. X., & Bergfelt, D. R. (2003). Mechanism of follicle deviation in monovular farm species. *Anim Reprod Sci*, *78*(3-4), 239-257.
- Ginther, O. J., Wiltbank, M. C., Fricke, P. M., Gibbons, J. R., & Kot, K. (1996). Selection of the Dominant Follicle in Cattle. *Biology of reproduction*, *55*(6), 1187-1194. doi:10.1095/biolreprod55.6.1187
- Greiner, E. F., Kirfel, J., Greschik, H., Huang, D., Becker, P., Kapfhammer, J. P., & Schule, R. (2000). Differential ligand-dependent protein-protein interactions between nuclear receptors and a neuronal-specific cofactor. *Proc Natl Acad Sci U S A*, *97*(13), 7160-7165. doi:10.1073/pnas.97.13.7160
- Gu, B., & Lee, M. G. (2013). Histone H3 lysine 4 methyltransferases and demethylases in self-renewal and differentiation of stem cells. *Cell & Bioscience*, *3*(1), 39. doi:10.1186/2045-3701-3-39
- Hamilton, M. J., Girke, T., & Martinez, E. (2018). Global isoform-specific transcript alterations and deregulated networks in clear cell renal cell carcinoma. *Oncotarget*, *9*(34), 23670-23680. doi:10.18632/oncotarget.25330
- Haring, M., Offermann, S., Danker, T., Horst, I., Peterhansel, C., & Stam, M. (2007). Chromatin immunoprecipitation: optimization, quantitative analysis and data normalization. *Plant Methods*, *3*, 11. doi:10.1186/1746-4811-3-11
- Hillier, S. G. (1994). Current concepts of the roles of follicle stimulating hormone and luteinizing hormone in folliculogenesis. *Human Reproduction*, *9*(2), 188-191. doi:10.1093/oxfordjournals.humrep.a138480
- Hisano, M., Erkek, S., Dessus-Babus, S., Ramos, L., Stadler, M. B., & Peters, A. H. (2013). Genome-wide chromatin analysis in mature mouse and human spermatozoa. *Nat Protoc*, *8*(12), 2449-2470. doi:10.1038/nprot.2013.145

- Hisano, M., Erkek, S., Dessus-Babus, S., Ramos, L., Stadler, M. B., & Peters, A. H. F. M. (2013). Genome-wide chromatin analysis in mature mouse and human spermatozoa. *Nat. Protocols*, 8(12), 2449-2470. doi:10.1038/nprot.2013.145
<http://www.nature.com/nprot/journal/v8/n12/abs/nprot.2013.145.html#supplementary-information>
- Hunzicker-Dunn, M., & Maizels, E. T. (2006). FSH signaling pathways in immature granulosa cells that regulate target gene expression: branching out from protein kinase A. *Cellular signalling*, 18(9), 1351-1359. doi:10.1016/j.cellsig.2006.02.011
- Ireland, J. J., & Roche, J. F. (1983). Growth and differentiation of large antral follicles after spontaneous luteolysis in heifers: changes in concentration of hormones in follicular fluid and specific binding of gonadotropins to follicles. *J Anim Sci*, 57(1), 157-167.
- Irving-Rodgers, H. F., Harland, M. L., Sullivan, T. R., & Rodgers, R. J. (2009). Studies of granulosa cell maturation in dominant and subordinate bovine follicles: novel extracellular matrix focimatrix is co-ordinately regulated with cholesterol side-chain cleavage CYP11A1. *137(5)*, 825. doi:10.1530/rep-08-0485
- Kumar, T. R., Wang, Y., Lu, N., & Matzuk, M. M. (1997). Follicle stimulating hormone is required for ovarian follicle maturation but not male fertility. *Nat Genet*, 15(2), 201-204. doi:10.1038/ng0297-201
- Kuo, M. H., & Allis, C. D. (1999). In vivo cross-linking and immunoprecipitation for studying dynamic Protein:DNA associations in a chromatin environment. *Methods*, 19(3), 425-433. doi:10.1006/meth.1999.0879
- Langmead, B., & Salzberg, S. L. (2012). Fast gapped-read alignment with Bowtie 2. *Nat Methods*, 9(4), 357-359. doi:10.1038/nmeth.1923
- Lee, L., Asada, H., Kizuka, F., Tamura, I., Maekawa, R., Taketani, T., . . . Sugino, N. (2013). Changes in Histone Modification and DNA Methylation of the StAR and Cyp19a1 Promoter Regions in Granulosa Cells Undergoing Luteinization during Ovulation In Rats. *Endocrinology*, 154(1), 458-470. doi:doi:10.1210/en.2012-1610
- Lei, Z. M., Mishra, S., Zou, W., Xu, B., Foltz, M., Li, X., & Rao, C. V. (2001). Targeted disruption of luteinizing hormone/human chorionic gonadotropin receptor gene. *Mol Endocrinol*, 15(1), 184-200. doi:10.1210/mend.15.1.0586
- Ma, X., Dong, Y., Matzuk, M. M., & Kumar, T. R. (2004). Targeted disruption of luteinizing hormone β -subunit leads to hypogonadism, defects in gonadal steroidogenesis, and infertility. *Proc Natl Acad Sci U S A*, 101(49), 17294-17299. doi:10.1073/pnas.0404743101
- Marmorstein, R., & Trievel, R. C. (2009). Histone modifying enzymes: structures, mechanisms, and specificities. *Biochim Biophys Acta*, 1789(1), 58-68. doi:10.1016/j.bbagr.2008.07.009
- Meinsohn, M. C., Morin, F., Bertolin, K., Duggavathi, R., Schoonjans, K., & Murphy, B. D. (2018). The Orphan Nuclear Receptor Liver Homolog Receptor-1 (Nr5a2) Regulates Ovarian Granulosa Cell Proliferation. *J Endocr Soc*, 2(1), 24-41. doi:10.1210/js.2017-00329
- Mihm, M., & Austin, E. J. (2002). The final stages of dominant follicle selection in cattle. *Domestic Animal Endocrinology*, 23(1), 155-166. doi:[https://doi.org/10.1016/S0739-7240\(02\)00153-4](https://doi.org/10.1016/S0739-7240(02)00153-4)

- Mozzetta, C., Boyarchuk, E., Pontis, J., & Ait-Si-Ali, S. (2015). Sound of silence: the properties and functions of repressive Lys methyltransferases. *Nat Rev Mol Cell Biol*, *16*(8), 499-513. doi:10.1038/nrm4029
- Nivet, A.-L., Dufort, I., Gilbert, I., & Sirard, M.-A. (2018). Short-term effect of FSH on gene expression in bovine granulosa cells *in vitro*. *Reproduction, Fertility and Development*, *30*(8), 1154-1160. doi:<https://doi.org/10.1071/RD17469>
- Pan, Q., Shai, O., Lee, L. J., Frey, B. J., & Blencowe, B. J. (2008). Deep surveying of alternative splicing complexity in the human transcriptome by high-throughput sequencing. *Nat Genet*, *40*(12), 1413-1415. doi:10.1038/ng.259
- Parakh, T. N., Hernandez, J. A., Grammer, J. C., Weck, J., Hunzicker-Dunn, M., Zeleznik, A. J., & Nilson, J. H. (2006). Follicle-stimulating hormone/cAMP regulation of aromatase gene expression requires β -catenin. *Proceedings of the National Academy of Sciences*, *103*(33), 12435-12440. doi:10.1073/pnas.0603006103
- Pimentel, H., Bray, N. L., Puente, S., Melsted, P., & Pachter, L. (2017). Differential analysis of RNA-seq incorporating quantification uncertainty. *Nat Methods*, *14*, 687. doi:10.1038/nmeth.4324
<https://www.nature.com/articles/nmeth.4324#supplementary-information>
- Raju, G. A. R., Chavan, R., Deenadayal, M., Gunasheela, D., Gutgutia, R., Haripriya, G., . . . Patki, A. S. (2013). Luteinizing hormone and follicle stimulating hormone synergy: A review of role in controlled ovarian hyper-stimulation. *Journal of human reproductive sciences*, *6*(4), 227-234. doi:10.4103/0974-1208.126285
- Richards, J. S. (1979). Hormonal Control of Ovarian Follicular Development: A 1978 Perspective. In R. O. Greep (Ed.), *Proceedings of the 1978 Laurentian Hormone Conference* (Vol. 35, pp. 343-373). Boston: Academic Press.
- Richards, J. S. (1994). Hormonal control of gene expression in the ovary. *Endocr Rev*, *15*(6), 725-751. doi:10.1210/edrv-15-6-725
- Richards, J. S. (2001). Perspective: The Ovarian Follicle—A Perspective in 2001*. *Endocrinology*, *142*(6), 2184-2193. doi:10.1210/endo.142.6.8223
- Robinson, J. T., Thorvaldsdóttir, H., Winckler, W., Guttman, M., Lander, E. S., Getz, G., & Mesirov, J. P. (2011). Integrative genomics viewer. *Nature Biotechnology*, *29*, 24. doi:10.1038/nbt.1754
<https://www.nature.com/articles/nbt.1754#supplementary-information>
- Santos-Rosa, H., Schneider, R., Bannister, A. J., Sherriff, J., Bernstein, B. E., Emre, N. C. T., . . . Kouzarides, T. (2002). Active genes are tri-methylated at K4 of histone H3. *Nature*, *419*(6905), 407-411. doi:http://www.nature.com/nature/journal/v419/n6905/supinfo/nature01080_S1.html
- Segers, I., Adriaenssens, T., Wathlet, S., & Smitz, J. (2012). Gene expression differences induced by equimolar low doses of LH or hCG in combination with FSH in cultured mouse antral follicles. *215*(2), 269. doi:10.1530/joe-12-0150
- Stocco, C. (2008). Aromatase expression in the ovary: hormonal and molecular regulation. *Steroids*, *73*(5), 473-487. doi:10.1016/j.steroids.2008.01.017
- Svotelis, A., Gevry, N., & Gaudreau, L. (2009). Chromatin immunoprecipitation in mammalian cells. *Methods Mol Biol*, *543*, 243-251. doi:10.1007/978-1-60327-015-1_16
- Teino, I., Matvere, A., Kuuse, S., Ingerpuu, S., Maimets, T., Kristjuhan, A., & Tiido, T. (2014). Transcriptional repression of the Ahr gene by LHCG signaling in preovulatory granulosa

- cells is controlled by chromatin accessibility. *Mol Cell Endocrinol*, 382(1), 292-301. doi:10.1016/j.mce.2013.10.011
- Verbraak, E. J. C., van 't Veld, E. M., Groot Koerkamp, M., Roelen, B. A. J., van Haefen, T., Stoorvogel, W., & Zijlstra, C. (2011). Identification of genes targeted by FSH and oocytes in porcine granulosa cells. *Theriogenology*, 75(2), 362-376. doi:<https://doi.org/10.1016/j.theriogenology.2010.09.008>
- Wen, Z., Pan, T., Yang, S., Liu, J., Tao, H., Zhao, Y., . . . Zhu, Y. (2017). Up-regulated NRIP2 in colorectal cancer initiating cells modulates the Wnt pathway by targeting ROR β . *Molecular cancer*, 16(1), 20-20. doi:10.1186/s12943-017-0590-2
- Wigglesworth, K., Eppig, J. J., Lee, K.-B., Emori, C., & Sugiura, K. (2015). Transcriptomic Diversification of Developing Cumulus and Mural Granulosa Cells in Mouse Ovarian Follicles1. *Biology of reproduction*, 92(1). doi:10.1095/biolreprod.114.121756
- Xia, J., Benner, M. J., & Hancock, R. E. W. (2014). NetworkAnalyst - integrative approaches for protein-protein interaction network analysis and visual exploration. *Nucleic Acids Research*, 42(W1), W167-W174. doi:10.1093/nar/gku443
- Xia, J., Gill, E. E., & Hancock, R. E. W. (2015). NetworkAnalyst for statistical, visual and network-based meta-analysis of gene expression data. *Nat Protoc*, 10, 823. doi:10.1038/nprot.2015.052
- Xia, J., Lyle, N. H., Mayer, M. L., Pena, O. M., & Hancock, R. E. (2013). INVEX--a web-based tool for integrative visualization of expression data. *Bioinformatics*, 29(24), 3232-3234. doi:10.1093/bioinformatics/btt562
- Xu, Z., Garverick, H. A., Smith, G. W., Smith, M. F., Hamilton, S. A., & Youngquist, R. S. (1995). Expression of follicle-stimulating hormone and luteinizing hormone receptor messenger ribonucleic acids in bovine follicles during the first follicular wave. *Biol Reprod*, 53(4), 951-957.
- Yu, G., Wang, L.-G., & He, Q.-Y. (2015). ChIPseeker: an R/Bioconductor package for ChIP peak annotation, comparison and visualization. *Bioinformatics*, 31(14), 2382-2383. doi:10.1093/bioinformatics/btv145
- Zhang, F. P., Poutanen, M., Wilbertz, J., & Huhtaniemi, I. (2001). Normal prenatal but arrested postnatal sexual development of luteinizing hormone receptor knockout (LuRKO) mice. *Mol Endocrinol*, 15(1), 172-183. doi:10.1210/mend.15.1.0582
- Zhang, X., Novera, W., Zhang, Y., & Deng, L. W. (2017). MLL5 (KMT2E): structure, function, and clinical relevance. *Cell Mol Life Sci*, 74(13), 2333-2344. doi:10.1007/s00018-017-2470-8
- Zhang, Y., Liu, T., Meyer, C. A., Eeckhoute, J., Johnson, D. S., Bernstein, B. E., . . . Liu, X. S. (2008). Model-based analysis of ChIP-Seq (MACS). *Genome biology*, 9(9), R137-R137. doi:10.1186/gb-2008-9-9-r137
- Zielak-Steciwo, A. E., & Evans, A. C. (2016). Genomic portrait of ovarian follicle growth regulation in cattle. *Reprod Biol*, 16(3), 197-202. doi:10.1016/j.repbio.2016.07.003
- Zubek, J., Stitzel, M. L., Ucar, D., & Plewczynski, D. M. (2016). Computational inference of H3K4me3 and H3K27ac domain length. *PeerJ*, 4, e1750. doi:10.7717/peerj.1750

CONNECTING STATEMENT 1

FSH induces follicular development in granulosa cells. Follicular development is the first step towards successful ovulation. In the first study, we identified previously known as well as novel FSH-regulated genes. We also looked at the H3K4me3 enrichment profile at the promoters of these genes and found a correlation between FSH regulated gene expression and the H3K4me3 profile at the promoter sites of some genes involved in follicular development such as *Cyp19a1* and *Lhcgr*. The next step is regulated by the LH surge that induces ovulation. In the next study, we investigated the role of ERK1/2 in the deposition of H3K4me3 at the promoter of LH-regulated genes using ChIP-Seq, RNA-Seq and pharmacological inhibition of ERK1/2.

CHAPTER 4

Manuscript in preparation for submission

LH surge-regulated trimethylation of lysine 4 of histone 3 drives gene expression in mouse granulosa cells via ERK1/2

Authors

Ejimedo Madogwe and Raj Duggavathi*

Affiliations

Department of Animal Science, McGill University, 21111, Lakeshore Road, Sainte-Anne-de-Bellevue, H9X 3V9.

Short title

LH and ERK1/2-regulated histone modification in granulosa cells

Correspondence

[*raj.duggavathi@mcgill.ca](mailto:raj.duggavathi@mcgill.ca); Department of Animal Science, McGill University, 21111, Lakeshore Road, Sainte-Anne-de-Bellevue, H9X 3V9

Conflict of interest statement

The authors have no conflicts of interest to declare

Key words (5)

Luteinizing hormone (LH), Granulosa cells, Ovulation, H3K4me3, ERK1/2

4.1 Abstract

The ERK1/2 signaling pathway, induced by the luteinizing hormone (LH) surge, is important for ovulation. Histone modifications such as trimethylation of lysine 4 of histone 3 (H3K4me3) are associated with gene transcription. Here, we hypothesized that LH regulates ovulatory genes through H3K4me3 and ERK1/2 modulates the H3K4me3 deposition at LH-regulated genes. We first analyzed the LH-regulated transcriptome in granulosa cells collected before (0h) or 4h after hCG treatment in superovulated immature mice. We then employed chromatin immunoprecipitation and sequencing to explore H3K4me3 enrichment prior to and 4h after hCG treatment. We found that there was an increase (from 66.2% to 82.6%) in the number of genes with H3K4me3 enrichment at the promoter region at 4h hCG. About a quarter (1198) of the LH-regulated genes, including *Pgr*, *Ptgs2*, *Star*, *Tnfaip6*, had differential enrichment of H3K4me3 at their promoters. Next, we analyzed the transcriptome profile of granulosa cells collected at 4h post-hCG from mice treated with vehicle or the MEK inhibitor PD0325901. Among the 2504 ERK1/2-dependent genes, 609 genes, including *Star*, *Pgr*, *Ptgs2*, *Sult1e1*, *Tnfaip6*, *Timp1* and *Cyp19a1*, were LH-regulated genes with differential H3K4me3 deposition. We were able to confirm these results using ChIP-qPCR analysis. In conclusion, these findings implicate ERK1/2 pathway in modulating H3K4me3 deposition on the LH-regulated ovulatory genes in granulosa cells.

4.2 Introduction

The process of ovulation, induced by the preovulatory LH surge, involves multiple processes including cumulus cell expansion, terminal differentiation of granulosa cells to luteal cells, oocyte meiotic resumption and follicle rupture (Duggavathi and Murphy, 2009, Richards et al., 2002b, Xu et al., 2011). Cumulus expansion involves secretion of hyaluronic acid by the cumulus cells of the ovulating follicle resulting in an increase in the space between the cells filled with extracellular matrix, a process that is vital for fertilization (Zhang et al., 2014, Brown et al., 2010). LH stimulates the expression of genes that are proposed to be involved in oocyte complex (COC) expansion such as *Ptgs2*, *Tnfrsf6*, *Has2*, *Ptx3* and *Pgr* (Wigglesworth et al., 2015, Fan et al., 2009b).

Luteinization is the process wherein granulosa cells terminally differentiate into luteal cells, which switch from estradiol producing cells to progesterone producing cells (Nimz et al., 2010, Richards, 1994). LH induces the expression of steroidogenic genes needed for progesterone production including *Star*, *Cyp11a1* and *Hsd3b1* (King and LaVoie, 2012). Depending on the species, LH also terminates estrogen synthesis in luteinizing cells by downregulating the expression of the estrogen synthesizing enzyme, *Cyp19a1* (Duffy et al, 2019) and by upregulating genes involved in estrogen metabolism such as *Sult1e1* (Duggavathi et al., 2008b). Follicle rupture and repair involves inflammatory-like processes that are regionally regulated within the ovulating follicle. High level mediators of inflammation include enzymes of prostaglandin E2 synthesis, angiogenic cytokines and chemotactic agents of immune cell trafficking. Of these, the genes involved in PGE2 synthesis and signaling are known to be directly induced by LH. Finally, follicular wall rupture and repair involves multiple extracellular matrix modifying enzymes such as matrix metalloproteinases (MMP and ADAMTS families) and their inhibitors (TIMP family),

which are expressed by granulosa and theca cells. However, with regards to genes involved in angiogenesis, immune cell trafficking and extracellular matrix modifying enzymes, it is not clear if LH regulates their expression directly or indirectly through other cytokines such as EGF-like growth factors; although, the LH surge is necessary for their expression.

LH induces several intracellular signaling pathways including the ERK1/2 signaling pathway. Both gene targeting and pharmacological inhibition models have been used to show that ERK1/2 plays a critical role in LH-induced gene expression in granulosa cells (Fan et al., 2009b, Schuermann et al., 2018, Siddappa et al., 2015). Transcription factors, *Cebpb* (Fan et al 2009) and *Egr1* (Siddappa 2015) have been shown to be ERK1/2 mediators in regulating LH-induced ovulatory genes. However, ERK1/2 is needed for the expression of these transcription factors themselves raising the question; *what are the transcriptional mechanisms by which activated ERK1/2 regulate expression of LH-induced genes?*

Therefore, we hypothesized that LH surge regulates the granulosa transcriptome through changes in trimethylation of lysine 4 of histone 3 (H3K4me3) at their promoters and that ERK1/2 signaling is required for LH-dependent changes in H3K4me3. Here, we have used chromatin immunoprecipitation, next-generation sequencing and bioinformatics tools along with pharmacological inhibition of ERK1/2 signaling to test these hypotheses in immature superovulated mice.

4.3 Materials and methods

4.3.1 Granulosa cell collection

Immature (post-natal 21-23 days) C57BL/6NCr1 female mice (Charles River) were housed in standard plastic rodent cages and maintained on a 12-h light and 12-h dark cycle with feed and water provided *ad libitum* (Rodent Diet from Harlan Teklad, Canada). All animal experiments were approved by the Animal Care and Use Committee of McGill University. Immature mice were injected intraperitoneally with 5 IU of eCG (Folligon, Merck) to stimulate follicular development. Forty-eight hours later, they were treated with a dose of 5 IU of hCG (Chorulon, Merck) to stimulate ovulation. In experiments testing the role of ERK1/2, eCG-stimulated mice were challenged with a dose of either vehicle (0.9% NaCl; Saline) or PD0325901 (a highly specific MEK inhibitor, Selleckchem) at 25µg/g body weight 30 minutes before hCG stimulation (Siddappa et al., 2015). Granulosa cells were collected at 0h and 4h timepoints relative to hCG stimulation as described in our previous studies (Duggavathi et al., 2008a, Dupuis et al., 2014). The authors acknowledge that LH surge-induced gene expression and histone modification would begin with the surge itself. However, we chose the 4h post-hCG timepoint to examine gene expression and histone modifications because it is the timepoint that is used by many studies to report LH-induced gene expression.

4.3.2 RNA purification and sequencing

Granulosa cells from one mouse yielded sufficient RNA for sequencing. RNA was purified from granulosa cells collected prior to (0 hCG) and 4h after hCG treatment (4h hCG Veh and 4h hCG PD) using the Direct-Zol RNA MiniPrep Isolation Kit (Zymo Research, Cedarlane Laboratories) as per the manufacturer's protocol. RNA was quantified using the Nanodrop 2000 spectrophotometer (Thermofisher Scientific). Samples were sent to the functional Genomics

platform (McGill University and Genome Quebec Innovation Centre) for library preparation using 250ng of RNA. Only RNA samples with an RNA integrity number (RIN) of 8 and above were used (N = 4 mice per group). The libraries were sequenced using the Illumina HiSeq 4000 chip with 100 base pair-ended sequencing. The RNA-Seq data will be available from the GEO data repository (submission in progress). RNA-Seq quality metrics are presented in Supplementary Table 1A. Upon confirmation of high-quality sequence data, we proceeded with bioinformatic analyses.

4.3.3 RNA-Seq data analysis

Sequenced reads were assessed for quality using FastQC; v 0.11.5 (Andrews, 2014). The STAR program, a splice aware aligner, was used for read alignment (Dobin et al., 2013) and uniquely mapped reads were 87-90 percent. The read counts were then uploaded to Network Analyst (Xia et al., 2015) for analysis of differential expression.

4.3.4 Chromatin Immunoprecipitation and sequencing

Since chromatin immunoprecipitation (ChIP) requires pooling of granulosa cells from multiple mice, we did not include ERK1/2 inhibited mice in the ChIP-seq experiment. For ChIP-seq, we collected granulosa cells 48h after eCG treatment but prior to hCG treatment (0h hCG) and 4h after hCG treatment (4h hCG). Chromatin immunoprecipitation was carried out using granulosa cells from four mice for each replicate (N = 2 replicates per timepoint). This protocol was adapted from previous reports (Haring et al., 2007, Hisano et al., 2013b, Kuo and Allis, 1999, Svtelis et al., 2009, Bianco et al., 2014b). Briefly, pelleted granulosa cells were crosslinked with 1% formaldehyde in PBS for 15 minutes at room temperature. Cells were lysed and sonicated (Q55 Sonicator, Fisher Scientific USA) to obtain chromatin fragments of 200-500bp. Ten percent of the sonicated chromatin was removed as input and 5% to evaluate sonication efficiency. The rest of

the chromatin was immunoprecipitated at 4° overnight with either H3K4me3 antibody (Abcam; ab8580) or Rabbit IgG (Abcam; ab171870). The next day, magnetic beads (Protein A Dynabeads; Life technologies) were added to the reaction and incubated with rotation at 4°C for 4 hours. DNA-protein complexes were eluted after washing with a low salt buffer, high salt buffer, LiCl buffer and three times with TE buffer and crosslinks were reversed by incubating overnight at 65° C. After treatment with RNase A and proteinase K, DNA was then purified using the Qiagen PCR Purification kit (Qiagen) and quantified using the Nanodrop 2000 spectrophotometer (Thermofisher Scientific). Samples were sent to the functional Genomics platform McGill University and Genome Quebec Innovation Centre for library preparation and sequencing using the Illumina HiSeq 2000 SR 50. The ChIP-Seq data will be available from the GEO data repository (submission in progress). ChIP-Seq quality metrics are presented in Supplementary Table 1B. Upon confirmation of high-quality sequence data, we proceeded with bioinformatic analyses.

4.3.5 ChIP-Seq data analysis

Sequenced reads were assessed for quality using FastQC; v 0.11.5 (Andrews, 2014) and adapters trimmed using Trimmomatic; v 0.36 (Bolger, 2014). Subsequently, sequences were mapped to the mouse genome (mm10) using Bowtie2; v 2.2.9 (Langmead and Salzberg, 2012) and peak calling was performed using MACS2; v 2.1.1 (Zhang et al., 2008) and a matrix of counts (enrichment) was obtained (Hisano et al., 2013b) that was then used to analyze differential enrichment of H3K4me3 using Network Analyst, a tool designed to enable statistical and visual analyses of gene expression data (Xia et al., 2015, Xia et al., 2013). Peaks were also annotated using ChIPseeker; v 1.18.0 (Yu et al., 2015) and peak data visualized using the integrative genomics viewer (IGV) (Robinson et al., 2011).

4.3.6 Pathway Analysis

EGSEA (Alhamdoosh et al., 2017) and Network Analyst (Xia et al., 2015) were used for Kyoto Encyclopedia of Genes and Genomes (KEGG) pathway analysis, as well as enrichment analysis of biological processes using the list of LH-regulated genes (DEGs; n = 4873) and ERK1/2-inhibited genes (DEGs; n=2504). This list was also uploaded and used for data analysis and interpretation using various functions in the Ingenuity pathway analysis (IPA; Ingenuity Systems Inc., Redwood City, CA) tool.

4.3.7 RT-PCR

For validation of RNA-Seq results and characterization of the histone modifying enzymes, total RNA was extracted (Qiagen microRNA kit; Qiagen, Toronto, CA) from granulosa cells collected at 0h hCG, 4h hCG Veh and 4h hCG PD (N = 4 biological replicates per timepoint). The purity and quantity of each sample was measured using the Nanodrop 2000 (ThermoScientific). We synthesized cDNA from 250ng of total RNA using the iScript cDNA Synthesis kit (BioRad) according to the manufacturer's instructions. All primers were purchased from Integrated DNA technologies (IDT, USA). We analyzed mRNA expression by RT-PCR using the CFX384 (BioRad). Expression data for each gene of interest was normalized to mean expression levels of four reference genes *Gapdh*, *B2m*, *L19* and *Sdha*. One-way analysis of variance (ANOVA) followed by Tukey's was used for statistical significance between timepoints. The sequences of the primer sets used are listed in (Table 1A).

4.3.8 ChIP-qPCR

Chromatin immunoprecipitation was carried out as previously described using H3K4me3 and IgG antibodies (Abcam). A 10% aliquot was taken from each sample after sonication but prior to incubation with the respective antibodies to serve as input for the qPCR reaction. Primers were

designed (IDT) to amplify a region within the H3K4me3 peaks identified in ChIP-seq data. The primer sequences for the promoters of *Pgr*, *Star*, *Ptgs2*, *Cyp19a1*, *Egr1*, *Sult1e1*, *Timp1*, *Tnfaip6*, *Nppc* and *Hsd17b1* are listed in (Table 1B). The purified DNA was then used in the qPCR reaction (ChIP-qPCR) using the CFX384 Real time PCR system (BioRad). Amplicon abundance in immunoprecipitated DNA was expressed as the percent relative to the input DNA. One-way analysis of variance (ANOVA) was used for statistical significance between groups.

4.4 Results

4.4.1 LH-regulated granulosa cell transcriptome

First, we sought to investigate the regulation of gene expression by LH at the level of the transcriptome. Sequenced reads were assessed for quality and then mapped to the mouse reference genome, mm10. Uniquely mapped reads accounted for 86-91% of the total reads (Supplementary Table 1A). Differential gene expression analysis using edgeR revealed 4873 differentially expressed genes (DEGs) between 0h hCG and 4h hCG. Of these, 2518 genes were upregulated, whereas 2355 genes were downregulated. Well known LH-induced genes among these DEGs were *Star*, *Pgr*, *Ptgs2* and *Tnfaip6*.

We used Ingenuity pathway analysis (IPA) to find functional categories among the 4873 LH-regulated genes using the core analysis function. Majority of these genes were located in the cytoplasm and plasma membrane, as well as the extracellular space and nucleus (Figure 1A). The top functional categories of these genes included enzymes, transcription regulators, ion channels/transporters, receptors, kinases, non-coding RNA and growth factors (Figure 1B). Among these, “enzymes” was the biggest class followed by ion channels/transporters. Some of the differentially regulated enzymes were *Cyp11a1*, *Cyp19a1* and *Hsd17b1*. Of interest were the genes among growth factors (*Areg* and *Vegfa*) and transcription regulators (*Cebpb* and *Foxo1*). The differentially regulated non-coding RNA genes included *Mir132* and *Snord37*.

4.4.2 Regulation of H3K4me3 in granulosa cells

We then evaluated LH-regulated changes in H3K4me3 in granulosa cells, because H3K4me3 is a histone modification that has been associated with active transcription in multiple cell types and species (Santos-Rosa et al., 2002, Lee et al., 2013, Zubek et al., 2016, Cao et al.,

2017, Dahl et al., 2016). Overall alignment rate of reads to the mouse reference genome (mm10) was above 97 percent for all samples (Supplementary Table 1B).

We first examined the nature of the genomic addresses with H3K4me3 peaks. At 0h hCG, about 66% of the peaks were located in the promoter region within 1 kilobase ($\leq 1\text{kb}$) from the transcription start site (TSS), the remainder being distributed over other gene features including the 3'-untranslated region (UTR), 5'-UTR, exons, introns and distal intergenic regions (Figure 2A). However, at 4h hCG, the number of peaks in the promoter region increased to about 82% (Figure 2A). Upon differential analysis using edgeR and applying a filter of absolute log fold change > 1 and FDR < 0.05 , we found that 8349 genes had differential H3K4me3 enrichment at 4h hCG compared to 0h hCG. Of these, 8255 genes, including *Ptgs2*, had increased H3K4me3 enrichment and 94 genes, including *Fshr*, had reduced H3K4me enrichment. Again, we used IPA to identify the functional categories and location of these genes. Top functional categories were enzymes, transcription regulators, ion channels/transporters, receptors, kinases, non-coding RNA and growth factors and the genes were located in the plasma membrane, cytoplasm, extracellular space and nucleus (Figure 2B).

4.4.3 Relationship between LH-regulated H3K4me3 enrichment and transcriptome

We explored if there were any changes in H3K4me3 enrichment associated with the genes that were differentially expressed in response to hCG treatment. Among the 4873 differentially expressed genes in RNA-Seq dataset and 8349 genes with differential H3K4me3 enrichment in ChIP-Seq dataset, 1198 genes were common to both datasets (Figure 3). Of these, 768 genes showed higher mRNA levels as well as higher H3K4me3 deposition including *Ptgs2*, *Pgr*, and *Star* (Figure 4A); while 75 genes that showed lower mRNA abundance as well as a lower H3K4me3 enrichment including *Nppc*, *Inhbb*, and *Hsd17b1* (Figure 4B). Conversely, 354 genes

showed lower mRNA levels despite elevated H3K4me3 enrichment including *Cyp19a1* (Figure 4C). Only one gene, *2810055G20Rik* showed higher mRNA levels with lower H3K4me3 enrichment. Nonetheless, 3675 genes showed an increase/decrease in gene expression but did not show differential H3K4me3 enrichment including *Nrip1* and 7151 genes showed differential H3K4me3 enrichment but no differential gene expression including *Esr2* (Figure 4C).

4.4.4 Effect of ERK1/2 inhibition on LH-regulated transcriptome

In order to test the role of ERK1/2 in LH-regulated histone modification, we first sought to profile ERK1/2-regulated genes using RNA-seq analysis. There were 2504 DEGs between granulosa cells from 4h hCG Veh and 4h hCG PD mice ($\text{abs}[\log\text{FC}] > 1$ and $\text{FDR} < 0.05$). Of these, 1129 genes were upregulated, whereas 1375 genes were downregulated. Well known ERK1/2-regulated genes among these DEGs were *Star*, *Pgr*, *Ptgs2*, *Cyp19a1* and *Tnfrsf10b*.

Functional categories identified by IPA included enzymes as the biggest class, followed by ion channels/transporters (*Cacna1a* and *Kcna4*), receptors (*Oxtr* and *Tshr*), transcription regulators (*Cited4* and *Fosl1*), kinases (*Fgr* and *Cdkn1a*), growth factors (*Epgn* and *Inhbb*), noncoding RNA (*Mir132* and *Snora23*), nuclear receptors (*Pgr* and *Nro2*) and translation regulators (*Eif4e* and *Celf4*) (Figure 5A). These genes were located in the cytoplasm (*Cyp19a1* and *Sult1e1*), plasma membrane (*Fshr* and *Npr1*), nucleus (*Pgr* and *Nupr1*) and extracellular space (*Il6* and *Timp1*) (Figure 5B).

4.4.5 Role of ERK1/2 signaling in LH-regulated cellular pathways

Next, we used datasets of LH-regulated DEGs and ERK1/2-regulated DEGs to uncover the role of ERK1/2 signaling at the level of cellular pathways. For this, we used EGSEA and IPA to identify KEGG pathways differentially regulated by hCG treatment (LH DEGs) and altered by ERK1/2 inhibition (ERK1/2 DEGs). The common KEGG pathways identified, using EGSEA, in

both datasets were TNF signaling pathway, MAPK signaling pathway, Transcriptional misregulation in cancer, VEGF signaling pathway and Chemokine signaling pathway (AdjP < 0.05). These pathways were enriched among LH DEGs but downregulated among ERK1/2 DEGs (Table 2). The top molecular and cellular functions in the LH DEGs, analyzed by IPA, were cellular movement, cellular growth and proliferation, cellular function and maintenance, cellular development and cellular assembly and organization (Supplementary Table 2A) ($p < 0.05$) all with a predicted increase. Among ERK1/2 DEGs, all these molecular and cellular functions were still among the top functions, but, with a predicted decrease. The top physiological functions among LH DEGs were tissue morphology, hematological system development and function, immune cell trafficking, organismal development and lymphoid tissue structure and development (Supplementary Table 2B) ($p < 0.05$). Similar to the molecular and cellular functions, these physiological functions also showed a predicted increase among LH DEGs and a predicted decrease among ERK1/2 DEGs.

The top upstream regulators predicted to be activated among the LH DEGs were lipopolysaccharide (LPS) with 636 target genes including *Areg*, *Ereg*, *Tnfrsf10b* and *Ptx3*. Other upstream regulators among LH DEGs were TNF (622 target genes), CG (194 target genes), TGF β 1 (600 target genes), STAT3 (223 target genes) and EGF (196 target genes), all of which were predicted to be activated. All these pathways showed a predicted inhibition among ERK1/2 DEGs (Supplementary Table 3). Further, U0126 and PD98059 (known ERK1/2 inhibitors) were identified as activated upstream regulators among ERK1/2 DEGs.

4.4.6 Relationship between LH-regulated ERK1/2-dependent genes and H3K4me3

Finally, to uncover the role of ERK1/2 in H3K4me3 deposition onto LH-induced genes we analyzed association between ERK1/2-regulated genes (2504 DEGs) with LH-regulated genes that

showed differential gene expression and associated H3K4me3 enrichment (1198 genes common to LH-regulated ChIP- and RNA- Seq datasets). This led to the discovery of 609 ERK1/2-dependent genes with changes in gene expression and H3K4me3 enrichment (*Star*, *Pgr*, *Ptgs2*, *Sult1e1*, *Tnfaip6*, *Btc*, *Hsd17b1*, *Fshr*, *Inhbb*, *Foxl2*, *Fosl1*, *Timp1*, *Runx2*, *Has1*, *Cited4*, *Nupr1*, *Nppc* and *Epgn*) (Figure 6).

The top PANTHER pathways for these 609 genes were Inflammation mediated by chemokine and cytokine signaling pathways, followed by Gonadotropin releasing hormone receptor pathway, integrin signaling pathway, interleukin signaling pathway and CCKR signaling. The top protein classes were signaling molecules, receptors, hydrolases, enzyme modulators and defense/immunity proteins (Table 3).

4.4.7 Confirmation of sequencing data using qPCR and ChIP-qPCR

We then undertook a targeted-gene approach to confirm the role of ERK1/2 in H3K4me3 deposition at the promoters of LH-regulated genes using qPCR and ChIP-qPCR, respectively. Using qPCR, we were able to show that there was higher mRNA abundance of *Pgr*, *Star*, *Ptgs2*, *Sult1e1*, *Timp1*, and *Tnfaip6* at 4h hCG Veh compared to 0h hCG (Figure 7A). The transcript abundance of these genes in 4h hCG PD group was significantly lower and was similar to the amounts seen in 0h hCG group ($P > 0.05$; Figure 7A). Similarly, we found lower mRNA abundance of *Cyp19a1*, *Hsd17b1* and *Nppc* at 4h hCG Veh compared to 0h hCG. For *Cyp19a1* and *Hsd17b1*, transcript abundance was significantly higher at 4h hCG PD compared to 4h hCG Veh ($p < 0.05$; Figure 7B).

Using ChIP-qPCR, we found higher H3K4me3 enrichment at the promoter regions of *Pgr*, *Star*, *Ptgs2*, *Sult1e1*, *Timp1*, and *Tnfaip6* ($p < 0.05$) at 4h hCG compared to 0h hCG ($p < 0.05$; Figure 7A). However, in 4h hCG PD granulosa cells, H3K4me3 enrichment was lower at the

promoter region of these genes ($p < 0.05$; Figure 7A). These higher and lower levels of H3K4me3 deposition at the promoter regions were similar to higher and lower mRNA levels for these genes. On the other hand, enrichment levels significantly increased between 4h hCG Veh and 4h hCG PD for *Cyp19a1* and *Hsd17b1*, two genes that are known to be downregulated by the LH surge ($p < 0.05$; Figure 7B).

4.4.8 Expression of H3K4me3 methylation and demethylation enzymes

We examined the genes coding for histone methyltransferases and demethylases in the RNA-Seq data and found that hCG treatment resulted in a 2-fold increase in the gene expression of demethylases, Kdm1a (*Lsd1*) and Kdm1b (*Lsd2*) (FDR $< 0.05\%$). The other methyltransferases – Kmt2a (*Mll1*), Kmt2c (*Mll3*), Kmt2e (*Mll5*) Ash11 (*Kmt2h*) and Setd1b (*Kmt2g*), or demethylases – Kdm5a (*Jarid1a*), Kdm5b (*Jarid1b*) and Kdm5c (*Jarid1c*) did not appear to be regulated by hCG treatment. Looking at H3K4me3 enrichment, none of the genes were found to have differential enrichment in the ChIP-Seq data. However, we found that the promoters of all these genes, except *Ash11*, did have H3K4me3 deposition.

We looked at the impact of ERK1/2 on these enzymes and found that Kdm1a (*Lsd1*) and Kdm1b (*Lsd2*) were ERK1/2-dependent as the expression of both genes was decreased 2-fold in granulosa cells of PD0325901-treated compared to vehicle-treated mice (FDR $< 0.05\%$). The other genes did not appear to be differentially regulated.

Confirmation of these genes via qPCR revealed that none of the methyltransferases showed a significant difference in mRNA abundance ($p > 0.05$; Figure 8A). For the demethylases, only *Kdm1a* and *Kdm5b* showed lower mRNA abundance in 4h hCG PD compared to 4h hCG Veh in granulosa cells ($p < 0.05$; Figure 8B) and there was no difference in mRNA levels of *Kdm1b* between vehicle- and PD0325901-treated granulosa cells.

4.5 Discussion

Initially thought to be regulated by a simple mechanism, ovulation has been shown to be a more complex process. Technological advancements have enabled a more accurate determination of the number (and function) of LH-regulated genes over the years (Espey and Richards, 2002, Xu et al., 2011, Liu et al., 2017, McRae et al., 2005). Sequencing of entire genomes as well as next generation sequencing have made vast contributions to our current body of knowledge.

Our RNA-Seq data revealed 4873 LH-regulated DEGs with 2518 upregulated and 2355 downregulated. A previous study found 563 LH-regulated DEGs, however, this study used a 4-fold change to classify DEGs (Fan et al., 2009b) in contrast to the 2-fold (1-log-fold) cut off used in this study. Our confidence in using the lower cut-off was based on the use of four biological replicates. Nonetheless, the top LH-regulated DEGs in both of these mouse studies were similar including well-known LH-regulated genes, *Star*, *Pgr*, *Ptgs2*, *Cyp19a1* and *Tnfaip6*.

LH induced genes such as progesterone receptor (*Pgr*) which is required for follicular rupture. We confirmed these via ChIP-Seq and RT-PCR. *Pgr*, a transcription factor and nuclear receptor, is required for ovulation (Dinh et al., 2019). Lack of *Pgr* expression leads to anovulation with trapped oocytes in mice (Lydon et al., 1995, Robker et al., 2000a) and this holds true for other species including rhesus monkeys and humans (Robker et al., 2018). *Pgr* mediates the expression of several downstream targets such as *Adamts1*, *Cxcr4* and *Edn2* (Palanisamy et al., 2006, Robker et al., 2000a, Choi et al., 2017) and hypoxia-inducible factors (*Hif1A*, *Hif1b* and *Hif2a*) (Kim et al., 2009). 454 genes were found to have altered regulation in *Pgr*-null mice, with 310 showing an increase and 114 showing a decrease in *Pgr* null mice compared to WT (fold change 1.5) (Kim et al., 2009). This study from Kim *et al.* (2009) used a microarray and looked at 0h hCG and 11h hCG.

Ovulation has been likened to an inflammatory reaction due to the similarities with injury-related inflammation (Espey, 1980, Duffy et al., 2019, Richards et al., 2002b). The LH surge induces genes associated with the inflammatory response. Progesterone and prostaglandins mediate this inflammatory response (Mo et al., 2006). LH also induces angiogenesis and extensive tissue remodeling (Duffy et al., 2019). In line with these observations, we found enrichment of functions associated with cellular movement, growth, organization and assembly among LH-regulated genes. Vascular endothelial growth factor (Vegf) signaling was one of the enriched pathways among LH-regulated genes. Indeed, Vegf has been reported to be induced by the LH surge and required for events surrounding tissue remodeling and follicular rupture [vascular permeability] (Redmer and Reynolds, 1996, Hazzard et al., 2000, Koos, 1995, Bianco et al., 2019, Schuermann et al., 2018). In line with this, chemokine signaling was also one of the top enriched pathways among LH-regulated genes including chemokine genes such as *Ccl2*, *Csf1*, *Cxcl1* and *Cxcl10*, along with the chemokine receptor, *Cxcr4*. The chemokine receptor, *Cxcr4*, reportedly plays a role in the ovulatory process and has been found to be upregulated in granulosa cells in women (Choi et al., 2017), equine and bovine (Sayasith and Sirois, 2014) and mice (Kim et al., 2009). The endothelins, *Edn1* and *Edn2*, were also among upregulated DEGs. It has been reported that *Edn2* is required for follicular rupture and is also involved in oocyte release (Cacioppo et al., 2017, Palanisamy et al., 2006, Ko et al., 2006).

Histone modifications and histone modifying enzymes regulate transcription by altering chromatin accessibility (Wu, 1997, Wozniak and Strahl, 2014). Previous studies have shown increases in chromatin accessibility post LH surge which have been proposed to make the promoter more amenable to binding of regulatory elements, thereby promoting transcription (Bianco et al., 2019). Our ChIP-Seq analysis revealed an increase in the percent of genes with H3K4me3 peaks

from 66.2% to 82.6% at the ≤ 1 kb promoter region suggesting that overall, the LH surge initiates events that favor the recruitment of regulatory elements that subsequently result in increased H3K4me3 deposition. We also identified 8349 genes with differential H3K4me3 enrichment, about 99% of which had higher H3K4me3 deposition in response to hCG treatment. This observation further buttresses the increased chromatin accessibility by the preovulatory LH surge. H3K4me3 was previously shown to increase at the promoter of *Star* and *Cyp19a1* post LH in rats (Lee et al., 2013), a finding we also observed in this study.

Intriguingly, of the 12024 genes with differential abundance of either mRNA or H3K4me3 enrichment, 1198 genes had both features differentially regulated by hCG treatment. A large proportion of these genes (843 genes) had similar differential abundance of mRNA and H3K4me3 demonstrating that increased or decreased expression of these genes was associated with concomitant increased or decreased H3K4me3 deposition at their promoters. The observation that there were many other genes that did not have both features regulated could be due to analysis at one time-point (4h post-hCG). Analyses at additional time-points during the 12-14h ovulation period may be necessary to correlate mRNA abundance with the level of H3K4me3 deposition. These findings may also suggest that for some genes, mechanisms besides H3K4me3 enrichment may be required for transcription.

In the present study, we used the drug PD0325901, a highly specific MEK1/2 inhibitor, to prevent the activation of hCG-induced ERK1/2 (Tee et al., 2014, Siddappa et al., 2015, Schuermann et al., 2018) and identified 2504 ERK1/2-regulated genes. Our previous studies have shown abrogation of ovulation when LH-induced ERK1/2 signaling was thwarted in mice (Siddappa et al., 2015) and cows (Schuermann et al., 2018). Transcriptome analyses in bovine (Schuermann et al., 2018) and mouse (Fan et al., 2009b) studies revealed 285 and 433 ERK1/2-

dependent genes, respectively. These studies reported *Pgr*, *Ptgs2*, *Star*, *Tnfaip6*, *Btc* and *Sult1e1* as LH-induced genes (Fan et al., 2009b, Schuermann et al., 2018) all of which were found to be altered in PD0325901-treated granulosa cells in our study. The top LH-enriched pathways; TNF signaling, VEGF signaling and MAPK signaling were decreased by ERK1/2 inhibition. Furthermore, the top cellular and molecular functions enriched by the LH surge including cellular movement, assembly and organization were also downregulated in response to ERK1/2 inhibition. Taken together, these studies demonstrate that LH-induced immediate early ERK1/2 signals are upstream of cellular and extracellular processes necessary for ovulation (Wigglesworth et al., 2015, Fan et al., 2009b, Robker et al., 2018).

We sought to understand the relationship between H3K4me3 enrichment and ERK1/2-regulated genes. We found that 609 genes that were regulated by hCG through H3K4me3 deposition were also ERK1/2-dependent genes. This suggests that H3K4me3 enrichment at these genes may require ERK1/2 signaling. We confirmed these findings using ChIP-qPCR for important LH-regulated genes known to be involved in ovulation. In a study using human melanoma cell lines, genetic and pharmacological inhibition of ERK1/2 resulted in lower H3K4me3 enrichment at the promoter of the telomerase reverse transcriptase (*TERT*) gene decreasing in its expression (Li et al., 2016). ERK1/2 has also been shown to regulate the deposition of the polycomb repressive complex 2 (PRC2) complex, which is an enzyme complex known to catalyze the transcriptional repression marker, H3K27me2/3 at the promoter of developmental genes in mouse embryonic stem cells (Tee et al., 2014). These studies demonstrate that ERK1/2 play a significant role in histone methylation thereby regulating gene expression. Thus, the data from our study demonstrate that ERK1/2 is necessary for LH-induced deposition of H3K4me3 at the promoters of ovulatory genes including *Pgr*, *Star*, *Ptgs2* among others.

There are several histone methyltransferases; however, the mechanisms of regulation are still poorly understood due to a combination of substrate specificity, cofactors and coactivators which differ between enzymes (Marmorstein and Trievel, 2009). We did not observe any significant changes in the levels of the H3K4 methyltransferases or demethylases. The fact that our ChIP-seq data showed no modulation of H3K4me3 at the promoter sites of histone modifying enzymes suggests that these enzymes may not be regulated at the transcriptional level. It is possible that recruitment of histone methylation enzymes at promoter sites may be regulated by the initial recruitment of phosphorylated ERK1/2 at the promoters of their target genes, as shown in mouse embryonic stem cells (Tee et al., 2014).

In conclusion, the data from our study suggest that the preovulatory LH surge regulates the ovulatory gene expression program, at least in part, through regulation of trimethylation of H3K4 at their promoters or other regions of the target genes. Most importantly, these findings implicate the ERK1/2 pathway in modulating H3K4me3 deposition on the LH-regulated ovulatory genes in granulosa cells. With the analyses used in this study, the mechanisms by which ERK1/2 regulate H3K4me3 deposition was not elucidated. Nonetheless, this study serves as the basis for a ChIP-seq study in ERK1/2 inhibited granulosa cells to identify global genomic regions where ERK1/2 directs LH-induced H3K4me3 modification.

4.6 Funding, Contributions and Acknowledgements

Funding

This work was supported by the National Science Research Council grant (NSERC RGPIN-2019-06667 - RD; NSERC-CREATE and Graduate Excellence Fellowship – EM

Author contribution

E.M. contributed to ideas, performed experiments, analyzed data, prepared figures and wrote manuscript; R.D. conceived the study, designed experiments, analyzed data, and edited the manuscript.

Acknowledgements

The authors would like to thank Dr Vilceu Bordignon, Dr Jean-Benoit Charron and Dr Sarah Kimmins for use of facilities. In addition, we would like to thank Deepak Tanwar and Milena Taibi for their invaluable assistance.

4.7 Figures

Figure 4.7.1 Functional categorization of 4873 LH DEGs using IPA (A) Location of genes; (B) Type of Genes.

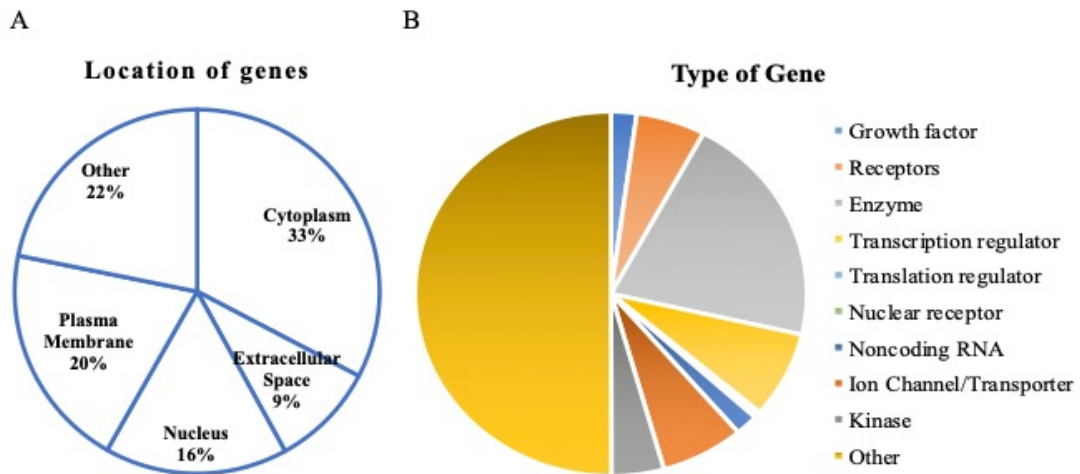
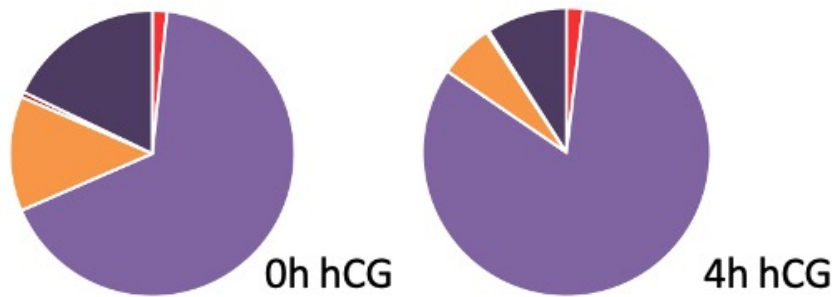


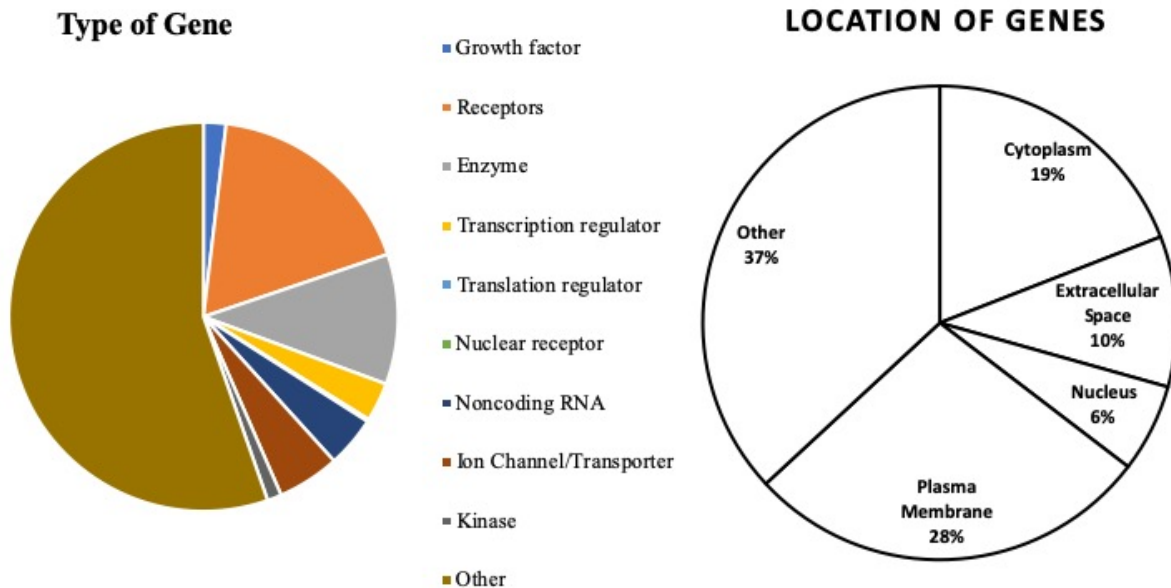
Figure 4.7.2 Genomic features and functional categorization (A) Genomic features of H3K4me3 peaks identified by Macs2 and annotated with ChIPseeker; (B) Functional categorization of 8349 genes with differential H3K4me3 enrichment using IPA.

A

	Prom (1-3kb)	Prom ≤ 1kb	Gene body	Downstream	Intergenic
0h hCG	1.7%	66.2%	12.9%	0.6%	17.7%
4h hCG	1.9%	82.6%	6.1%	0.3%	9.1%

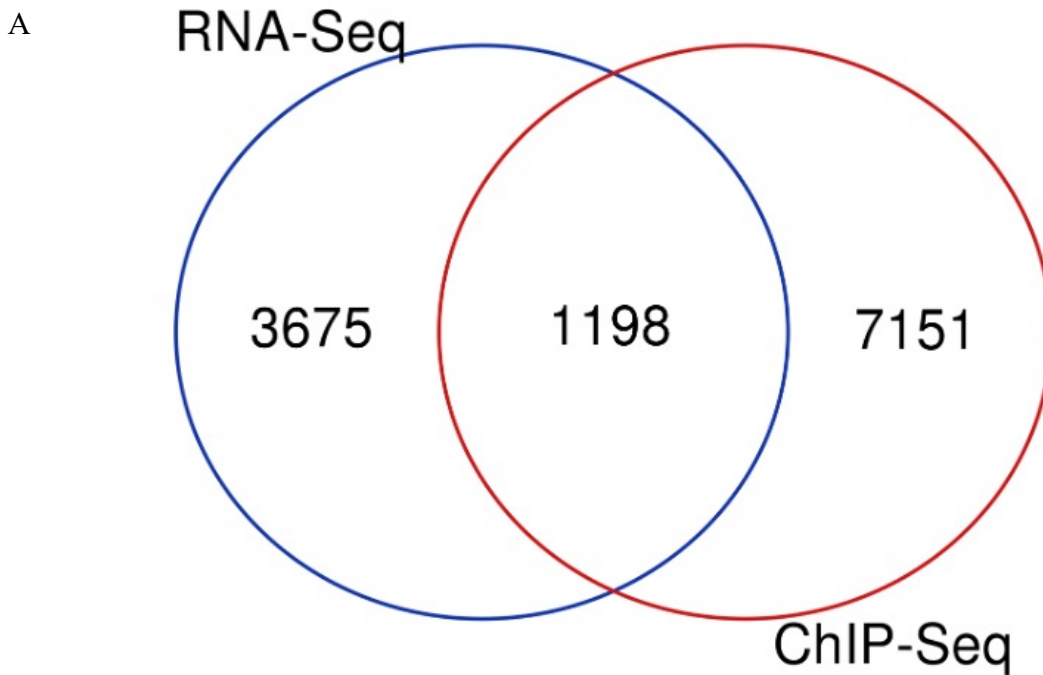


B



4.7.3 Interaction of ChIP- and RNA-Seq regulated genes

(A) Venn diagram showing the interaction of the 4873 DEGs with the 8349 genes with differential H3K4me3 enrichment; (B) Number of genes in each category



B

LH RNA Seq	LH H3K4me3	Number of Genes
Up	Up	768
Down	Up	354
Down	Down	75
Up	Down	1
Up/Down	Not regulated	3675
Not regulated	Up/Down	7151

Figure 4.7.4 Representative IGV images showing genes (A) Upregulated in RNA-Seq and ChIP-Seq (B) Downregulated in RNA-Seq and ChIP-Seq (C) Other categories

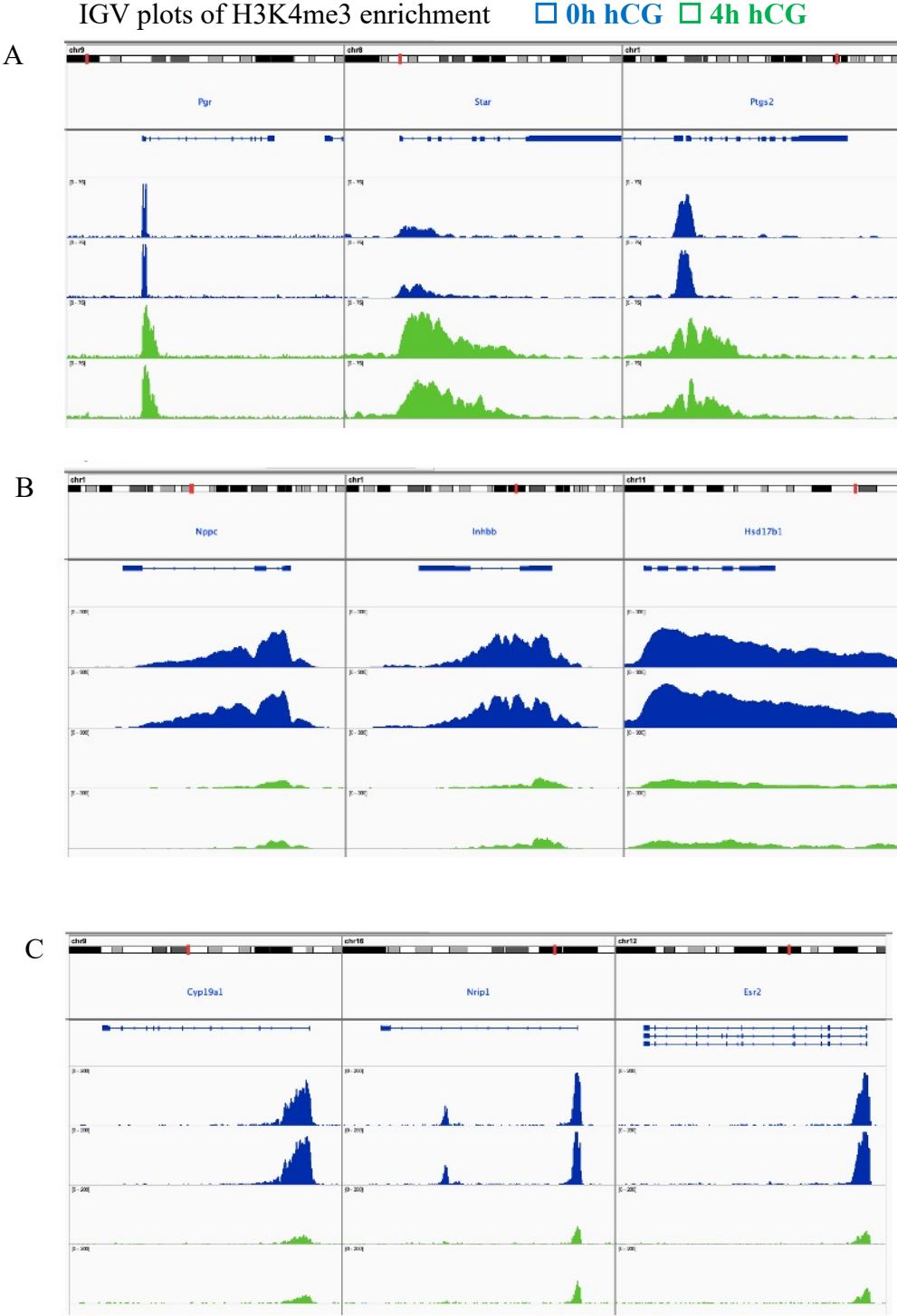


Figure 4.7.5 Functional categorization of 2504 ERK1/2-regulated genes using IPA

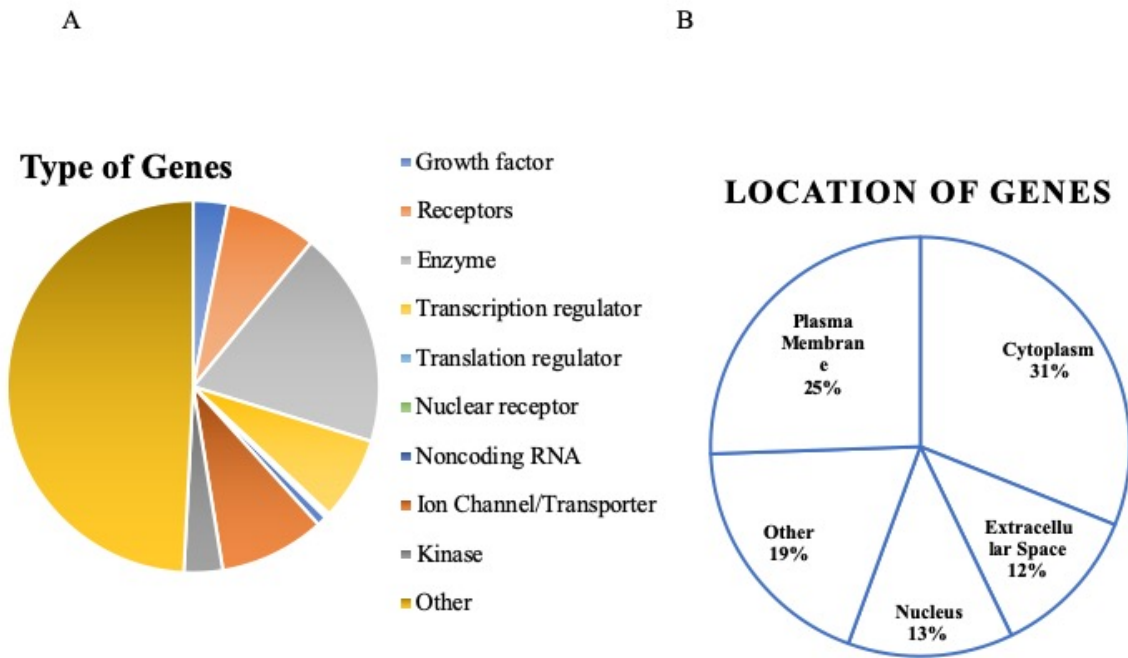


Figure 4.7.6 Interaction of ChIP- and RNA-Seq regulated genes with ERK1/2 regulated genes

Interaction between 1198 genes common to both LH RNA- and ChIP-Seq and 2504 ERK1/2 regulated genes. All genes meet the criteria of $\text{abs}[\log\text{FC}] > 1$ and $\text{FDR} < 0.05$

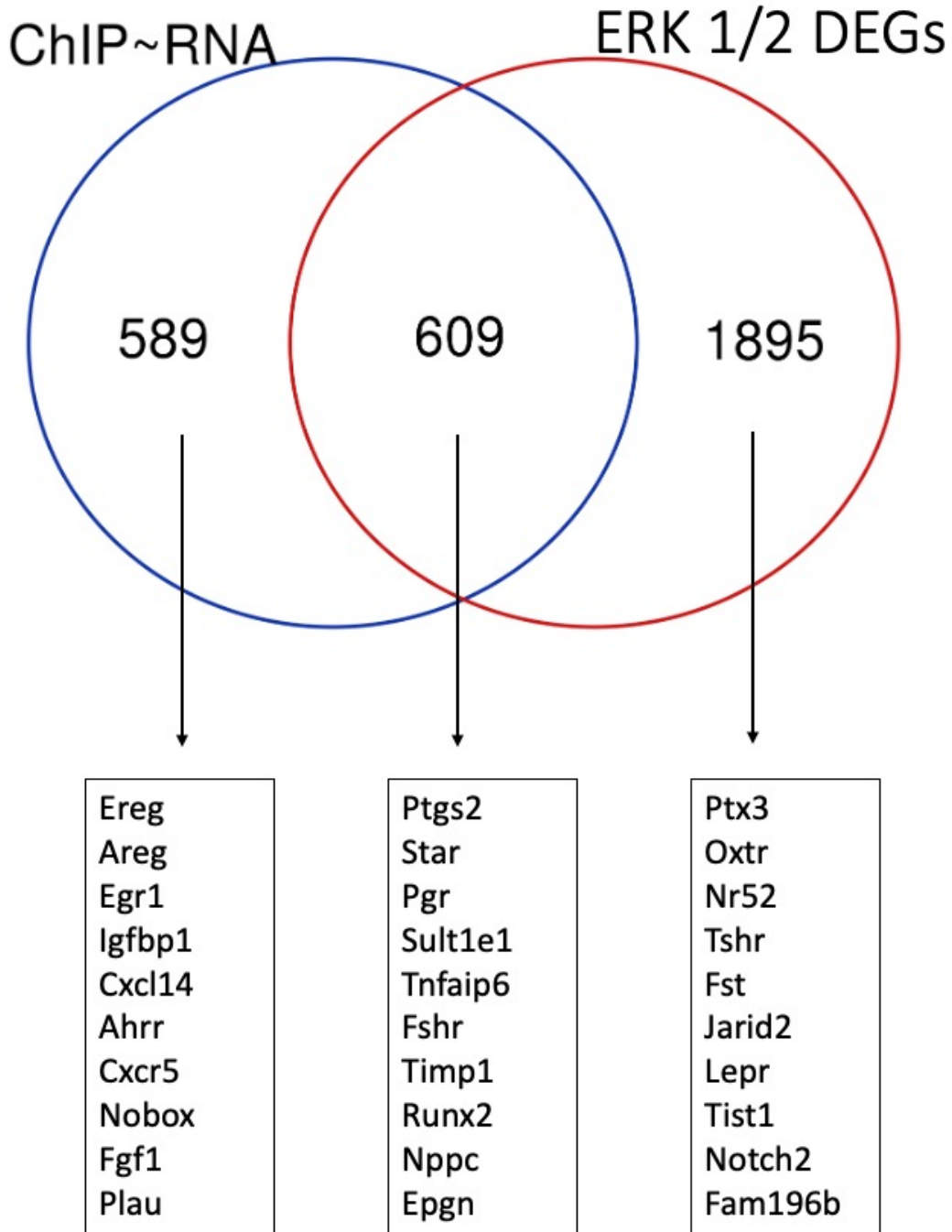
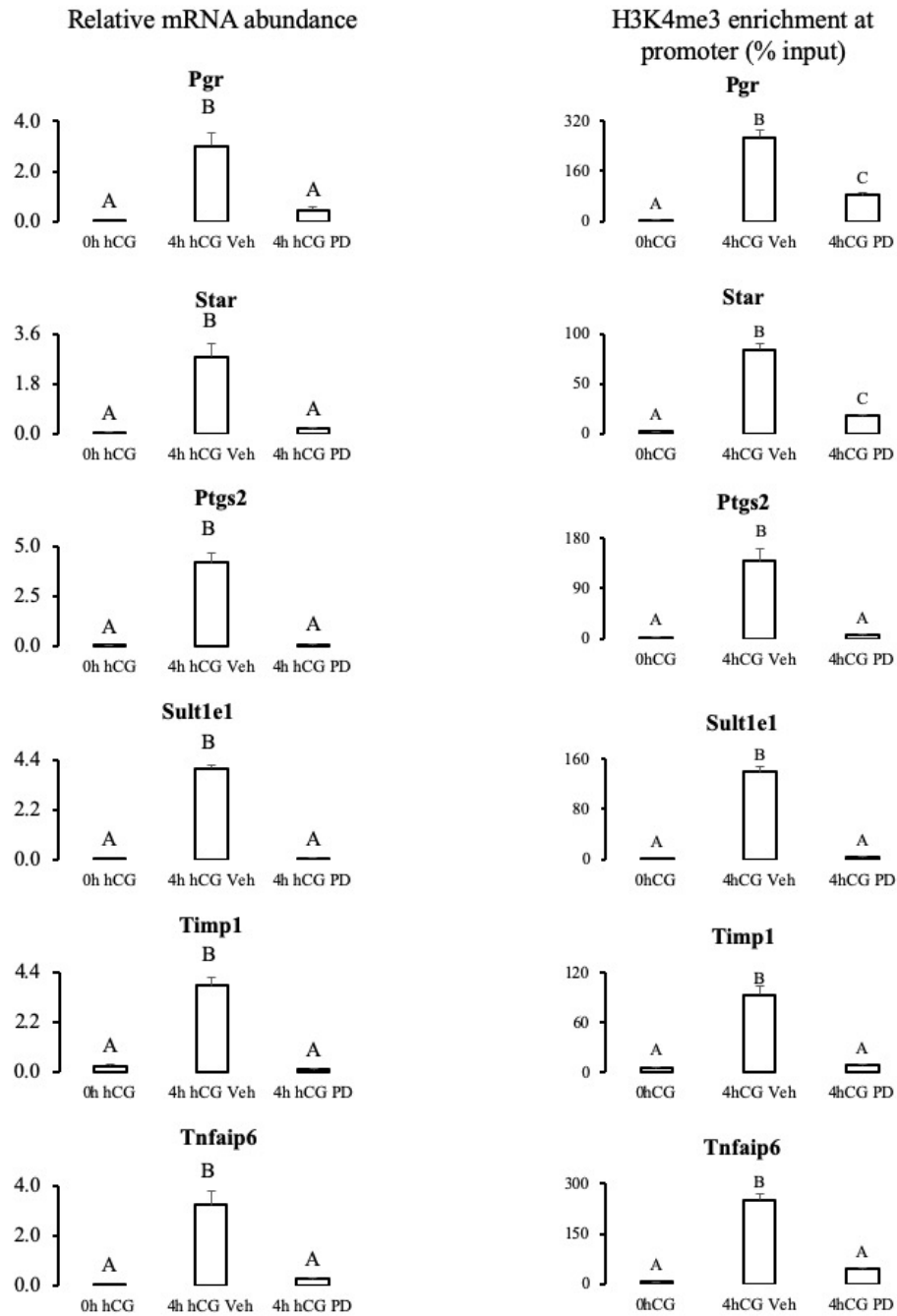


Figure 4.7.7 RT-PCR and ChIP-qPCR graphs

Graphs showing mRNA abundance (RT-PCR) and percent input (ChIP-qPCR) of (A) *Pgr*, *Ptgs2*, *Star*, *Ptgs2*, *Sult1e1*, *Timp1* and *Tnfaip6*, (B) *Cyp19a1*, *Hsd17b1* and *Nppc*

All data are expressed as a mean \pm S.E.M, where different letters represent differences at $p < 0.05$ after a one-way ANOVA followed by Tukey's test. *AC signifies a trend

A



B

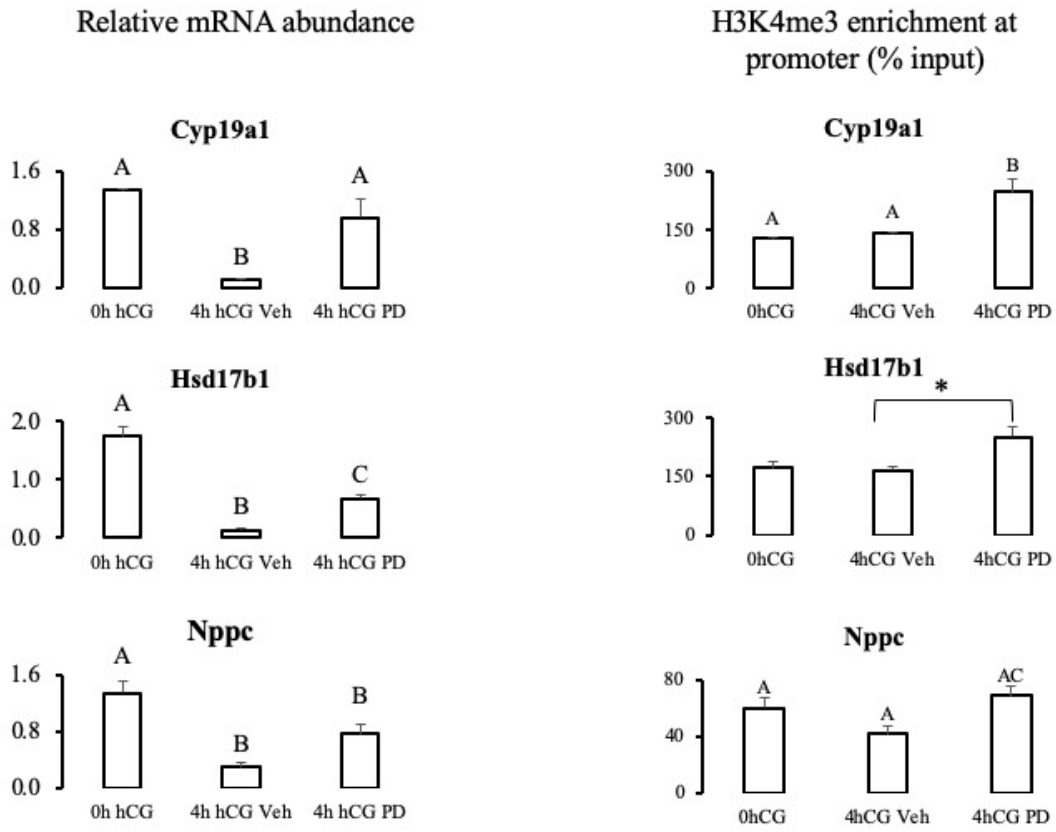
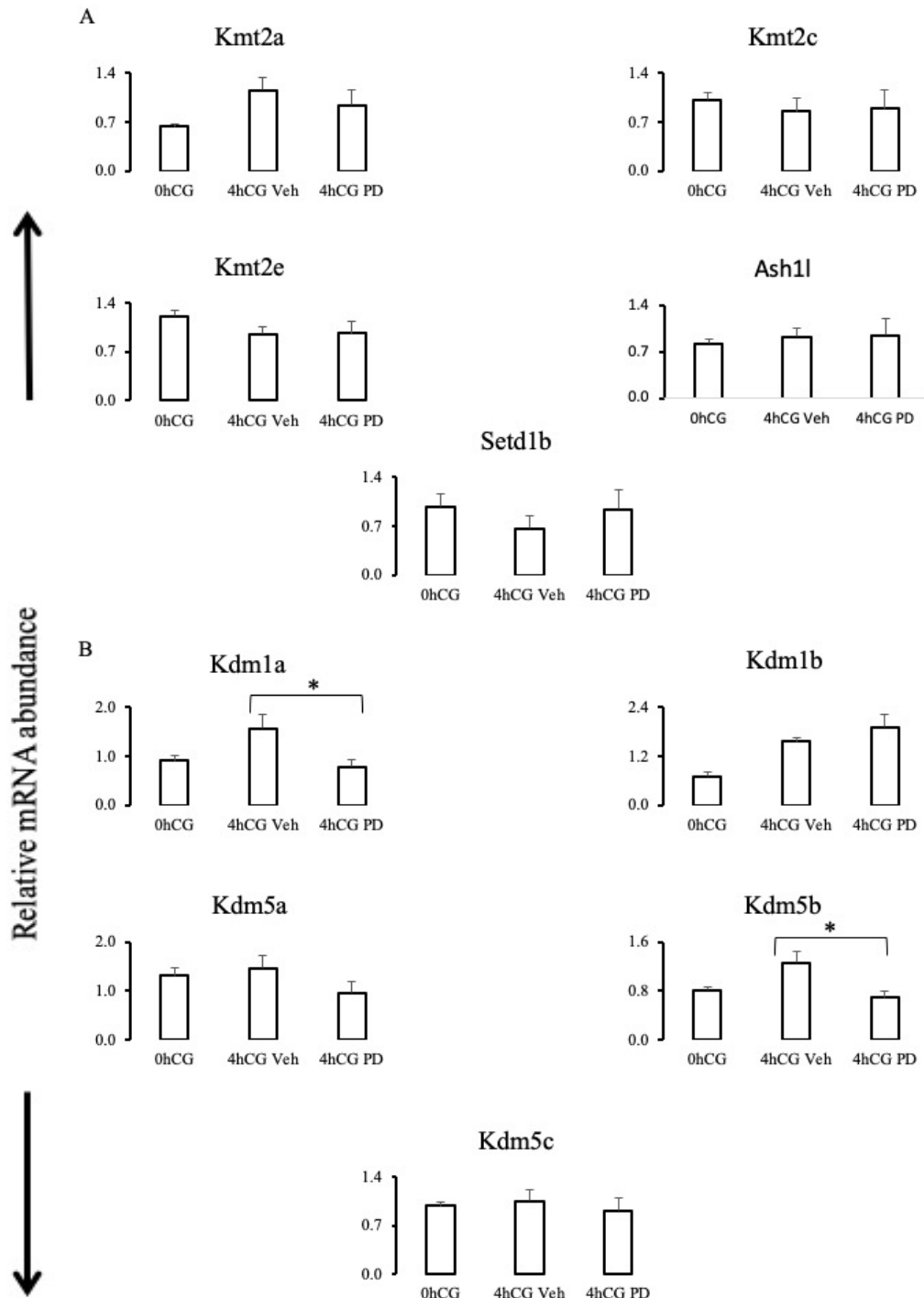


Figure 4.7.8 Expression of H3K4me3 methylases and demethylases

Graphs showing mRNA abundance (RT-PCR) of (A) Histone methyltransferases *Kmt2a*, *Kmt2c*, *Kmt2e*, *Ash1l* and *Setd1b* (B) Histone demethylases *Kdm1a*, *Kdm1b*, *Kdm5a*, *Kdm5b* and *Kdm5c*. All data are expressed as a mean \pm S.E.M, where different letters represent differences at $p < 0.05$ after a one-way ANOVA followed by Tukey's test



4.8 Tables

Table 4.8.1 List of primer sequences

(A) Primer sequences for RT-PCR (B) Primer sequences for ChIP-qPCR (C) Primer sequences for RT-PCR: Histone modifying enzymes

A

Gene symbol	Sequence (5' - 3')
mGapdh-F	AGGTCGGTGTGAACGGATTG
mGapdh-R	TGTAGACCATGTAGTTGAGGTCA
mL19-F	ATGAGTATGCTCAGGCTACAGA
mL19-R	GCATTGGCGATTTCATTGGTC
mB2m-F	TTCTGGTGCTTGCTCACTGA
mB2m-R	CAGTATGTTCCGGCTCCCATTC
mSdha-F	GGAACACTCCAAAAACAGACCT
mSdha-R	CCACCCTGGGTATTGAGTAGAA
mPgr-F	CATGCTGTACGACCTCCAC
mPgr-R	GTAGTCAAATGGTCTAAATCTCTGC
mStar-F	CCTCCAAGCGAAACACCTT
mStar-R	GGCATACTCAACAACAGGAA
mPtgs2-F	TGAGCAACTATTCCAAACCAGC
mPtgs2-R	GCACGTAGTCTTCGATCACTATC
mSult1e1-F	ATGGAGACTTCTATGCCTGAGT
mSult1e1-R	ACACAACCTCACTAATCCAGGTG
mTimp1-F	GCAACTCGACCTGGTCATAA
mTimp1-R	CGGCCCGTGATGAGAACT
mTnfaip6-F	GGGATTCAAGAACGGGATCTTT
mTnfaip6-R	TCAAATCACATACGGCCTTGG
mCyp19a1-F	ATGTTCTTGGAAATGCTGAACCC
mCyp19a1-R	AGGACCTGGTATTGAAGACGAG
mHsd17b1-F	ACTTGGCTGTCGCCTAGC
mHsd17b1-R	GAGGGCATCCTTGAGTCCTG
mNppc-F	CAGAAAAAGGGTGACAAGACTCC
mNppc-R	ATCCAGACCGCTCATGGA
mEgr1-F	TCGGCTCTTCTCACTCA
mEgr1-R	CTCATAGGGTTGTTCCGTCGG

B

Gene name	Sequence (5' - 3')
Pgr-F	GCTTACCTACCATACACTGAG
Pgr-R	GTGCTGGAACAGAAAGCATT
Star-F	AACACATTACAGGGCAGAG
Star-R	TCCAGTTGAGAACCTGCATAC
Ptgs2-F	CACTACATCTGACCCACTTC
Ptgs2-R	AAACAAGGGAGGGTTGTACTT
Sult1e1-F	GCTTCTTCTCCCACTT
Sult1e1-R	GGCACCTATTACCTCCTTATG
Timp1-F	CGTCTCCGCTCCCTTATTC
Timp1-R	CCAGACCAACGGCTTACAT
Tnfaip6-F	GTTTCATCAGGTTTGGCTCTTC
Tnfaip6-R	TAGCCCAAGTCATTCTTACAC
Cyp19a1-F	AGAAGAAGCACAGCTACAAG
Cyp19a1-R	GGGAGCATCTAACCCCATTT
Hsd17b1-F	CAAAGGTATAGGACGGGAAAGG
Hsd17b1-R	CCGCAATGTGGCATAAACTAAA
Nppc-F	ACACTTGATCCCATGCCTAAAT
Nppc-R	CCAAGAGAGCCAAGCTCTTATC
Egr1-F	GATGGAAGATCTCAGAGCCAAG
Egr1-R	GGCAGGGATGGTAAGTGAAA

C

Gene symbol	Sequence (5' - 3')
mKmt2a-F	ATGAGCAGTCTTAGGTTTGGC
mKmt2a-R	CTCCCGGAGGTTTTCGAG
mKmt2c-F	TGTTACAGTGTGGTCAATGTT
mKmt2c-R	GAGGGTCTAGGCAGTAGGTATG
mKmt2e-F	AGATGCACTTACAATCAAGAGGG
mKmt2e-R	AGGGCTGGTATAACCAATAGTCT
mSetd1b-F	TCCTCAAGCTCCGACAAGGAT
mSetd1b-R	CGTCGATGCTGAATCAATCTGG
mAsh1l-F	TTAGGATTGGGTTCTGATTCCGA
mAsh1l-R	CGATTCCGCTTTCGAGGAT
mKdm1a-F	GTTGGTGTATGCTTTGACCGT
mKdm1a-R	GCTGCCAAAAATCCCTTTGAGA
mKdm1b-F	TACGAGTCCCAGAGTATTCGC
mKdm1b-R	GGATGAGGTTTCTCAAAGCCAG
mKdm5a-F	GCCCTTTGCGGAGAAAAACG
mKdm5a-R	TGGACTCTAGGAGTGAAACGG
mKdm5b-F	CTGGGAAGAGTTCCGGGAC
mKdm5b-R	CGCGGGTGAAATGAAGTTTAT
mKdm5c-F	GAGGCCAGACAAGAGTGAAA
mKdm5c-R	TTGGGAATCTTTAAGGATGAGCC

Table 4.8.2 KEGG pathways

KEGG Pathways identified by EGSEA and IPA for 4874 LH DEGs and 2504 ERK1/2 DEGs

LH

Top KEGG Pathways	Avg Rank
TNF signaling pathway	2.0
MAPK signaling pathway	1.5
Transcriptional misregulation in cancer	1.9
Osteoclast differentiation	1.9
Proteoglycans in cancer	1.6
NF-kappa B signaling pathway	1.8
Legionellosis	2.1
Leishmaniasis	2.1
Salmonella infection	1.7
Tuberculosis	1.7
VEGF signaling pathway	1.7
Peroxisome	-1.1
Glyoxylate and dicarboxylate metabolism	-1.3
Chemokine signaling pathway	1.6
Toll-like receptor signaling pathway	1.6
NOD-like receptor signaling pathway	1.8
Pertussis	1.9
Glycine, serine and threonine metabolism	-1.3
Valine, leucine and isoleucine degradation	-1.2
Pathways in cancer	1.7

ERK

Top KEGG Pathways	Avg Rank
TNF signaling pathway	-1.6
MAPK signaling pathway	-1.2
Transcriptional misregulation in cancer	-1.3
Osteoclast differentiation	-1.6
Leishmaniasis	-1.7
Legionellosis	-2.2
Tuberculosis	-1.5
VEGF signaling pathway	-1.3
Chemokine signaling pathway	-1.5
Fc gamma R-mediated phagocytosis	-1.2
Salmonella infection	-1.7
Other types of O-glycan biosynthesis	1.0
MAPK signaling pathway	-1.2
B cell receptor signaling pathway	-1.1
Fc epsilon RI signaling pathway	-1.2
Natural killer cell mediated cytotoxicity	-1.7
Pertussis	-1.9
NF-kappa B signaling pathway	-1.3
Glycosaminoglycan biosynthesis - chondroitin sulfate / dermatan sulfate	1.0
NOD-like receptor signaling pathway	-1.7
Glycosphingolipid biosynthesis - ganglio series	1.9

Table 4.8.3 Pathways and Protein classes

(A) Top pathways for the 609 genes regulated by LH and ERK1/2 identified by PANTHER

(B) Top protein classes for the 609 genes regulated by LH and ERK1/2 identified by PANTHER

A

Category name	Number of genes	Percent of gene hits against total # genes	Percent of gene hits against total # pathway hits
Inflammation mediated by chemokine and cytokine signaling pathway	25	4.70%	11.90%
Gonadotropin-releasing hormone receptor pathway	12	2.30%	5.70%
Integrin signalling pathway	11	2.10%	5.20%
Interleukin signaling pathway	9	1.70%	4.30%
CCKR signaling map	8	1.50%	3.80%
Nicotinic acetylcholine receptor signaling pathway	8	1.50%	3.80%
Heterotrimeric G-protein signaling pathway-Gi alpha and Gs alpha mediated pathway	6	1.10%	2.90%
Alzheimer disease-presenilin pathway	5	0.90%	2.40%
Wnt signaling pathway	5	0.90%	2.40%
Thyrotropin-releasing hormone receptor signaling pathway	5	0.90%	2.40%
TGF-beta signaling pathway	5	0.90%	2.40%
Apoptosis signaling pathway	4	0.80%	1.90%
Plasminogen activating cascade	4	0.80%	1.90%
Endothelin signaling pathway	4	0.80%	1.90%

B

Category name	Number of genes	Percent of gene hits against total # genes	Percent of gene hits against total # pathway hits
Signaling molecule	51	9.60%	15.20%
Receptor	41	7.80%	12.20%
Hydrolase	40	7.60%	11.90%
Enzyme modulator	39	7.40%	11.60%
Defense/immunity protein	24	4.50%	7.20%
Transporter	21	4.00%	6.30%
Oxidoreductase	16	3.00%	4.80%
Transcription factor	16	3.00%	4.80%
Transferase	15	2.80%	4.50%
Nucleic acid binding	14	2.60%	4.20%
Cell adhesion molecule	12	2.30%	3.60%
Cytoskeletal protein	11	2.10%	3.30%
Membrane traffic protein	8	1.50%	2.40%
Extracellular matrix protein	6	1.10%	1.80%
Cell junction protein	5	0.90%	1.50%

Supplementary Table 4.8.1: Quality control metrics

(A) Quality control metrics for the RNA-Sequencing data; (B) Quality control metrics for the ChIP-Sequencing data

A

Sample		Number of Reads (Millions)	Aligned exactly one time (Millions)
0h hCG	1	19	17 (88.48%)
	2	34	31 (90.75%)
	3	17	15 (87.94%)
4h hCG Veh	1	15	14 (87.17%)
	2	38	34 (87.97%)
	3	29	26 (86.99%)
4h hCG PD	1	20	18 (89.47%)
	2	21	18 (88.10%)
	3	21	18 (86.67%)

B

Sample		Number of Reads (millions)	Overall Alignment rate	Aligned Exactly 1 time (millions)
0h hCG	1	32	97.83%	24 (74.52%)
	2	34	97.95%	24 (69.39%)
4h hCG	1	31	97.66%	21 (68.01%)
	2	26	98.03%	17 (65.59%)

Supplementary Table 4.8.2: Top functions

(A) Top molecular and cellular functions of 4873 LH regulated genes identified by IPA; (B) Top physiological system development and function of 4873 LH regulated genes identified by IPA

A

Top Molecular and Cellular Functions	Number of Genes	Including:
Movement	1113	Sult1e1, Npy, Nts, Ptgs2, Ereg, Tnfaip6
Growth and proliferation	1426	Adcyap1, Il6, Cxcr4, mir-17, Tnf, Trem1, mir-21
Function and Maintenance	1337	Il6, Tnf, Slc2a1, Ptx3, Fpr1, Ch25h,
Development	1447	Lepr, Il6, Il7, Egr3, Sult1e1, Epgn
Assembly and Organization	840	Ptx3, Vgf, Fgf5, mir-132, Has2,

B

Top Physiological System Development and Function	Number of Genes	Including:
Tissue Morphology	1202	Sult1e1, Vgf, Tnfaip6, Il6, Adcyap1, Btc, Trh
Hematological System Development and Function	1057	Nmu, Il6, F3, Il17a, Cxcr4, Cebpe, Gpr83, Ccl11,
Organismal Development	1672	Ptgs2, Egr3, Lepr, Il6, Spp1, Il17a, Cnr1, Hgf, Fgf2, Vegfa,
Immune cell trafficking	651	Npy, Ptgs2, Il6, Olr1, F3, Il17a, Cxcr4, Itgs2, Tnf, Cxcl3, Ccr9
Lymphoid Tissue structure and Development	747	Il6, F3, Il17a, Cxcr4, Il7, Kl, Serpinb2, Runx1, Timp1

Supplementary Table 4.8.3: Top Upstream regulators of LH and ERK1/2 regulated genes

Top Upstream Regulators	LH	ERK
Lipopolysaccharide	Activated	Inhibited
TNF	Activated	Inhibited
CG	Activated	Inhibited
TGFB1	Activated	Inhibited

4.9 References

- ALHAMDOOSH, M., LAW, C., TIAN, L., SHERIDAN, J., NG, M. & RITCHIE, M. 2017. Easy and efficient ensemble gene set testing with EGSEA [version 1; referees: 1 approved, 3 approved with reservations]. *F1000Research*, 6.
- ANDREWS, S. 2014. *FastQC A Quality Control tool for High Throughput Sequence Data*.
- BIANCO, S., BELLEFLEUR, A.-M., BEAULIEU, É., BEAUPARLANT, C. J., BERTOLIN, K., DROIT, A., SCHOONJANS, K., MURPHY, B. D. & GÉVRY, N. 2019. The Ovulatory Signal Precipitates LRH-1 Transcriptional Switching Mediated by Differential Chromatin Accessibility. *Cell reports*, 28, 2443-2454.e4.
- BIANCO, S., BRUNELLE, M., JANGAL, M., MAGNANI, L. & GÉVRY, N. 2014. LRH-1 governs vital transcriptional programs in endocrine-sensitive and -resistant breast cancer cells. *Cancer research*, 74, 2015-2025.
- BOLGER, A. M., LOHSE, M., & USADEL, B. 2014. Trimmomatic: A flexible trimmer for Illumina Sequence Data. *Bioinformatics*, btu170.
- BROWN, H. M., DUNNING, K. R., ROBKER, R. L., BOERBOOM, D., PRITCHARD, M., LANE, M. & RUSSELL, D. L. 2010. ADAMTS1 cleavage of versican mediates essential structural remodeling of the ovarian follicle and cumulus-oocyte matrix during ovulation in mice. *Biol Reprod*, 83, 549-57.
- CACIOPPO, J. A., LIN, P.-C. P., HANNON, P. R., MCDUGLE, D. R., GAL, A. & KO, C. 2017. Granulosa cell endothelin-2 expression is fundamental for ovulatory follicle rupture. *Scientific reports*, 7, 817-817.
- CAO, F., FANG, Y., TAN, H. K., GOH, Y., CHOY, J. Y. H., KOH, B. T. H., HAO TAN, J., BERTIN, N., RAMADASS, A., HUNTER, E., GREEN, J., SALTER, M., AKOULITCHEV, A., WANG, W., CHNG, W. J., TENEN, D. G. & FULLWOOD, M. J. 2017. Super-Enhancers and Broad H3K4me3 Domains Form Complex Gene Regulatory Circuits Involving Chromatin Interactions. *Scientific Reports*, 7, 2186.
- CHOI, Y., PARK, J. Y., WILSON, K., ROSEWELL, K. L., BRÄNNSTRÖM, M., AKIN, J. W., CURRY, T. E., JR. & JO, M. 2017. The expression of CXCR4 is induced by the luteinizing hormone surge and mediated by progesterone receptors in human preovulatory granulosa cells. *Biology of reproduction*, 96, 1256-1266.
- DAHL, J. A., JUNG, I., AANES, H., GREGGAINS, G. D., MANAF, A., LERDRUP, M., LI, G., KUAN, S., LI, B., LEE, A. Y., PREISSEL, S., JERMSTAD, I., HAUGEN, M. H., SUGANTHAN, R., BJØRÅS, M., HANSEN, K., DALEN, K. T., FEDORCSAK, P., REN, B. & KLUNGLAND, A. 2016. Broad histone H3K4me3 domains in mouse oocytes modulate maternal-to-zygotic transition. *Nature*, 537, 548-552.
- DINH, D. T., BREEN, J., AKISON, L. K., DEMAYO, F. J., BROWN, H. M., ROBKER, R. L. & RUSSELL, D. L. 2019. Tissue-specific progesterone receptor-chromatin binding and the regulation of progesterone-dependent gene expression. *Sci Rep*, 9, 11966.
- DOBIN, A., DAVIS, C. A., SCHLESINGER, F., DRENKOW, J., ZALESKI, C., JHA, S., BATUT, P., CHAISSON, M. & GINGERAS, T. R. 2013. STAR: ultrafast universal RNA-seq aligner. *Bioinformatics*, 29, 15-21.
- DUFFY, D. M., KO, C., JO, M., BRANNSTROM, M. & CURRY, T. E. 2019. Ovulation: Parallels With Inflammatory Processes. *Endocr Rev*, 40, 369-416.
- DUGGAVATHI, R. & MURPHY, B. D. 2009. Development. Ovulation signals. *Science*, 324, 890-1.

- DUGGAVATHI, R., VOLLE, D., MATAKI, C., ANTAL, M., MESSADDEQ, N., AUWERX, J., MURPHY, B., SCHOONJANS, K., DUGGAVATHI, R., VOLLE, D., MATAKI, C., ANTAL, M., MESSADDEQ, N., AUWERX, J., MURPHY, B. & SCHOONJANS, K. 2008a. Liver receptor homolog 1 is essential for ovulation. *Genes and Development*, 22, 1871-1876.
- DUGGAVATHI, R., VOLLE, D. H., MATAKI, C., ANTAL, M. C., MESSADDEQ, N., AUWERX, J., MURPHY, B. D. & SCHOONJANS, K. 2008b. Liver receptor homolog 1 is essential for ovulation. *Genes Dev*, 22, 1871-6.
- DUPUIS, L., SCHUERMAN, Y., COHEN, T., SIDDAPPA, D., KALAISELVANRAJA, A., PANSERA, M., BORDIGNON, V. & DUGGAVATHI, R. 2014. Role of leptin receptors in granulosa cells during ovulation. 147, 221.
- ESPEY, L. L. 1980. Ovulation as an inflammatory reaction--a hypothesis. *Biology of reproduction*, 22, 73-106.
- ESPEY, L. L. & RICHARDS, J. S. 2002. Temporal and spatial patterns of ovarian gene transcription following an ovulatory dose of gonadotropin in the rat. *Biology of reproduction*, 67, 1662-1670.
- FAN, H. Y., LIU, Z., SHIMADA, M., STERNECK, E., JOHNSON, P. F., HEDRICK, S. M. & RICHARDS, J. S. 2009. MAPK3/1 (ERK1/2) in ovarian granulosa cells are essential for female fertility. *Science*, 324, 938-41.
- HARING, M., OFFERMANN, S., DANKER, T., HORST, I., PETERHANSEL, C. & STAM, M. 2007. Chromatin immunoprecipitation: optimization, quantitative analysis and data normalization. *Plant Methods*, 3, 11.
- HAZZARD, T. M., CHRISTENSON, L. K. & STOUFFER, R. L. 2000. Changes in expression of vascular endothelial growth factor and angiopoietin-1 and -2 in the macaque corpus luteum during the menstrual cycle. *Molecular Human Reproduction*, 6, 993-998.
- HISANO, M., ERKEK, S., DESSUS-BABUS, S., RAMOS, L., STADLER, M. B. & PETERS, A. H. F. M. 2013. Genome-wide chromatin analysis in mature mouse and human spermatozoa. *Nat. Protocols*, 8, 2449-2470.
- KIM, J., BAGCHI, I. C. & BAGCHI, M. K. 2009. Signaling by hypoxia-inducible factors is critical for ovulation in mice. *Endocrinology*, 150, 3392-3400.
- KING, S. R. & LAVOIE, H. A. 2012. Gonadal transactivation of STARD1, CYP11A1 and HSD3B. *Frontiers in bioscience (Landmark edition)*, 17, 824-846.
- KO, C., GIESKE, M. C., AL-ALEM, L., HAHN, Y., SU, W., GONG, M. C., IGLARZ, M. & KOO, Y. 2006. Endothelin-2 in ovarian follicle rupture. *Endocrinology*, 147, 1770-1779.
- KOOS, R. D. 1995. Increased expression of vascular endothelial growth/permeability factor in the rat ovary following an ovulatory gonadotropin stimulus: potential roles in follicle rupture. *Biology of reproduction*, 52, 1426-1435.
- KUO, M. H. & ALLIS, C. D. 1999. In vivo cross-linking and immunoprecipitation for studying dynamic Protein:DNA associations in a chromatin environment. *Methods*, 19, 425-33.
- LANGMEAD, B. & SALZBERG, S. L. 2012. Fast gapped-read alignment with Bowtie 2. *Nat Methods*, 9, 357-9.
- LEE, L., ASADA, H., KIZUKA, F., TAMURA, I., MAEKAWA, R., TAKETANI, T., SATO, S., YAMAGATA, Y., TAMURA, H. & SUGINO, N. 2013. Changes in Histone Modification and DNA Methylation of the StAR and Cyp19a1 Promoter Regions in Granulosa Cells Undergoing Luteinization during Ovulation In Rats. *Endocrinology*, 154, 458-470.

- LI, Y., CHENG, H. S., CHNG, W. J. & TERGAONKAR, V. 2016. Activation of mutant TERT promoter by RAS-ERK signaling is a key step in malignant progression of BRAF-mutant human melanomas. *Proceedings of the National Academy of Sciences of the United States of America*, 113, 14402-14407.
- LYDON, J. P., DEMAYO, F. J., FUNK, C. R., MANI, S. K., HUGHES, A. R., MONTGOMERY, C. A., JR., SHYAMALA, G., CONNEELY, O. M. & O'MALLEY, B. W. 1995. Mice lacking progesterone receptor exhibit pleiotropic reproductive abnormalities. *Genes Dev*, 9, 2266-78.
- MARMORSTEIN, R. & TRIEVEL, R. C. 2009. Histone modifying enzymes: structures, mechanisms, and specificities. *Biochim Biophys Acta*, 1789, 58-68.
- MO, R., RAO, S. M. & ZHU, Y. J. 2006. Identification of the MLL2 complex as a coactivator for estrogen receptor alpha. *J Biol Chem*, 281, 15714-20.
- NIMZ, M., SPITSCHAK, M., FURBASS, R. & VANSELOW, J. 2010. The pre-ovulatory luteinizing hormone surge is followed by down-regulation of CYP19A1, HSD3B1, and CYP17A1 and chromatin condensation of the corresponding promoters in bovine follicles. *Mol Reprod Dev*, 77, 1040-8.
- PALANISAMY, G. S., CHEON, Y.-P., KIM, J., KANNAN, A., LI, Q., SATO, M., MANTENA, S. R., SITRUK-WARE, R. L., BAGCHI, M. K. & BAGCHI, I. C. 2006. A novel pathway involving progesterone receptor, endothelin-2, and endothelin receptor B controls ovulation in mice. *Molecular endocrinology (Baltimore, Md.)*, 20, 2784-2795.
- REDMER, D. A. & REYNOLDS, L. P. 1996. Angiogenesis in the ovary. *Reviews of reproduction*, 1, 182-192.
- RICHARDS, J. S. 1994. Hormonal control of gene expression in the ovary. *Endocr Rev*, 15, 725-51.
- RICHARDS, J. S., RUSSELL, D. L., OCHSNER, S. & ESPEY, L. L. 2002. Ovulation: new dimensions and new regulators of the inflammatory-like response. *Annu Rev Physiol*, 64, 69-92.
- ROBINSON, J. T., THORVALDSDÓTTIR, H., WINCKLER, W., GUTTMAN, M., LANDER, E. S., GETZ, G. & MESIROV, J. P. 2011. Integrative genomics viewer. *Nature Biotechnology*, 29, 24.
- ROBKER, R. L., HENNEBOLD, J. D. & RUSSELL, D. L. 2018. Coordination of Ovulation and Oocyte Maturation: A Good Egg at the Right Time. *Endocrinology*, 159, 3209-3218.
- ROBKER, R. L., RUSSELL, D. L., ESPEY, L. L., LYDON, J. P., O'MALLEY, B. W. & RICHARDS, J. S. 2000. Progesterone-regulated genes in the ovulation process: ADAMTS-1 and cathepsin L proteases. *Proc Natl Acad Sci U S A*, 97, 4689-94.
- SANTOS-ROSA, H., SCHNEIDER, R., BANNISTER, A. J., SHERRIFF, J., BERNSTEIN, B. E., EMRE, N. C. T., SCHREIBER, S. L., MELLOR, J. & KOUZARIDES, T. 2002. Active genes are tri-methylated at K4 of histone H3. *Nature*, 419, 407-411.
- SAYASITH, K. & SIROIS, J. 2014. Expression and regulation of stromal cell-derived factor-1 (SDF1) and chemokine CXC motif receptor 4 (CXCR4) in equine and bovine preovulatory follicles. *Molecular and cellular endocrinology*, 391, 10-21.
- SCHUERMAN, Y., ROVANI, M. T., GASPERIN, B., FERREIRA, R., FERST, J., MADOGWE, E., GONCALVES, P. B., BORDIGNON, V. & DUGGAVATHI, R. 2018. ERK1/2-dependent gene expression in the bovine ovulating follicle. *Sci Rep*, 8, 16170.

- SIDDAPPA, D., BEAULIEU, E., GEVRY, N., ROUX, P. P., BORDIGNON, V. & DUGGAVATHI, R. 2015. Effect of the transient pharmacological inhibition of Mapk3/1 pathway on ovulation in mice. *PLoS One*, 10, e0119387.
- SVOTELIS, A., GEVRY, N. & GAUDREAU, L. 2009. Chromatin immunoprecipitation in mammalian cells. *Methods Mol Biol*, 543, 243-51.
- TEE, W. W., SHEN, S. S., OKSUZ, O., NARENDRA, V. & REINBERG, D. 2014. Erk1/2 activity promotes chromatin features and RNAPII phosphorylation at developmental promoters in mouse ESCs. *Cell*, 156, 678-90.
- WIGGLESWORTH, K., EPPIG, J. J., LEE, K.-B., EMORI, C. & SUGIURA, K. 2015. Transcriptomic Diversification of Developing Cumulus and Mural Granulosa Cells in Mouse Ovarian Follicles1. *Biology of Reproduction*, 92.
- WOZNAK, G. G. & STRAHL, B. D. 2014. Hitting the 'mark': Interpreting lysine methylation in the context of active transcription. *Biochim Biophys Acta*.
- WU, C. 1997. Chromatin remodeling and the control of gene expression. *J Biol Chem*, 272, 28171-4.
- XIA, J., GILL, E. E. & HANCOCK, R. E. W. 2015. NetworkAnalyst for statistical, visual and network-based meta-analysis of gene expression data. *Nature Protocols*, 10, 823.
- XIA, J., LYLE, N. H., MAYER, M. L., PENA, O. M. & HANCOCK, R. E. 2013. INVEX--a web-based tool for integrative visualization of expression data. *Bioinformatics*, 29, 3232-4.
- XU, F., STOUFFER, R. L., MÜLLER, J., HENNEBOLD, J. D., WRIGHT, J. W., BAHAR, A., LEDER, G., PETERS, M., THORNE, M., SIMS, M., WINTERMANTEL, T. & LINDENTHAL, B. 2011. Dynamics of the transcriptome in the primate ovulatory follicle. *Molecular Human Reproduction*, 17, 152-165.
- YU, G., WANG, L.-G. & HE, Q.-Y. 2015. ChIPseeker: an R/Bioconductor package for ChIP peak annotation, comparison and visualization. *Bioinformatics*, 31, 2382-2383.
- ZHANG, Y., LIU, T., MEYER, C. A., ECKHOUTE, J., JOHNSON, D. S., BERNSTEIN, B. E., NUSBAUM, C., MYERS, R. M., BROWN, M., LI, W. & LIU, X. S. 2008. Model-based analysis of ChIP-Seq (MACS). *Genome biology*, 9, R137-R137.
- ZHANG, Y. L., XIA, Y., YU, C., RICHARDS, J. S., LIU, J. & FAN, H. Y. 2014. CBP-CITED4 is required for luteinizing hormone-triggered target gene expression during ovulation. *Mol Hum Reprod*, 20, 850-60.
- ZUBEK, J., STITZEL, M. L., UCAR, D. & PLEWCZYNSKI, D. M. 2016. Computational inference of H3K4me3 and H3K27ac domain length. *PeerJ*, 4, e1750.

CONNECTING STATEMENT 2

In Study 2, we established that inhibition of the LH-induced immediate early ERK1/2 signaling abrogates ovulation through altered gene expression program in granulosa cells. We also observed that Rps6ka2 was induced by LH surge hinting that it may participate in prolongation of ERK1/2 signals beyond immediate early time-points of ovulation. In Study 3, we sought to clarify the role of sustained ERK1/2 signaling on cumulus expansion, oocyte meiotic resumption and luteinization by inhibiting ERK1/2 at 4h post hCG.

CHAPTER 5

Manuscript under Review by the peer reviewed journal '*Reproduction*'

REP-20-0087

Sustained ERK1/2 signaling is necessary for follicular rupture during ovulation in mice

Ejimedo Madogwe¹, Yasmin Schuermann^{1,#}, Dayananda Siddappa^{1,#}, Vilceu Bordignon¹, Philippe P. Roux² and Raj Duggavathi^{1*}

Affiliations

¹Department of Animal Science, McGill University, Sainte-Anne-de-Bellevue, QC H9X 3V9

²Institute for Research in Immunology and Cancer, Université de Montréal, Montreal, QC H3C 3J7

*Corresponding author: raj.duggavathi@mcgill.ca, Ph: +1 514 398-7803

Authors' contributed equally

Short Title: Sustained ERK1/2 signaling during ovulation

Key words: Granulosa cells, ERK1/2, knockout, PD0325901, RSK3, ovulation, extracellular matrix, follicle rupture.

Word count of full article: 4704

5.1 Abstract

Abolition of LH-induced ERK1/2 pathway leads to dramatic changes in gene expression in granulosa cells, subsequently abrogating ovulation. Here we explored whether sustained ERK1/2 signaling beyond immediate early hours of the LH surge is important for ovulation in mice. First, we examined the effect of inhibition of ERK1/2 activity at 4h after hCG stimulation on ovulation in superovulated immature mice. Treatment with the ERK1/2 pathway inhibitor PD0325901 at 4h post-hCG disrupted follicular rupture without altering cumulus expansion, oocyte meiotic maturation and luteinization. Profiling the expression pattern of genes of the RSK family of ERK1/2 signal mediators revealed that *RSK3*, but not other isoforms, was induced by hCG treatment. Further, *RSK3*-knockout mice were sub-fertile with reduced ovulation rate and smaller litter size compared to wild type mice. Given that PD0325901 inhibits all mediators of ERK1/2 signaling, we chose to evaluate the gene expression underlying deficient follicular rupture in ERK1/2-inhibited mice. We found that inhibition of ERK1/2 signaling at 4h post-hCG resulted in imbalance in the expression of genes involved in extracellular matrix degradation and leukocyte infiltration necessary for follicular rupture. In conclusion, our data demonstrate that sustained ERK1/2 signaling during ovulation is not required for cumulus expansion, oocyte meiotic maturation and luteinization, but is required for follicular rupture.

5.2 Introduction

Ovulation is a unique biological event, which is essential for reproductive success in all mammals. It is a prolonged process (12-16h in mice and 36-40h in primates) involving multiple events including oocyte maturation, luteinization and follicular rupture. The single trigger for the initiation of ovulation is the preovulatory surge of luteinizing hormone (LH) from the pituitary. Acting through its receptors (Lhcgr), LH triggers multiple signaling pathways (Richards, 2005). Some of the important signaling pathways through which LH brings about ovulatory events are cAMP/PKA pathway, ERK1/2 pathway and PI3K-Akt pathway (Ben-Ami et al., 2009, Ashkenazi et al., 2005, Park et al., 2004, Fan et al., 2008). These signaling pathways initiate an intricate gene expression program that underpins oocyte maturation, follicular rupture and luteinization.

Signals from extracellular signal-regulated kinases 1 and 2 (ERK1/2) are mediated through multiple proteins both in the cytoplasm and the nucleus. Among the cytoplasmic targets of ERK1/2 are the 90 kDa ribosomal S6 kinases (RSKs), which belong to the family of serine/threonine kinases (Anjum and Blenis, 2008a). In mice and humans, there are four isoforms of RSKs (RSK1, 2, 3 and 4), encoded by four genes *Rps6ka1*, *Rps6ka3*, *Rps6ka2* and *Rps6ka6*, respectively (Anjum and Blenis, 2008a, Kim et al., 2006). Abolition of LH-induced ERK1/2 pathway leads to dramatic changes in gene expression in granulosa cells, subsequently abrogating ovulation (Siddappa et al., 2015, Fan et al., 2009b). However, these studies inherently tested the role of ERK1/2 signaling as part of the immediate early response to LH surge by abrogating ERK1/2 signal prior to the LH surge. One of the important mediators of ERK1/2 signals, RSK3 (*Rps6ka2*), was shown to be induced in granulosa cells by the LH surge (Fan et al., 2009b). This indicates that ERK1/2 signals may continue to be activated by the mediators that become available later during the ovulatory process. Consistent with this, *RPS6KA2* expression in human cumulus cells was shown to be

associated with higher quality of embryos (Adriaenssens et al., 2010). Therefore, it is possible that the lingering ERK1/2 signals may play important roles in the later processes of ovulation. We hypothesized that the continued ERK1/2 signaling beyond immediate early hours of LH surge is important for ovulation in mice. To test this hypothesis, we inhibited periovulatory ERK1/2 signaling by administering the pharmacological inhibitor, PD0325901, 4h after hCG stimulation in superovulated immature mice. We also examined the role of the ERK1/2 mediator, RSK3, in ovulation and fertility using RSK3-knockout mice (Li et al., 2013). Here we show that sustained ERK1/2 signaling later during the ovulatory process regulates follicular rupture.

5.3 Materials and methods

5.3.1 Animal Model

We used immature superovulated C57BL/6NCrl mice (Charles River) to investigate the effect of abolition of ERK1/2 signaling 4h after hCG stimulus on ovulation. The animal use protocol for the use of C57BL/6NCrl mice (PD0325901 studies) was approved by the Facility Animal Care and Use Committee of McGill University. We also used wild type (*RSK3^{+/+}*) and knockout (*RSK3^{-/-}*) mice, which have been previously described (Li et al., 2013), for studies investigating the role of RSK3 in the ovary. The animal use protocol for the use of RSK3 wildtype and knockout mice was approved by the animal care committee of Université de Montréal. Mice were housed in standard animal cages and provided water and feed (Rodent Diet, Harlan Teklad, Montreal, Canada) *ad libitum*. They were maintained under a 12-hour light and 12-hour dark cycle.

5.3.2 Superovulation and sample collection

Immature mice (23-25d old) were first treated with equine chorionic gonadotropin (eCG; Sigma Life Sciences; 5 IU i.p.) to stimulate follicle development. Forty-eight hours later, mice were treated with human chorionic gonadotropin (hCG; Sigma Life Sciences; 5 IU i.p.) to induce

ovulation and luteinization. In this protocol, ovulation occurs at 12-14h post-hCG (Richards et al., 2002a, Duggavathi et al., 2008b). Ovaries were collected at specific time-points relative to superovulation as described for each experiment. Granulosa cell and cumulus-oocyte-complex samples, when needed, were collected by follicular puncture as described previously (Dupuis et al., 2014). These samples were either processed immediately or stored at -80°C until further use.

5.3.3 Inhibition of ERK1/2 activity

We have used the Mp2k1/Mp2k2 (MEK1/2) inhibitor PD0325901 (Selleckchem, USA) previously to inhibit ERK1/2 activation in the ovary (Siddappa et al., 2015). A dosing solution of $2.5\ \mu\text{g}/\mu\text{l}$ in 5% DMSO in saline was prepared just before treatment. For inhibition of ERK1/2 activity, mice were administered a single dose of PD0325901 ($25\ \mu\text{g}/\text{g}$ body weight, i.p.) at 4h after hCG stimulation. Mice treated with 5% DMSO in saline served as vehicle controls. We determined ERK1/2 activity by measuring the abundance of the phosphorylated isoform of ERK1/2 (at Thr202/Tyr204) relative to its total isoform.

5.3.4 Assessment of ovulation rate, oocyte maturation and ovarian histology in vehicle and PD0325901 treated mice

To test the effect of ERK1/2 inhibition at 4h post-hCG, we collected oviducts from vehicle- and PD0325901-treated mice (N=7-10 per group) at 18h post-hCG to count the number of cumulus-oocyte complexes (COCs) ovulated. To evaluate the maturation status of oocytes ovulated, the COCs were denuded using hyaluronidase enzyme to get rid of cumulus cells from oocytes. These denuded oocytes were stained using DAPI and observed under fluorescent microscope (Nikon) to evaluate oocyte meiotic maturation. For histological evaluation, ovaries collected at 18h post-hCG from these mice were fixed in 10% neutral buffered formalin for at least 2 days. Ovaries were also frozen in liquid nitrogen and stored at -80°C for protein extraction. For

histology, ovaries were embedded in paraffin and were cut (4-5 μ thickness) using a rotatory microtome (Leica RM2125RT). Sections were stained by hematoxylin and eosin for histological observation under Leica DM200 microscope attached to a Leica EC3 camera.

5.3.5 Reproductive phenotyping of *RSK3*^{-/-} mice

We first assessed ovulation rate in immature superovulated mice and also in adult cyclic mice. Oviducts from immature superovulated *RSK3*^{+/+} and *RSK3*^{-/-} (N=5-6 per genotype) mice were collected at 18h post-hCG to count the number of COCs ovulated. To assess ovulation rate in adult mice, post-pubertal knockout and wildtype females (8-9 weeks) were housed with C57BL/6NCrl proven males and inspected for vaginal plugs daily 08:30-9:30 am. On the day when the vaginal plug was observed, confirming that mating had occurred, oviducts were collected from *RSK3*^{+/+} and *RSK3*^{-/-} females (N=4 per genotype). A 27G needle was used to puncture oviducts and allow the oocytes to flow out so as to determine the number of ovulations. Finally, fertility was assessed by mating C57BL/6NCrl proven males with female *RSK3*^{-/-} mice (N=4) or *RSK3*^{+/+} mice (N=4) for six months. The frequency and number of pups per litter were noted for each female.

5.3.6 RT PCR

Total RNA was purified from granulosa cells or isolated ovulating follicles (described in Results section) using the Direct-zol RNA miniprep isolation kit from Zymo Research (R2050). The purity and quantity of RNA was evaluated using the Nanodrop 2000 (Thermo Scientific), followed by cDNA synthesis from 250ng of total RNA using the iScript cDNA Synthesis kit (BioRad). qPCR assays to determine relative mRNA abundance were conducted on CFX384 (BioRad) with diluted cDNA samples. The succeeding conditions were performed by CFX384: an initial denaturation of 95°C for 5 minutes followed by 39 cycles of 95°C for 15 seconds, 58°C for

30 seconds for annealing and 95°C for 10 seconds. The primers, used for the experiments with efficiencies ranging from 90-110% and a correlation coefficient of 0.95-1.00, are given in Table 1. Transcript abundance was normalized to four control genes (*B2m*, *Gapdh*, *L19* and *Sdha*).

5.3.7 PCR arrays

We performed three PCR arrays using RNA from isolated ovulating follicles of superovulated immature mice treated with PD0325901 and vehicle (N=3 mice per group). Each plate had samples from one vehicle and one inhibitor treated mice. Ovaries were collected at 8h after hCG stimulation and 2 follicles were isolated per mouse (1 follicle per ovary). Next, we purified RNA from these 2 follicles and carried out cDNA synthesis using the RT² First strand Kit (Qiagen #330401) to synthesize cDNA from 400ng of total RNA. We ran the RT² Wound Healing Profiler PCR Array (Qiagen #330231 PAMM1212E-4) with 84 genes (associated with tissue remodeling and leukocyte infiltration), 5 reference genes and 7 proprietary controls to monitor genomic DNA contamination, first strand synthesis and real time PCR efficiency. We chose the Wound Healing array as it contains genes involved in both tissue remodeling (e.g. *Actc1*, *Coll1a1* and *Ctsl*) and leukocyte infiltration (e.g. *Ccl7*, *Cxcl11* and *Fgf2*). The array was performed according to the manufacturer's instructions. Briefly, we prepared the PCR components in a loading reservoir and added 10µl of mix to each well using a multichannel pipette and EZ load covers (included in the kit). We ran the recommended qPCR program of 1 cycle for 10 minutes at 95 °C, 40 cycles of 15 seconds at 60 °C and 1 minute at 60 °C. We also ran a dissociation (melting) curve analysis to verify PCR specificity. The threshold cycle (C_q) values were transferred to a blank excel sheet, formatted, and uploaded to the Qiagen website for analysis. We then performed qPCR to confirm the differentially expressed genes from the PCR arrays.

5.3.8 Protein extraction and immunoblotting

Total protein was extracted from either a pure population of granulosa cells collected at 8h post-hCG (for ERK1/2 pathway evaluation) or whole ovaries collected at 18h post-hCG (for quantifying Star abundance). Samples were homogenized in total extract lysis buffer (25mM Tris-HCl pH 7.5, 5mM MgCl₂, 10% glycerol, 100mM NaCl, 0.01% NP-40, 500µM dithiothreitol and distilled water) with freshly added 1% protease and phosphatase inhibitors (G Biosciences, St. Louis, MO, U.S.A) and stored at -80°C until further use. At the time of immunoblotting, 5% Laemmli solution was added to each sample, which was subsequently boiled at 95°C for 5 minutes. A 10% SDS-PAGE gel was used to separate proteins by electrophoresis and then transferred onto a nitrocellulose membrane followed by blocking in 5% milk in Tris-buffered saline with 0.1% Tween-20 (TBS-T) at room temperature. Membranes were incubated overnight at 4°C with primary antibodies against: phospho-ERK1/2 (Thr202/Tyr204; #4376, Cell Signaling, dilution of 1:1000), total-ERK1/2 (#4695, Cell Signaling, 1:1000), Star (#sc-25806, Santa Cruz, 1:500) and beta-actin (Actb; ab8227, Abcam, 1:10 000). Membranes were washed three times for 10 minutes in TBS-T before and after incubation with secondary antibody goat anti-rabbit-IgG (1:10000, #ab6721, Abcam) for 1.5 hours at room temperature. The Immun-Star Western Chemi luminescent Kit (Bio-Rad) and Chemidoc Analyzer were used to detect immunoblotted proteins. Densitometry of the protein bands was measured using ImageLab software. For measurement of ERK1/2 activity, the membranes were first blotted with phospho-ERK1/2 antibody and following its readout, the membranes were stripped using stripping buffer (10 % SDS – 20 ml, 0.5 M Tris – Hcl, pH 6.8 – 12.5 ml, DEPC H₂O – 67.5 ml and 2-mercaptoethanol – 0.8 ml) and re-blotted with total-ERK1/2 antibody.

5.3.9 Statistical Analysis

Ovulation data and mRNA abundance data were expressed as mean \pm SEM and analyses were performed using SigmaPlot 12.3 Software, San Jose, CA, U.S.A. The data was checked for normality by the Shapiro-Wilke test and analyzed via the unpaired Student's *t*-test. Data involving more than one time point were analyzed by one-way ANOVA. A significance level of $P < 0.05$ was used for statistical inference.

5.4 Results

5.4.1 PD0325901 treatment at 4h post-hCG inhibits ERK1/2 activity in granulosa cells

We have previously demonstrated that PD0325901 pretreatment 2h before hCG stimulus inhibits immediate early ERK1/2 activity in granulosa cells leading to anovulation (Siddappa et al., 2015). In the present study we wanted to test if PD0325901 at 4h after hCG treatment impacts ovulation in mice. First, we examined if this treatment resulted in inactivation of ERK1/2 signaling as measured by phospho-ERK1/2 levels in purified granulosa cells at 8h post-hCG (Fig. 1A).

5.4.2 PD0325901 treatment at 4h post-hCG inhibits follicular rupture without altering oocyte maturation and luteinization

In our previous study, we showed that inhibition of ERK1/2 activity at 2h before hCG treatment resulted in anovulation with trapped oocytes within large antral follicles. The oocytes within these non-luteinized follicles were in germinal vesicle (GV) stage indicating failure of meiotic resumption and cumulus cells failed to undergo expansion. In the current study, we found that inhibition of ERK1/2 activity 4h after the LH surge dramatically reduced the ovulation rate ($P < 0.05$) compared to vehicle-treated mice (Fig. 1B). Histologically, the ovaries of vehicle-treated mice showed numerous well-developed corpora lutea (Fig. 1C). Conversely, the ovaries of PD0325901-treated mice showed numerous distended unruptured preovulatory follicles with

sporadic corpora lutea compared to vehicle-treated mice (Fig. 1C). Upon close observation, cumulus expansion was evident in follicles of PD0325901-treated mice (Fig. 2A) and was comparable to those of vehicle-treated mice. Some of the oocytes in histological sections showed polar body (Fig. 2A). We also examined the ovulated oocytes collected from the oviducts in both vehicle and PD0325901-treated mice for meiotic resumption. Polar bodies, indicative of metaphase II, were evident upon DAPI staining of ovulated oocytes in PD0325901-treated mice (Fig. 2B), similar to those of vehicle-treated mice (data not shown). These observations demonstrated that inhibition of ERK1/2 at 4h post-hCG did not affect oocyte maturation.

Further, observation at higher magnification revealed that the unruptured ovulatory-sized follicles in PD0325901-treated mice appeared to have undergone luteinization as evidenced by granulosa cells showing morphological features of luteal cells (Fig. 2C). There was also evidence of neovascularization as indicated by presence of numerous capillaries containing red blood cells among granulosa cells within unruptured ovulatory-sized follicles in PD0325901-treated mice (Fig. 2C). Immunoblot analysis of ovaries from PD0325901-treated mice collected at 18h post-hCG revealed similar levels of Star protein compared to those of vehicle-treated mice even though inhibitor treated mice had markedly fewer ovulations (Fig. 2D).

5.4.3 Expression profile of RSK isoforms in granulosa cells

It was reported that RSK3 is one of the ERK1/2 targets that is induced by LH surge in granulosa cells of ovulating follicles (Fan et al., 2009b). Therefore, we wanted to test if RSK3, as mediator of continued ERK1/2 signaling, plays a role in the mouse ovary. First, we determined the expression pattern of all four RSK isoforms in granulosa and luteal cells collected at specific stages of gonadotropin stimulated follicular and luteal growth. The mRNA abundance of *Rps6ka2* (RSK3) remained unchanged through eCG-induced follicular growth, but its relative amounts were

higher by about 5-fold at 4h post-hCG compared to 48h post-eCG ($P < 0.003$, Fig. 3). The levels of RSK3 mRNA remained high at 7 and 12h post-hCG and returned to baseline by 24h post-hCG. On the contrary, there were no significant changes in *Rps6ka1* (RSK1), *Rps6ka3* (RSK2) and *Rps6ka6* (RSK4) transcript abundance through follicular and luteal development ($P > 0.05$; Fig. 3).

5.4.4 Ovulation rate and fertility of *RSK3*^{-/-} mice

Based on unique hCG-induced expression of *Rps6ka2*, we hypothesized that RSK3 may play a significant role in ovulation in mice. We used the recently developed *RSK3* knockout mice (*RSK3*^{-/-}) (Li et al., 2013) to investigate the potential role of RSK3 in ovulation and fertility. First, we examined the expression of *RSK3* in granulosa cells at peak expression time-point, 4h post-hCG. As expected, transcript abundance of *Rps6ka2* was 13-fold lower in *RSK3*^{-/-} granulosa cells compared to *RSK3*^{+/+} granulosa cells ($P < 0.01$, Fig. 4A). On the contrary, mRNA levels of *Rps6ka1*, *Rps6ka3* and *Rps6ka6* genes were similar between granulosa cells of both genotypes (data not shown) demonstrating that there was no compensatory expression of other RSK isoforms.

As part of reproductive phenotyping, we first examined the superovulatory response in immature *RSK3*^{-/-} and *RSK3*^{+/+} mice. Ovulation rate in response to superovulation treatment was about 80% lower in *RSK3*^{-/-} than *RSK3*^{+/+} mice ($P < 0.01$; Fig. 4B). We then examined ovulation rate in adult *RSK3*-knockout and wildtype mice. Ovulation rate, as measured by the number of oocytes in the oviducts on the day of vaginal plug, was about 40% lower in *RSK3*^{-/-} than *RSK3*^{+/+} mice ($P < 0.05$; Fig. 4C). In line with this aberrant ovulatory phenotype, breeding trials revealed that *RSK3*^{-/-} mice were sub-fertile with smaller litter size than *RSK3*^{+/+} mice ($P < 0.05$; Fig. 4D).

5.4.5 PD0325901 treatment at 4h post-hCG results in aberrant expression of genes involved in tissue remodeling and leukocyte infiltration in ovulating follicles

Data from both pharmacological and genetic models showed that lack of ERK1/2 signaling beyond 4h post-hCG results in defective follicular rupture. We sought to define the molecular determinants of this deficient follicular rupture. We chose to use a pharmacological inhibition model for two reasons. First, the pharmacological model allows us to inhibit ERK1/2 signals at a precise time point during the ovulatory process. Second, the pharmacological model would inhibit all downstream mediators of ERK1/2 signals resulting in robust anovulatory phenotype, whereas sub-fertile *RSK3*^{-/-} mice lacked one of the many ERK1/2 mediators.

Our initial qPCR analyses of RNA from granulosa cells collected from the whole ovaries at 8h post-hCG showed mostly non-significant differences in transcript abundance between vehicle and PD0325901-treated mice (data not shown). We reasoned that this may be because collection of granulosa cells from the whole ovary may not enrich the small number of cells with gene expression differences localized to a small area of the ovulatory follicle. For that reason, we chose to isolate two ovulatory follicles per mouse (one per ovary) and purify RNA from the whole follicles. Even though this method would yield a mixture of granulosa, theca and oocytes, it is still a better option to obtain an enriched population of cells expressing genes involved in follicle rupture.

First, we examined the transcript abundance of the genes involved in extracellular matrix remodeling during ovulation in ovulating follicles of vehicle and PD0325901-treated mice (Duffy et al., 2019). There were higher levels of *Timp2*, *Adamts10*, and *Mmp11*, but lower level of *Timp1* at 8h post-hCG in ovulating follicles of PD0325901-treated than those of vehicle-treated mice (Fig. 5A). With this observation of imbalance in the expression of the extracellular matrix

proteases and their inhibitors, we sought to identify other dysregulated genes involved in tissue remodeling and leukocyte infiltration associated with follicular rupture (Oakley et al., 2010). We used a PCR-array to identify differentially expressed genes between vehicle and PD0325901-treated follicles. Upon running the arrays in three replicates using follicular samples from separate groups of mice, we found one upregulated gene (*Actc1*) and four downregulated genes (*Ccl7*, *Ccl12*, *Cxcl1* and *Cxcl3*) common for the three array replicates (Fig. 5B). Of these, we were able to confirm higher levels of *Actc1* and lower levels of *Ccl7* transcripts in ovulating follicles of PD0325901-treated compared to those of vehicle-treated mice (Fig. 5C).

5.5 Discussion

In the present study, inhibition of ERK1/2 activity at 4h after hCG stimulation disrupted follicular rupture without altering cumulus expansion and oocyte meiotic maturation. Reduced ovulation rate due to ERK1/2 inhibition in our current model is different from previous studies (Siddappa et al., 2015, Fan et al., 2009b), which demonstrated anovulation due to lack of LH-induced ERK1/2 activity. In those studies, ERK1/2 signals were absent right from the beginning of the ovulatory process. Whereas in the present study, initial ERK1/2 activity was not affected as the inhibitor was administered only at 4h after hCG treatment. Like those previous studies, there were large distended unruptured preovulatory follicles in ovaries of mice with ERK1/2 inhibition at 4h hCG. However, contrary to those previous studies, trapped oocytes within the unruptured follicles from PD0325901-treated mice in this study were meiotically mature with normally expanded cumulus. This observation is consistent with the fact that cumulus expansion and oocyte meiotic resumption would have started by 4h post-hCG when the inhibitor was administered. Indeed, genes critical for meiotic resumption and cumulus expansion such as *Has2*, *Areg*, *Ereg*,

Ptx3 and others are all highly expressed, by 4h post-hCG in mice (Wigglesworth et al., 2015, Fan et al., 2009b, Robker et al., 2018).

Another important contrast between this study and the previous studies (Siddappa et al., 2015, Fan et al., 2009b) with ERK1/2 signal abrogation from the beginning of the ovulatory process is luteinization. In both studies, abolition of ERK1/2 signal at the time of hCG treatment resulted in dramatically reduced expression of *Star* and complete absence of epithelial-to-mesenchymal transition, which is the hallmark of luteinization (Irving-Rodgers et al., 2004). In this study, we found that although the follicles that ovulated formed corpus luteum, the granulosa cells of large distended follicles that remained unruptured appeared to have undergone luteinization. This was supported by the fact that *Star* levels were similar in the ovaries of both vehicle and PD0325901-treated mice. In addition, the presence of blood-filled capillaries among granulosa cells indicated that the luteinization process was underway (Murphy, 2000). Since the marker of luteinization, *Star* as well as the driver of neovascularization, *Vegfa* are induced by immediate early transcription factors such as *Cebpa/b* (Sterneck et al., 1997, Fan et al., 2011), *Nr5a2* (Duggavathi et al., 2008b) and *Hif1/2* (Kim et al., 2009), it is possible that inhibition of ERK1/2 after their activation does not impact luteinization and angiogenesis. In line with this, intra luteal infusion of another ERK1/2 inhibitor PD98059 to bonnet monkeys on day 9 of luteal phase (period of high functioning corpus luteum), did not affect STAR mRNA levels and circulating progesterone concentration (Yadav and Medhamurthy, 2006). All these studies indicate that ERK1/2 signals beyond 4h post-hCG may not be necessary for luteinization and cumulus expansion.

Our data showed a dramatic induction of RSK3 in granulosa cells of ovulating follicles indicating that ERK1/2 signals are sustained beyond 4h and may play a role during mouse

ovulation. Confirming this hypothesis, *RSK3*^{-/-} showed reduced ovulation rate both in adult and superovulated immature mice and they were sub-fertile. These data clearly demonstrate that RSK3, one of the many ERK1/2 signal mediators, is important for ovulation. As it was shown that RSK3 in the oocyte is not necessary for maturation and meiotic progression (Dumont et al., 2005), it is likely that infertility in *RSK3*^{-/-} mice is due to molecular defects in other cell types in ovulating follicles. Taken together, data from both pharmacological and genetic models demonstrate that ERK1/2 signals beyond 4h post-hCG are needed for follicular rupture.

While most parts of the ovulating follicle are undergoing luteinization and angiogenesis, a small region in the follicular wall towards the ovarian surface undergoes a separate set of morphological changes (reviewed in (Duffy et al., 2019)). These unique regional changes lead to breaching of the follicular wall so that the COCs will be released into oviduct. This region-specific regulation of cellular differentiation and extracellular matrix remodeling has been a barrier to studying molecular mechanisms regulating follicular rupture. There have been several studies proposing various cytokines, cell types (granulosa, theca and leukocytes) and tissue remodeling enzymes involved in the ovulatory processes of angiogenesis, cell motility and follicular rupture (Brown et al., 2010, Cacioppo et al., 2017, Choi et al., 2017, Fraser and Duncan, 2005, Hazzard et al., 2000, Ko et al., 2006, Oakley et al., 2010, Palanisamy et al., 2006, Redmer and Reynolds, 1996). At the time of follicular rupture, proteinases degrade extracellular matrix and connective tissues at the apex of follicle in a circumferential manner (Russell and Robker, 2007). Important proteinases involved in the proteolysis of the extracellular matrix during follicular rupture include matrix metalloproteinases (MMPs), serine proteinases (Plasminogen activators and plasmin), a disintegrin and metalloproteinase domain with thrombospondin motifs (ADAMTSs) and cathepsin L (Ohnishi et al., 2005). Tissue inhibitors of metalloproteinases (TIMPs) regulate proteolytic

activities of MMPs and a ratio in favor of MMP activity results in ECM degradation whereas a ratio in favor of TIMP inhibits ECM degradation (McIntush and Smith, 1998). Among the tissue remodeling enzymes, TIMPs play contrasting roles because of their ability to regulate membrane-bound and secreted MMPs. For example, while TIMP2 inhibits MMP2 by direct binding in extracellular space, TIMP2 also participates in the activation of MMP2 through membrane-bound MMP14 (Jezierska and Motyl, 2009, Wang et al., 2000). These data demonstrate that both higher and lower expression of TIMPs can have negative impact on the activity of MMPs. Thus, a balanced expression of various tissue remodeling enzymes is necessary for normal follicular rupture. Our data of lower *Timp1* and higher *Timp2* demonstrated an imbalance of TIMPs in ovulatory follicles of PD0325901-treated mice. Supporting this, it has been reported that presence of excessive TIMP2 can inhibit MMP14 activity and decrease the processing of proMMP2 to active MMP2 in BS-C-1 cells (Hernandez-Barrantes et al., 2000, Bernardo and Fridman, 2003). Further, our data of abnormal expression of *Adams10* and *Mmp11* are consistent with dysregulated matrix protease machinery in ovulating follicles in which ERK1/2 signaling was inhibited at 4h post-hCG. This imbalance in matrix proteases and their inhibitors may have resulted in inefficient proteolysis of the extracellular matrix, which is required for normal follicular rupture.

In conclusion, our data from both pharmacological and genetic models demonstrate that lack of ERK1/2 signaling during ovulation results in abnormal follicular rupture. Most importantly, our pharmacological inhibition of ERK1/2 at 4h post-hCG inhibited follicular rupture without affecting luteinization, oocyte meiosis and cumulus expansion. Our molecular phenotyping indicate that sustained ERK1/2 signals play a critical role in balanced expression of genes involved in extracellular matrix degradation and leukocyte infiltration necessary for successful follicular rupture (Figure 8). Finally, this pharmacological method of separation of

follicular rupture from luteinization and oocyte maturation offers an excellent experimental model to study molecular mechanisms of divergent tissue remodeling processes associated with luteinization and follicular rupture.

5.6 Acknowledgements

We would like to thank Rodrigo Bohrer for his invaluable assistance, as well as Kim Lévesque for expert technical help with animal work. We also thank Professors Sarah Kimmins, Jaswinder Singh and Luis Agellon for allowing us to use their laboratory facilities for this study.

Funding

This work was partly funded by the National Science and Engineering Research Council (NSERC) of Canada (RGPIN-371850 and RGPIN-2019-06667 to RD, and RGPIN-2017-04736 to PPR). This work was also supported by grants from the Canadian Institutes for Health Research (CIHR; MOP-142374 to PPR). EM was funded by NSERC-CREATE and McGill Graduate Excellence Fellowship. DS was funded by McGill Graduate Student Fellowship, Department of Animal Science, Graduate Excellence Fellowship and RQR. YS was funded by RQR-CREATE and McGill Graduate Excellence Fellowship. PPR is a senior scholar of the Fonds de la recherche du Québec - Santé (FRQS).

Author contribution

E.M. designed experiments, collected and processed samples, analyzed and interpreted data, prepared figures and wrote manuscript; D.S. and Y.S. contributed to ideas, designed experiments, collected and processed samples, interpreted data and reviewed the manuscript; P.P.R. performed reproductive phenotyping of RSK3 mice and reviewed the manuscript and V.B. performed analyses of oocyte maturation, contributed to experimental design and reviewed the manuscript; R.D. conceived the study, designed experiments, analyzed and interpreted data, and edited the manuscript.

Disclosure and conflict of interest

Authors do not have any conflicts of interest.

5.7 Figures

Figure 5.7.1 Inhibition of ERK1/2 at 4h post-hCG results in reduced ovulation rate

(A) Transient inhibition of hCG induced ERK1/2 activity by PD0325901 treatment. Granulosa cells from mice treated with PD0325901 at 4h after hCG administration were collected at 7h after hCG treatment and showed absence of phosphorylation of ERK1/2 at Thr202/Tyr204 compared to vehicle-treated mice. N=2 mice/group. (B) Treatment of immature mice with a single dose of 25 μ g/g of PD0325901 at 4h hCG reduced the ovulation rate compared to vehicle-treated mice during superovulation. (Vehicle control, n=7 mice, PD0325901 n=10 mice). * indicates significant difference between the two groups ($P < 0.05$). (C) Histology of the ovaries collected at 18h after hCG from PD0325901 or vehicle treated mice. Numerous corpora lutea were observed in ovaries collected from mice which were treated with vehicle. Ovaries from PD0325901-treated mice showed distended unruptured preovulatory follicles with reduced number of corpus luteum compared to vehicle treated mice.

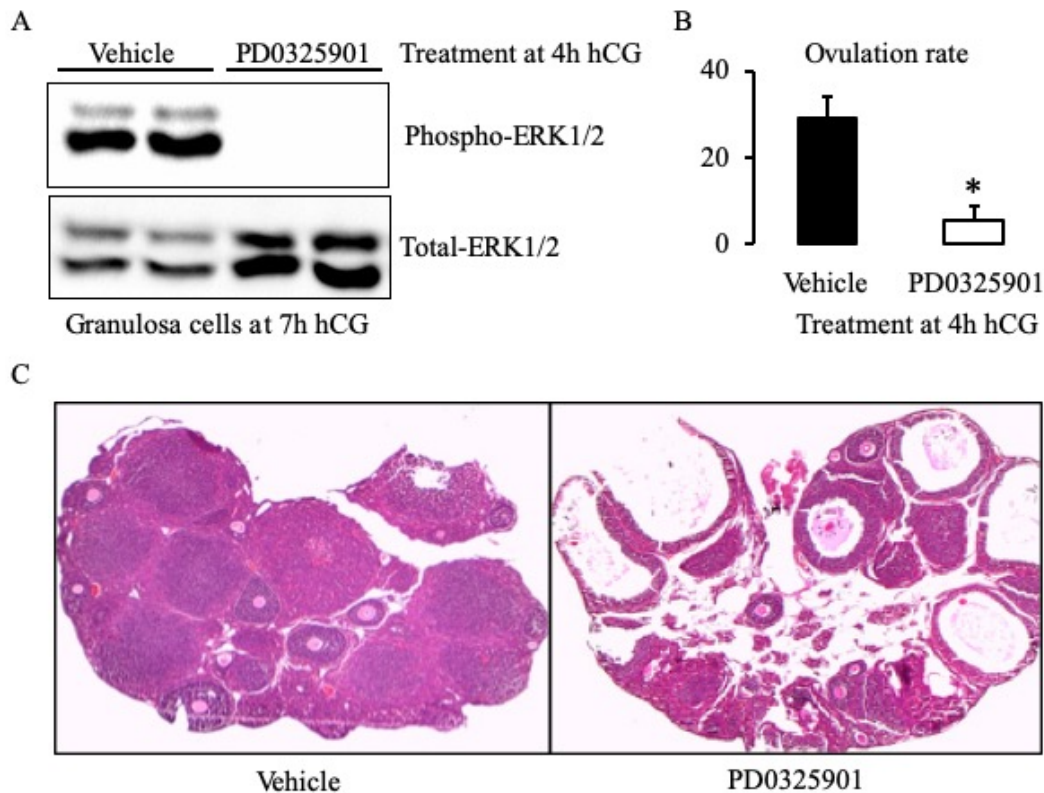


Figure 5.7.2 Inhibition of ERK1/2 at 4h post-hCG disrupts follicular rupture without affecting cumulus expansion, oocyte maturation and luteinization

(A) Metaphase II oocyte that was trapped inside the unruptured follicle showing extruded polar body (arrow) indicating unaltered oocyte maturation. Trapped cumulus-oocyte complexes inside the unruptured follicles showed normal cumulus expansion (arrowhead). Mice were administered with PD0325901 at 4h hCG during superovulation and ovaries were collected at 18h after hCG. (B) Metaphase II oocytes with extruded polar body in PD0325901 treated mice. COCs were collected from the oviduct at 18h hCG. (C) In response to the LH surge, granulosa cells adjacent to the basement membrane inside the distended unruptured follicle underwent luteinization and neovascularization. (D) Expression of steroidogenesis related protein Star was unaltered in mice treated with PD0325901 at 4h after hCG. Ovaries were collected at 18h after hCG.

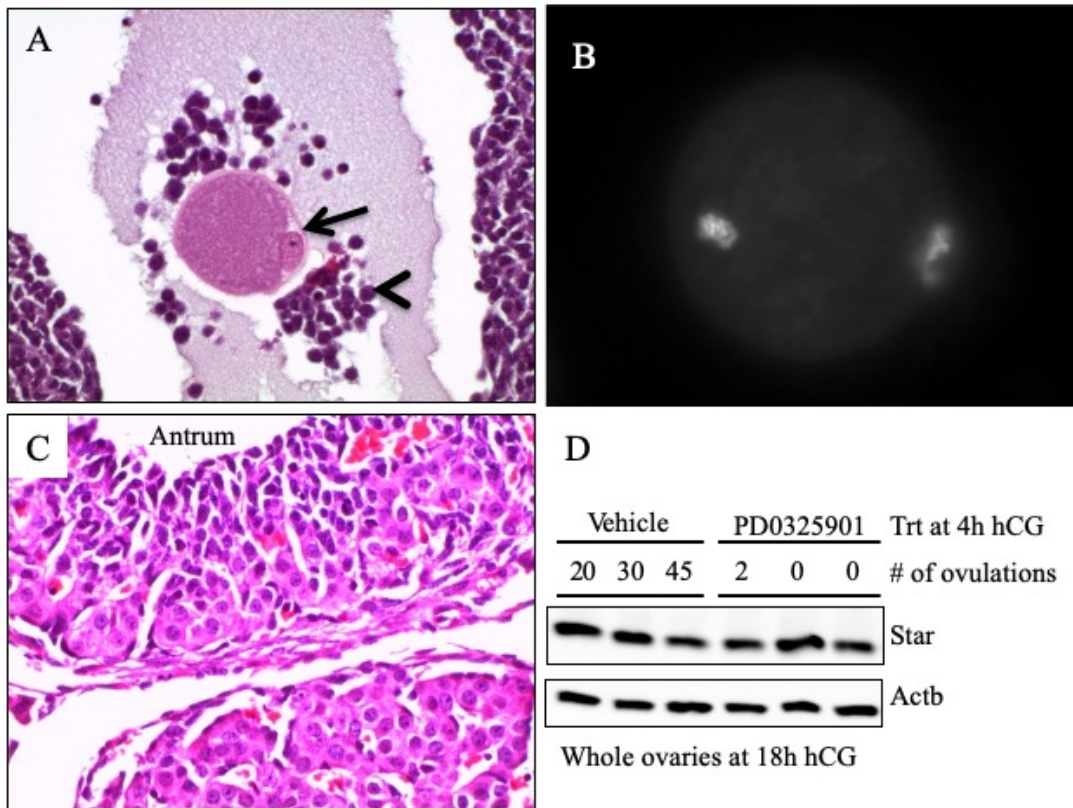


Figure 5.7.3 RSK3 is dramatically induced by hCG treatment

Relative mRNA levels of *Rps6ka2*, *Rps6ka1*, *Rps6ka3* and *Rps6ka6* in granulosa and luteal cells collected at different time points of superovulation from murine ovaries. Data are expressed as a mean \pm S.E.M. **P<0.01

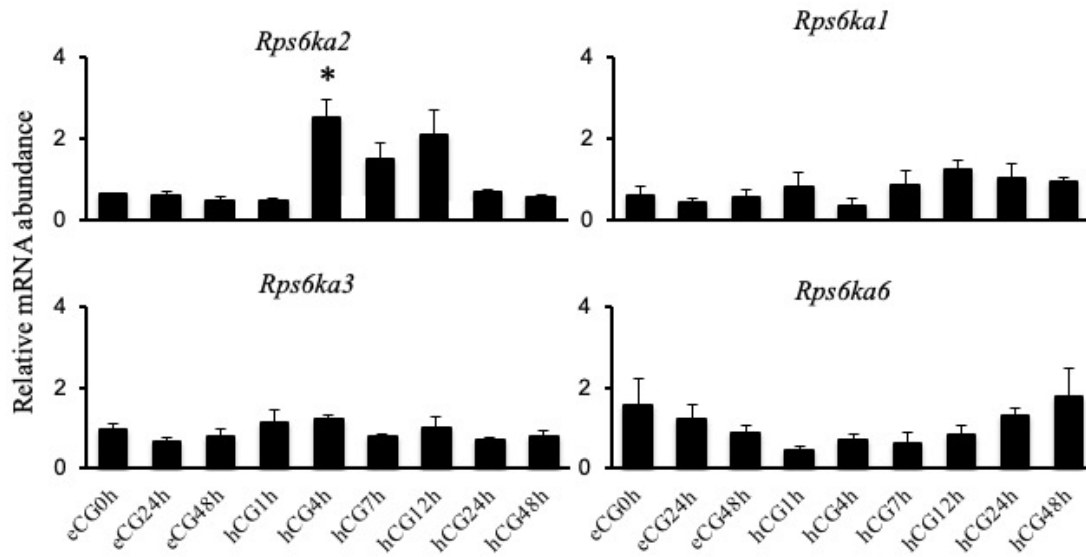


Figure 5.7.4 Reproductive phenotype of *RSK3*^{-/-} mice

(A) Relative mRNA levels of *Rps6ka2* in granulosa cells from *RSK3*^{+/+} and *RSK3*^{-/-} mice (N=3 per genotype) collected at 4h post-hCG. Data are expressed as a mean \pm S.E.M. *P<0.05

(B and C) *RSK3*^{+/+} and *RSK3*^{-/-} mice have different ovulation rates. Ovulation rate was established by counting the number of oocytes in the oviducts of superovulated mice wild-type (N=5) mice and *RSK3*-knockout (N=6) mice 18h-post hCG administration.

(D) Litter sizes from wild-type mice (N=4) and *RSK3*-knockout mice (N=4) were averaged amongst litters per mouse over a 6-month breeding trial. Data are expressed as mean \pm S.E.M. from both genotyped groups. *P<0.05 and **P<0.01

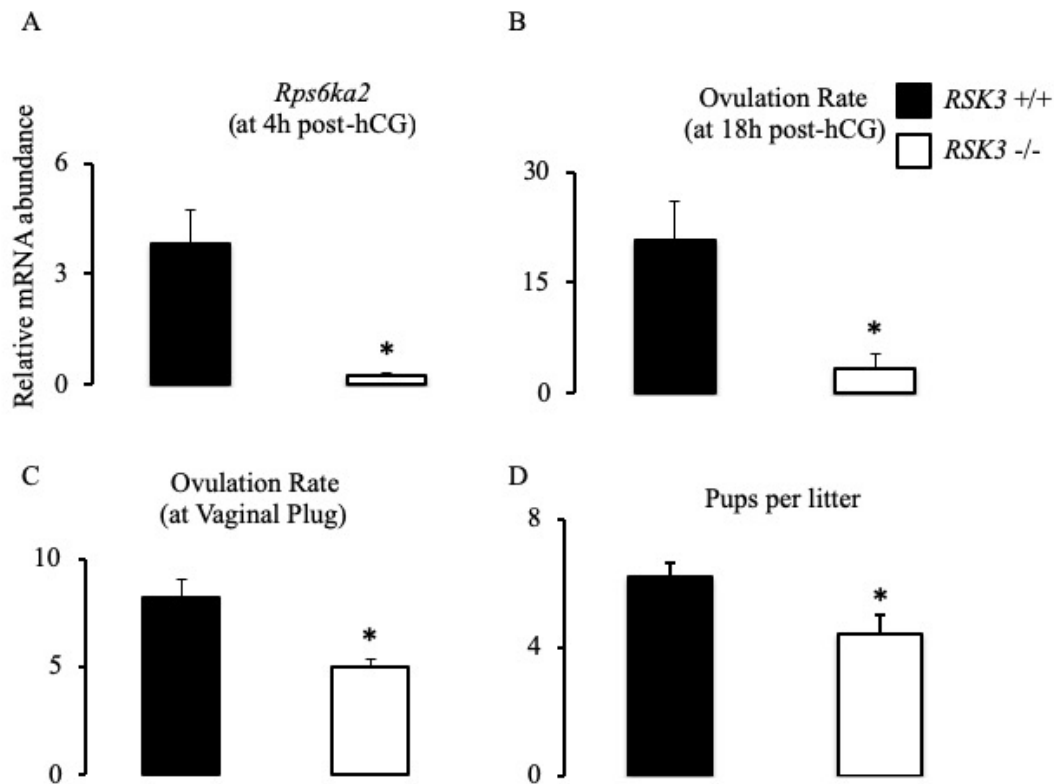


Figure 5.7.5 Inhibition of ERK1/2 at 4h post-hCG results in abnormal expression of genes associated with extracellular matrix degradation and leukocyte infiltration

(A) Gene expression of *Timp1*, *Timp2*, *Adamts10* and *Mmp11* was measured in granulosa cells collected by follicular puncture at 8h post-hCG with or without inhibition of ERK1/2 at 4h hCG. Data are expressed as a mean \pm S.E.M. *P<0.05 (B) Number of upregulated and downregulated genes in the PCR arrays. (C) Relative mRNA levels of *Actc1*, *Ccl7*, *Ccl12* and *Cxcl1* in granulosa cells collected at 8h hCG with or without inhibition of ERK1/2 at 4h hCG. Data are expressed as a mean \pm S.E.M. *P<0.05

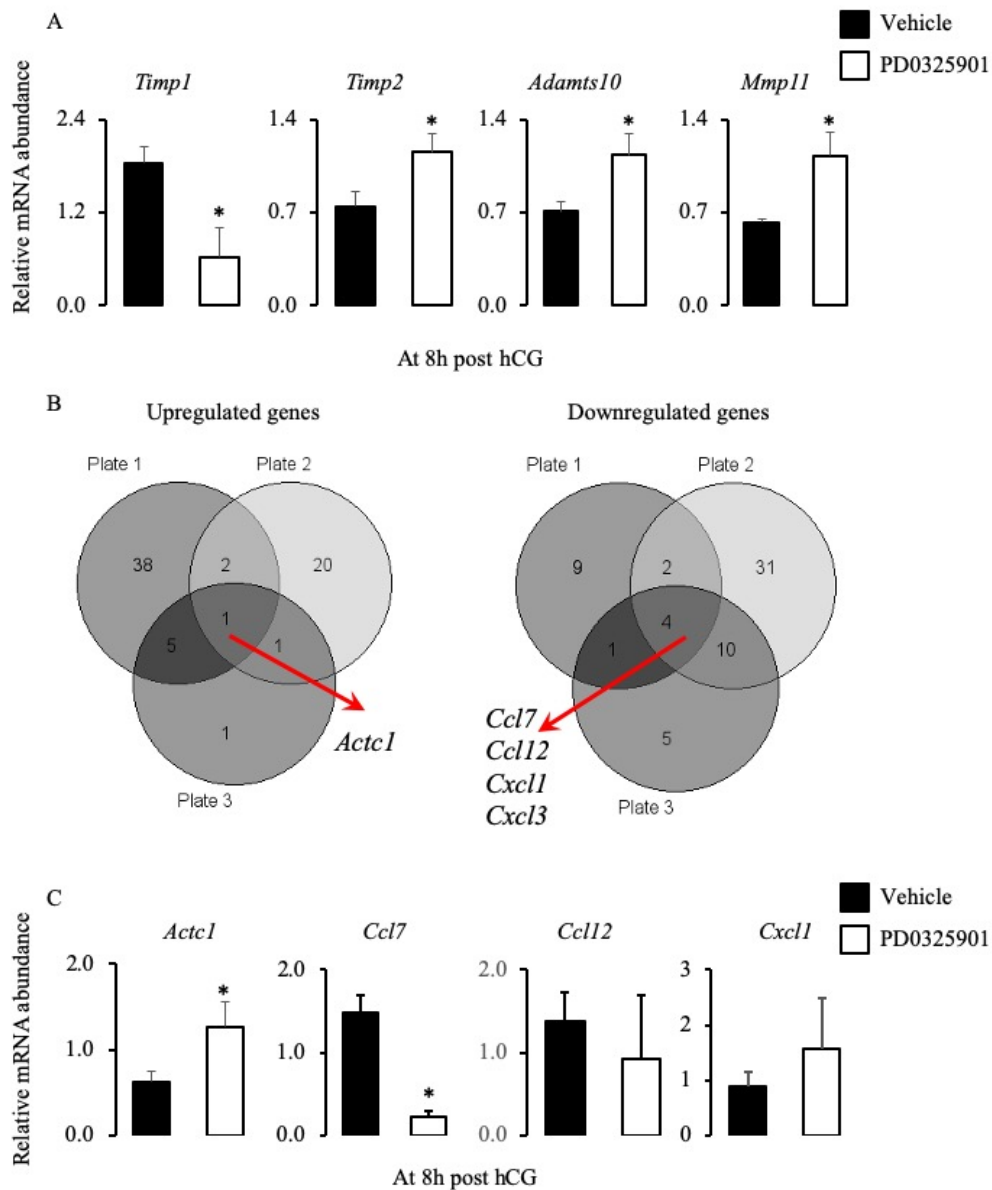
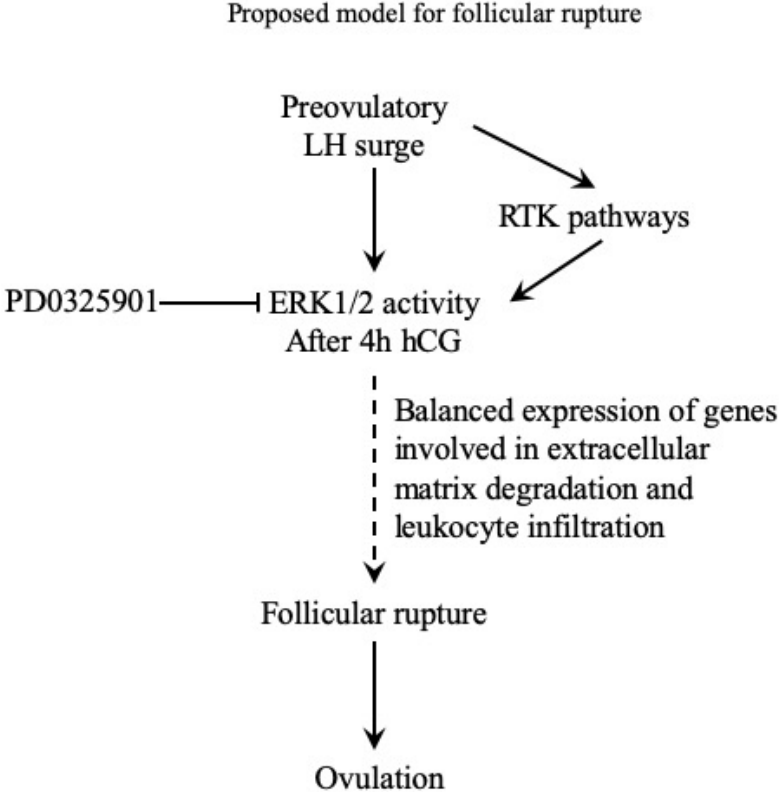


Figure 5.7.6 Proposed mechanism for ERK1/2 regulation of follicular rupture.



5.8 Tables

Table 5.8.1 List of primer sequences used in RT-PCR

Gene	Forward Primer	Reverse Primer
Actc1	CTGGATTCTGGCGATGGTGTA	CGGACAATTTACGTTTCAGCA
Adamts10	GGCTGGGCCTCACATTCAA	GAAGGCAATCTCATAGCTCTCC
B2m	TTCTGGTGCTTGTCTCACTGA	CAGTATGTTCTGGCTTCCCATTTC
Ccl12	ATTTCCACACTTCTATGCCTCCT	ATCCAGTATGGTCCTGAAGATCA
Ccl7	GCTGCTTTCAGCATCCAAGTG	CCAGGGACACCGACTACTG
Cxcl1	CTGGGATTCACCTCAAGAACATC	CAGGGTCAAGGCAAGCCTC
Gapdh	AGGTCGGTGTGAACGGATTTG	TGTAGACCATGTAGTTGAGGTCA
L19	ATGAGTATGCTCAGGCTACAGA	GCATTGGCGATTTTCATTGGTC
Mmp11	CCGGAGAGTCACCGTCATC	GCAGGACTAGGGACCCAATG
Rps6ka1	CCATCACACACCACGTCAAG	TTGCGTACCAGGAAGACTTTG
Rps6ka2	GCAGGTTCTTCTCCGTGTACC	GAGGGGTCTGCCTTCTCAA
Rps6ka3	ATGGATGAACCTATGGGAGAGG	AAGCTGTCTAGCATCAGAGCC
Rps6ka6	CGCCATCAGCCAAACTCAGAT	ATGTTTCGCTTTTTTCATGTTCCG
Sdha	GGAACACTCCAAAAACAGACCT	CCACCACTGGGTATTGAGTAGAA
Timp1	GCAACTCGGACCTGGTCATAA	CGGCCCGTGATGAGAAACT
Timp2	TCAGAGCCAAAGCAGTGAGC	GCCGTGTAGATAAACTCGATGTC

5.9 Bibliography

- ADRIAENSSENS, T., WATHLET, S., SEGERS, I., VERHEYEN, G., DE VOS, A., VAN DER ELST, J., COUCKE, W., DEVROEY, P. & SMITZ, J. 2010. Cumulus cell gene expression is associated with oocyte developmental quality and influenced by patient and treatment characteristics. *Hum Reprod*, 25, 1259-70.
- ANJUM, R. & BLENIS, J. 2008. The RSK family of kinases: emerging roles in cellular signalling. *Nat Rev Mol Cell Biol*, 9, 747-58.
- ASHKENAZI, H., CAO, X., MOTOLA, S., POPLIKER, M., CONTI, M. & TSAFRIRI, A. 2005. Epidermal growth factor family members: endogenous mediators of the ovulatory response. *Endocrinology*, 146, 77-84.
- BEN-AMI, I., ARMON, L., FREIMANN, S., STRASSBURGER, D., RON-EL, R. & AMSTERDAM, A. 2009. EGF-like growth factors as LH mediators in the human corpus luteum. *Hum Reprod*, 24, 176-84.
- BERNARDO, M. & FRIDMAN, R. 2003. TIMP-2 (tissue inhibitor of metalloproteinase-2) regulates MMP-2 (matrix metalloproteinase-2) activity in the extracellular environment after pro-MMP-2 activation by MT1 (membrane type 1)-MMP. *Biochem. J*, 374, 739-745.
- DUFFY, D. M., KO, C., JO, M., BRANNSTROM, M. & CURRY, T. E. 2019. Ovulation: Parallels With Inflammatory Processes. *Endocr Rev*, 40, 369-416.
- DUGGAVATHI, R., VOLLE, D. H., MATAKI, C., ANTAL, M. C., MESSADDEQ, N., AUWERX, J., MURPHY, B. D. & SCHOONJANS, K. 2008. Liver receptor homolog 1 is essential for ovulation. *Genes Dev*, 22, 1871-6.
- DUMONT, J., UMBHAUER, M., RASSINIER, P., HANAUER, A. & VERLHAC, M.-H. 2005. p90Rsk is not involved in cytosolic factor arrest in mouse oocytes. *The Journal of cell biology*, 169, 227-231.
- DUPUIS, L., SCHUERMANN, Y., COHEN, T., SIDDAPPA, D., KALAISELVANRAJA, A., PANSERA, M., BORDIGNON, V. & DUGGAVATHI, R. 2014. Role of leptin receptors in granulosa cells during ovulation. *Reproduction*, 147, 221-9.
- FAN, H. Y., LIU, Z., JOHNSON, P. F. & RICHARDS, J. S. 2011. CCAAT/enhancer-binding proteins (C/EBP)-alpha and -beta are essential for ovulation, luteinization, and the expression of key target genes. *Mol Endocrinol*, 25, 253-68.
- FAN, H. Y., LIU, Z., SHIMADA, M., STERNECK, E., JOHNSON, P. F., HEDRICK, S. M. & RICHARDS, J. S. 2009. MAPK3/1 (ERK1/2) in ovarian granulosa cells are essential for female fertility. *Science*, 324, 938-41.
- FAN, H. Y., SHIMADA, M., LIU, Z., CAHILL, N., NOMA, N., WU, Y., GOSSEN, J. & RICHARDS, J. S. 2008. Selective expression of KrasG12D in granulosa cells of the mouse ovary causes defects in follicle development and ovulation. *Development*, 135, 2127-37.
- HERNANDEZ-BARRANTES, S., TOTH, M., BERNARDO, M. M., YURKOVA, M., GERVASI, D. C., RAZ, Y., SANG, Q. A. & FRIDMAN, R. 2000. Binding of active (57 kDa) membrane type 1-matrix metalloproteinase (MT1-MMP) to tissue inhibitor of metalloproteinase (TIMP)-2 regulates MT1-MMP processing and pro-MMP-2 activation. *Journal of Biological Chemistry*, 275, 12080-12089.
- IRVING-RODGERS, H. F., HARLAND, M. L. & RODGERS, R. J. 2004. A novel basal lamina matrix of the stratified epithelium of the ovarian follicle. *Matrix biology : journal of the International Society for Matrix Biology*, 23, 207-217.

- JEZIERSKA, A. & MOTYL, T. 2009. Matrix metalloproteinase-2 involvement in breast cancer progression: a mini-review. *Medical science monitor : international medical journal of experimental and clinical research*, 15, RA32-RA40.
- KIM, J., BAGCHI, I. C. & BAGCHI, M. K. 2009. Signaling by hypoxia-inducible factors is critical for ovulation in mice. *Endocrinology*, 150, 3392-3400.
- KIM, M., LEE, J. H., KOH, H., LEE, S. Y., JANG, C., CHUNG, C. J., SUNG, J. H., BLENIS, J. & CHUNG, J. 2006. Inhibition of ERK-MAP kinase signaling by RSK during *Drosophila* development. *EMBO J*, 25, 3056-67.
- LI, J., KRITZER, M. D., MICHEL, J. J., LE, A., THAKUR, H., GAYANILO, M., PASSARIELLO, C. L., NEGRO, A., DANIAL, J. B., OSKOU EI, B., SANDERS, M., HARE, J. M., HANAUER, A., DODGE-KAFKA, K. & KAPILOFF, M. S. 2013. Anchored p90 ribosomal S6 kinase 3 is required for cardiac myocyte hypertrophy. *Circ Res*, 112, 128-39.
- MCINTUSH, E. W. & SMITH, M. F. 1998. Matrix metalloproteinases and tissue inhibitors of metalloproteinases in ovarian function. *Reviews of Reproduction*, 3, 23-30.
- MURPHY, B. D. 2000. Models of luteinization. *Biology of reproduction*, 63, 2-11.
- OAKLEY, O. R., KIM, H., EL-AMOURI, I., LIN, P.-C. P., CHO, J., BANI-AHMAD, M. & KO, C. 2010. Perioovulatory leukocyte infiltration in the rat ovary. *Endocrinology*, 151, 4551-4559.
- OHNISHI, J., OHNISHI, E., SHIBUYA, H. & TAKAHASHI, T. 2005. Functions for proteinases in the ovulatory process. *Biochimica et Biophysica Acta (BBA)-Proteins and Proteomics*, 1751, 95-109.
- PARK, J. Y., SU, Y. Q., ARIGA, M., LAW, E., JIN, S. L. & CONTI, M. 2004. EGF-like growth factors as mediators of LH action in the ovulatory follicle. *Science*, 303, 682-4.
- RICHARDS, J. A. S., RUSSELL, D. L., OCHSNER, S. & ESPEY, L. L. 2002. Ovulation: new dimensions and new regulators of the inflammatory-like response. *Annual review of physiology*, 64, 69-92.
- RICHARDS, J. S. 2005. Ovulation: new factors that prepare the oocyte for fertilization. *Molecular and cellular endocrinology*, 234, 75-79.
- ROBKER, R. L., HENNEBOLD, J. D. & RUSSELL, D. L. 2018. Coordination of Ovulation and Oocyte Maturation: A Good Egg at the Right Time. *Endocrinology*, 159, 3209-3218.
- RUSSELL, D. L. & ROBKER, R. L. 2007. Molecular mechanisms of ovulation: co-ordination through the cumulus complex. *Human reproduction update*, 13, 289-312.
- SIDDAPPA, D., BEAULIEU, E., GEVRY, N., ROUX, P. P., BORDIGNON, V. & DUGGAVATHI, R. 2015. Effect of the transient pharmacological inhibition of mapk3/1 pathway on ovulation in mice. *PLoS One*, 10, e0119387.
- STERNECK, E., TESSAROLLO, L. & JOHNSON, P. F. 1997. An essential role for C/EBPbeta in female reproduction. *Genes & development*, 11, 2153-2162.
- WANG, Z., JUTTERMANN, R. & SOLOWAY, P. D. 2000. TIMP-2 is required for efficient activation of proMMP-2 in vivo. *The Journal of biological chemistry*, 275, 26411-26415.
- WIGGLESWORTH, K., EPPIG, J. J., LEE, K.-B., EMORI, C. & SUGIURA, K. 2015. Transcriptomic Diversification of Developing Cumulus and Mural Granulosa Cells in Mouse Ovarian Follicles1. *Biology of Reproduction*, 92.
- YADAV, V. & MEDHAMURTHY, R. 2006. Dynamic changes in mitogen-activated protein kinase (MAPK) activities in the corpus luteum of the bonnet monkey (*Macaca radiata*)

during development, induced luteolysis, and simulated early pregnancy: a role for p38 MAPK in the regulation of luteal function. *Endocrinology*, 147, 2018-2027.

CHAPTER 6

General discussion and conclusions

Problems associated with ovulation account for 30 percent of fertility problems in women (Health Canada). Polycystic ovary syndrome (PCOS), luteinized unruptured follicle (LUF) syndrome and other ovulatory disorders show phenotypes that can be associated with improper development (signaling) and dysregulation of gene expression of the preovulatory follicle leading to ovulatory failure (Duffy et al., 2019). Furthermore, luteinization is essential for maintenance of pregnancy and early embryonic losses occur as a result of defective luteinization. It is therefore necessary to improve our knowledge of the mechanisms by which FSH and LH regulate these events in order to better understand and consequently, provide a basis for the development of therapeutics tailored to addressing these challenges.

There is a paucity of information on the impact of FSH on the transcriptome as well as the involvement of histone modifications such as H3K4me3. The expression profile of FSH-regulated genes have mostly come from studies in the bovine, utilizing the dominant and subordinate follicles (Xu et al., 1995, Fortune et al., 2001, Ginther et al., 1996, Bao et al., 1997). Furthermore, majority of these studies used microarrays. We used RNA-Sequencing to study the effects of FSH in granulosa cells and found 1463 FSH-regulated genes, including previously identified genes such as *Lhcgr* and *Cyp19a1*. Next, we explored the role of FSH in the regulation of the active transcription marker, H3K4me3 using ChIP-Sequencing. Our data suggests that FSH regulates follicular development through changes in the transcriptome through deposition of H3K4me3 at the promoters of these genes.

Many studies have established that the LH surge positively regulates genes involved in inflammation, cellular movement, tissue remodeling and angiogenesis, while switching off the

expression of genes involved in metabolism and proliferation in multiple species (Rao et al., 2011, Wissing et al., 2014, Liu et al., 2017). The LH-induced ERK1/2 pathway has also been shown to be essential for ovulation. Inhibition of ERK1/2 *in vivo* results in an anovulatory phenotype with trapped oocytes and defective follicular rupture (Fan et al., 2009b, Schuermann et al., 2018, Siddappa et al., 2015). The switch from estrogen to progesterone production is a key factor in LH regulation of ovulation. However, ERK1/2 inhibition interferes with this switch and the follicle continues to produce high levels of estradiol. *Sult1e1* misregulation results in high estradiol concentrations which affects fertility as shown in *Sult1e1* knockout mice (Gershon et al., 2007). Additionally, *Cyp19a1* expression, which is usually repressed by LH, was not downregulated in the ERK1/2 inhibited granulosa cells, contributing to the increased estrogen levels.

We were interested in exploring the LH-regulated transcriptome. However, we also sought to understand how ERK1/2 and histone modifications such as H3K4me3 play a role in the regulation of the many genes that are required for ovulation. By combining data from ChIP-Sequencing, RNA-Sequencing and pharmacological inhibition of ERK1/2, we found that ERK1/2 regulates the deposition of H3K4me3 on the promoter region of 609 LH-regulated genes. Similar findings have been reported in developmental cells in mice and human melanoma cell lines, but not in granulosa cells (Li et al., 2016, Tee et al., 2014). Moreover, we were able to confirm our findings using qPCR and ChIP-qPCR. We also observed an enrichment of LH-induced pathways involved in TNF signaling, MAPK signaling and VEGF signaling, which was reversed by ERK1/2 inhibition.

Finally, having established the effect of inhibition of early ERK1/2 signaling on ovulation, we decided to take it a step further by exploring the role of sustained ERK1/2 signaling. We did this by pharmacological inhibition of ERK1/2 at four hours after the LH surge. Surprisingly, we did not find any effect on COC expansion, meiotic resumption and luteinization. However, follicular

rupture was disrupted, and genes involved in the regulation of the extracellular matrix and leukocyte were affected. We also looked at the RSK family which are effectors of the ERK1/2 signal (Anjum and Blenis, 2008b, Dumont et al., 2005) and found that LH induced the expression of RSK3 (we found a 3.5 fold increase in our RNA-Seq data) but not the other RSKs in granulosa cells of ovulating follicles. Therefore, we explored the role of RSK3 using a knockout mouse model and found a decrease in ovulation rate and smaller litter size. Thus, sustained ERK1/2 signaling appears to be critical for follicular rupture but not cumulus expansion, resumption of meiosis or luteinization.

Ovulation runs like a well-oiled machine, with different genes and pathways working in a temporal and spatial manner for the sole purpose of releasing a fertilizable oocyte in preparation for fertilization and pregnancy. The wealth of data in these studies have contributed in taking us one step closer to understanding the basic mechanisms of FSH and LH regulation of follicular development and ovulation. Furthermore, we have also highlighted the role of ERK1/2 in H3K4me3 deposition at the promoters of several ovulatory genes in granulosa cells.

Further studies need to be done to investigate the mechanism by which ERK1/2 regulates H3K4me3 deposition during follicular development and ovulation. It will also be interesting to understand the mechanism of regulation of H3K4me3 in terms of the precise enzymes that lead to its enrichment. In developmental genes, chromatin has been reported to exist in a poised state consisting of a bivalent domain with the presence of both a transcriptional activator (such as H3K4me3) and a transcriptional repressor (H3K27me3), which supposedly keeps these genes primed for activation (Tee et al., 2014). Thus, it will be interesting to see if a similar mechanism exists for the interaction of H3K4me3 with the deposition or removal of other histone marks such as H3K9me3 during follicular development and ovulation in granulosa cells. Finally, the

significance of differential transcript expression involving isoform switching events and differential transcript usage as well as their regulatory mechanisms need to be further explored.

Bibliography

- ADRIAENSSENS, T., WATHLET, S., SEGERS, I., VERHEYEN, G., DE VOS, A., VAN DER ELST, J., COUCKE, W., DEVROEY, P. & SMITZ, J. 2010. Cumulus cell gene expression is associated with oocyte developmental quality and influenced by patient and treatment characteristics. *Hum Reprod*, 25, 1259-70.
- ALHAMDOOSH, M., LAW, C., TIAN, L., SHERIDAN, J., NG, M. & RITCHIE, M. 2017. Easy and efficient ensemble gene set testing with EGSEA [version 1; referees: 1 approved, 3 approved with reservations]. *F1000Research*, 6.
- ANDREWS, S. 2014. *FastQC A Quality Control tool for High Throughput Sequence Data*.
- ANJUM, R. & BLENIS, J. 2008a. The RSK family of kinases: emerging roles in cellular signalling. *Nat Rev Mol Cell Biol*, 9, 747-58.
- ANJUM, R. & BLENIS, J. 2008b. The RSK family of kinases: emerging roles in cellular signalling. *Nature Reviews Molecular Cell Biology*, 9, 747-758.
- ASHKENAZI, H., CAO, X., MOTOLA, S., POPLIKER, M., CONTI, M. & TSAFRIRI, A. 2005. Epidermal growth factor family members: endogenous mediators of the ovulatory response. *Endocrinology*, 146, 77-84.
- ASSEY, R. J., HYTTEL, P., GREVE, T. & PURWANTARA, B. 1994. Oocyte morphology in dominant and subordinate follicles. *Molecular Reproduction and Development*, 37, 335-344.
- BAKER, J., HARDY, M. P., ZHOU, J., BONDY, C., LUPU, F., BELLVÉ, A. R. & EFSTRATIADIS, A. 1996. Effects of an Igf1 gene null mutation on mouse reproduction. *Molecular Endocrinology*, 10, 903-918.
- BALEY, J. & LI, J. 2012. MicroRNAs and ovarian function. *Journal of Ovarian Research*, 5, 8.
- BAO, B. & GARVERICK, H. A. 1998. Expression of steroidogenic enzyme and gonadotropin receptor genes in bovine follicles during ovarian follicular waves: a review. *Journal of animal science*, 76, 1903-1921.
- BAO, B., GARVERICK, H. A., SMITH, G. W., SMITH, M. F., SALFEN, B. E. & YOUNGQUIST, R. S. 1997. Changes in messenger ribonucleic acid encoding luteinizing hormone receptor, cytochrome P450-side chain cleavage, and aromatase are associated with recruitment and selection of bovine ovarian follicles. *Biol Reprod*, 56, 1158-68.
- BEN-AMI, I., ARMON, L., FREIMANN, S., STRASSBURGER, D., RON-EL, R. & AMSTERDAM, A. 2009. EGF-like growth factors as LH mediators in the human corpus luteum. *Hum Reprod*, 24, 176-84.
- BERNARDO, M. & FRIDMAN, R. 2003. TIMP-2 (tissue inhibitor of metalloproteinase-2) regulates MMP-2 (matrix metalloproteinase-2) activity in the extracellular environment after pro-MMP-2 activation by MT1 (membrane type 1)-MMP. *Biochem. J*, 374, 739-745.
- BERNSTEIN, B. E., MIKKELSEN, T. S., XIE, X., KAMAL, M., HUEBERT, D. J., CUFF, J., FRY, B., MEISSNER, A., WERNIG, M., PLATH, K., JAENISCH, R., WAGSCHAL, A., FEIL, R., SCHREIBER, S. L. & LANDER, E. S. 2006. A bivalent chromatin structure marks key developmental genes in embryonic stem cells. *Cell*, 125, 315-26.
- BIANCO, S., BELLEFLEUR, A.-M., BEAULIEU, É., BEAUPARLANT, C. J., BERTOLIN, K., DROIT, A., SCHOONJANS, K., MURPHY, B. D. & GÉVRY, N. 2019. The Ovulatory Signal Precipitates

- LRH-1 Transcriptional Switching Mediated by Differential Chromatin Accessibility. *Cell reports*, 28, 2443-2454.e4.
- BIANCO, S., BRUNELLE, M., JANGAL, M., MAGNANI, L. & GEVRY, N. 2014a. LRH-1 governs vital transcriptional programs in endocrine-sensitive and -resistant breast cancer cells. *Cancer Res*, 74, 2015-25.
- BIANCO, S., BRUNELLE, M., JANGAL, M., MAGNANI, L. & GÉVRY, N. 2014b. LRH-1 governs vital transcriptional programs in endocrine-sensitive and -resistant breast cancer cells. *Cancer research*, 74, 2015-2025.
- BILLON, P. & COTE, J. 2013. Precise deposition of histone H2A.Z in chromatin for genome expression and maintenance. *Biochim Biophys Acta*, 1819, 290-302.
- BINDER, A. K., RODRIGUEZ, K. F., HAMILTON, K. J., STOCKTON, P. S., REED, C. E. & KORACH, K. S. 2013. The absence of ER-beta results in altered gene expression in ovarian granulosa cells isolated from in vivo preovulatory follicles. *Endocrinology*, 154, 2174-87.
- BOLGER, A. M., LOHSE, M., & USADEL, B. 2014. Trimmomatic: A flexible trimmer for Illumina Sequence Data. *Bioinformatics*, btu170.
- BRAY, N. L., PIMENTEL, H., MELSTED, P. & PACTER, L. 2016. Near-optimal probabilistic RNA-seq quantification. *Nature Biotechnology*, 34, 525.
- BROWN, H. M., DUNNING, K. R., ROBKER, R. L., BOERBOOM, D., PRITCHARD, M., LANE, M. & RUSSELL, D. L. 2010. ADAMTS1 cleavage of versican mediates essential structural remodeling of the ovarian follicle and cumulus-oocyte matrix during ovulation in mice. *Biol Reprod*, 83, 549-57.
- CACIOPPO, J. A., LIN, P.-C. P., HANNON, P. R., MCDUGLE, D. R., GAL, A. & KO, C. 2017. Granulosa cell endothelin-2 expression is fundamental for ovulatory follicle rupture. *Scientific reports*, 7, 817-817.
- CAO, F., FANG, Y., TAN, H. K., GOH, Y., CHOY, J. Y. H., KOH, B. T. H., HAO TAN, J., BERTIN, N., RAMADASS, A., HUNTER, E., GREEN, J., SALTER, M., AKOULITCHEV, A., WANG, W., CHNG, W. J., TENEN, D. G. & FULLWOOD, M. J. 2017. Super-Enhancers and Broad H3K4me3 Domains Form Complex Gene Regulatory Circuits Involving Chromatin Interactions. *Scientific Reports*, 7, 2186.
- CHENG, F., LIU, J., ZHOU, S. H., WANG, X. N., CHEW, J. F. & DENG, L. W. 2008. RNA interference against mixed lineage leukemia 5 resulted in cell cycle arrest. *Int J Biochem Cell Biol*, 40, 2472-81.
- CHOI, Y., PARK, J. Y., WILSON, K., ROSEWELL, K. L., BRÄNNSTRÖM, M., AKIN, J. W., CURRY, T. E., JR. & JO, M. 2017. The expression of CXCR4 is induced by the luteinizing hormone surge and mediated by progesterone receptors in human preovulatory granulosa cells. *Biology of reproduction*, 96, 1256-1266.
- CHRISTENSON, L. K., GUNWARDENA, S., HONG, X., SPITSCHAK, M., BAUFELD, A. & VANSELOW, J. 2013. Research resource: preovulatory LH surge effects on follicular theca and granulosa transcriptomes. *Mol Endocrinol*, 27, 1153-71.
- CONNELLY, O. M. 2010. Progesterone receptors and ovulation. *Handb Exp Pharmacol*, 37-44.
- CRAIG, J. M. 2005. Heterochromatin—many flavours, common themes. *BioEssays*, 27, 17-28.
- DAHL, J. A., JUNG, I., AANES, H., GREGGAINS, G. D., MANAF, A., LERDRUP, M., LI, G., KUAN, S., LI, B., LEE, A. Y., PREISSEL, S., JERMSTAD, I., HAUGEN, M. H., SUGANTHAN, R., BJØRÅS, M., HANSEN, K., DALEN, K. T., FEDORCSAK, P., REN, B. & KLUNGLAND, A. 2016. Broad

- histone H3K4me3 domains in mouse oocytes modulate maternal-to-zygotic transition. *Nature*, 537, 548-552.
- DALBIÈS-TRAN, R. & MERMILLOD, P. 2003. Use of heterologous complementary DNA array screening to analyze bovine oocyte transcriptome and its evolution during in vitro maturation. *Biology of reproduction*, 68, 252-261.
- DINH, D. T., BREEN, J., AKISON, L. K., DEMAYO, F. J., BROWN, H. M., ROBKER, R. L. & RUSSELL, D. L. 2019. Tissue-specific progesterone receptor-chromatin binding and the regulation of progesterone-dependent gene expression. *Sci Rep*, 9, 11966.
- DOBIN, A., DAVIS, C. A., SCHLESINGER, F., DRENKOW, J., ZALESKI, C., JHA, S., BATUT, P., CHAISSON, M. & GINGERAS, T. R. 2013. STAR: ultrafast universal RNA-seq aligner. *Bioinformatics*, 29, 15-21.
- DRAIN COURT, M. A., FRY, R. C., CLARKE, I. J. & CAHILL, L. P. 1987. Follicular growth and regression during the 8 days after hypophysectomy in sheep. *J Reprod Fertil*, 79, 635-41.
- DUFFY, D. M., KO, C., JO, M., BRANNSTROM, M. & CURRY, T. E. 2019. Ovulation: Parallels With Inflammatory Processes. *Endocr Rev*, 40, 369-416.
- DUGGAVATHI, R. & MURPHY, B. D. 2009. Development. Ovulation signals. *Science*, 324, 890-1.
- DUGGAVATHI, R., VOLLE, D., MATAKI, C., ANTAL, M., MESSADDEQ, N., AUWERX, J., MURPHY, B., SCHOONJANS, K., DUGGAVATHI, R., VOLLE, D., MATAKI, C., ANTAL, M., MESSADDEQ, N., AUWERX, J., MURPHY, B. & SCHOONJANS, K. 2008a. Liver receptor homolog 1 is essential for ovulation. *Genes and Development*, 22, 1871-1876.
- DUGGAVATHI, R., VOLLE, D. H., MATAKI, C., ANTAL, M. C., MESSADDEQ, N., AUWERX, J., MURPHY, B. D. & SCHOONJANS, K. 2008b. Liver receptor homolog 1 is essential for ovulation. *Genes Dev*, 22, 1871-6.
- DÜMMLER, B. A., HAUGE, C., SILBER, J., YNTEMA, H. G., KRUSE, L. S., KOFOED, B., HEMMING, B. A., ALESSI, D. R. & FRÖDIN, M. 2005. Functional characterization of human RSK4, a new 90-kDa ribosomal S6 kinase, reveals constitutive activation in most cell types. *Journal of Biological Chemistry*, 280, 13304-13314.
- DUMONT, J., UMBHAUER, M., RASSINIER, P., HANAUER, A. & VERLHAC, M.-H. 2005. p90Rsk is not involved in cytostatic factor arrest in mouse oocytes. *The Journal of cell biology*, 169, 227-231.
- DUPUIS, L., SCHUERMANN, Y., COHEN, T., SIDDAPPA, D., KALAISELVANRAJA, A., PANSERA, M., BORDIGNON, V. & DUGGAVATHI, R. 2014. Role of leptin receptors in granulosa cells during ovulation. 147, 221.
- EPPIG, J. J., O'BRIEN, M. & WIGGLESWORTH, K. 1996. Mammalian oocyte growth and development in vitro. *Molecular Reproduction and Development*, 44, 260-273.
- ESPEY, L. L. 1980. Ovulation as an inflammatory reaction--a hypothesis. *Biology of reproduction*, 22, 73-106.
- ESPEY, L. L. & RICHARDS, J. S. 2002. Temporal and spatial patterns of ovarian gene transcription following an ovulatory dose of gonadotropin in the rat. *Biology of reproduction*, 67, 1662-1670.
- EVANS, A. C. O., IRELAND, J. L. H., WINN, M. E., LONERGAN, P., SMITH, G. W., COUSSENS, P. M. & IRELAND, J. J. 2004. Identification of Genes Involved in Apoptosis and Dominant Follicle Development During Follicular Waves in Cattle1. *Biology of Reproduction*, 70, 1475-1484.

- FAN, H.-Y., GONZALEZ-ROBAYNA, I., HERNANDEZ-GONZALEZ, I., RUDD, M. D., LIU, Z., RICHARDS, J. S. & ZELEZNIK, A. J. 2009a. FSH and FOXO1 Regulate Genes in the Sterol/Steroid and Lipid Biosynthetic Pathways in Granulosa Cells. *Molecular Endocrinology*, 23, 649-661.
- FAN, H. Y., LIU, Z., JOHNSON, P. F. & RICHARDS, J. S. 2011. CCAAT/enhancer-binding proteins (C/EBP)-alpha and -beta are essential for ovulation, luteinization, and the expression of key target genes. *Mol Endocrinol*, 25, 253-68.
- FAN, H. Y., LIU, Z., SHIMADA, M., STERNECK, E., JOHNSON, P. F., HEDRICK, S. M. & RICHARDS, J. S. 2009b. MAPK3/1 (ERK1/2) in ovarian granulosa cells are essential for female fertility. *Science*, 324, 938-41.
- FAN, H. Y., SHIMADA, M., LIU, Z., CAHILL, N., NOMA, N., WU, Y., GOSSEN, J. & RICHARDS, J. S. 2008. Selective expression of KrasG12D in granulosa cells of the mouse ovary causes defects in follicle development and ovulation. *Development*, 135, 2127-37.
- FIEDLER, S. D., CARLETTI, M. Z., HONG, X. & CHRISTENSON, L. K. 2008. Hormonal Regulation of MicroRNA Expression in Periovarian Mouse Mural Granulosa Cells. *Biology of Reproduction*, 79, 1030-1037.
- FINDLAY, J. K. & DRUMMOND, A. E. 1999. Regulation of the FSH Receptor in the Ovary. *Trends in Endocrinology & Metabolism*, 10, 183-188.
- FISCHLE, W., WANG, Y. & ALLIS, C. D. 2003. Histone and chromatin cross-talk. *Curr Opin Cell Biol*, 15, 172-83.
- FORTUNE, J. E., RIVERA, G. M., EVANS, A. C. & TURZILLO, A. M. 2001. Differentiation of dominant versus subordinate follicles in cattle. *Biol Reprod*, 65, 648-54.
- FRASER, H. M. & DUNCAN, W. C. 2005. Vascular morphogenesis in the primate ovary. *Angiogenesis*, 8, 101-16.
- GASPERIN, B. G., FERREIRA, R., ROVANI, M. T., BORDIGNON, V., DUGGAVATHI, R., BURATINI, J., OLIVEIRA, J. F. C. & GONÇALVES, P. B. D. 2014. Expression of receptors for BMP15 is differentially regulated in dominant and subordinate follicles during follicle deviation in cattle. *Animal Reproduction Science*, 144, 72-78.
- GEBREMEDHN, S., SALILEW-WONDIM, D., AHMAD, I., SAHADEVAN, S., HOSSAIN, M. M., HOELKER, M., RINGS, F., NEUHOFF, C., THOLEN, E., LOOFT, C., SCHELLANDER, K. & TESFAYE, D. 2015. MicroRNA Expression Profile in Bovine Granulosa Cells of Preovulatory Dominant and Subordinate Follicles during the Late Follicular Phase of the Estrous Cycle. *PLoS one*, 10, e0125912-e0125912.
- GEORGE, J. W., DILLE, E. A. & HECKERT, L. L. 2011. Current concepts of follicle-stimulating hormone receptor gene regulation. *Biology of reproduction*, 84, 7-17.
- GERSHON, E., HOURVITZ, A., REIKHAV, S., MAMAN, E. & DEKEL, N. 2007. Low expression of COX-2, reduced cumulus expansion, and impaired ovulation in SULT1E1-deficient mice. *The FASEB Journal*, 21, 1893-1901.
- GILBERT, I., ROBERT, C., DIELEMAN, S., BLONDIN, P. & SIRARD, M. A. 2011. Transcriptional effect of the LH surge in bovine granulosa cells during the peri-ovulation period. *Reproduction*, 141, 193-205.
- GINTHER, O. J. 2000. Selection of the dominant follicle in cattle and horses. *Animal Reproduction Science*, 60, 61-79.
- GINTHER, O. J., BEG, M. A., DONADEU, F. X. & BERGFELT, D. R. 2003. Mechanism of follicle deviation in monovular farm species. *Anim Reprod Sci*, 78, 239-57.

- GINTHER, O. J., WILTBANK, M. C., FRICKE, P. M., GIBBONS, J. R. & KOT, K. 1996. Selection of the Dominant Follicle in Cattle. *Biology of Reproduction*, 55, 1187-1194.
- GRANOT, I. & DEKEL, N. 1998. Cell-to-cell communication in the ovarian follicle: developmental and hormonal regulation of the expression of connexin43. *Hum Reprod*, 13 Suppl 4, 85-97.
- GREINER, E. F., KIRFEL, J., GRESCHIK, H., HUANG, D., BECKER, P., KAPFHAMMER, J. P. & SCHULE, R. 2000. Differential ligand-dependent protein-protein interactions between nuclear receptors and a neuronal-specific cofactor. *Proc Natl Acad Sci U S A*, 97, 7160-5.
- GU, B. & LEE, M. G. 2013. Histone H3 lysine 4 methyltransferases and demethylases in self-renewal and differentiation of stem cells. *Cell & Bioscience*, 3, 39.
- HAMILTON, M. J., GIRKE, T. & MARTINEZ, E. 2018. Global isoform-specific transcript alterations and deregulated networks in clear cell renal cell carcinoma. *Oncotarget*, 9, 23670-23680.
- HARING, M., OFFERMANN, S., DANKER, T., HORST, I., PETERHANSEL, C. & STAM, M. 2007. Chromatin immunoprecipitation: optimization, quantitative analysis and data normalization. *Plant Methods*, 3, 11.
- HAZZARD, T. M., CHRISTENSON, L. K. & STOUFFER, R. L. 2000. Changes in expression of vascular endothelial growth factor and angiopoietin-1 and -2 in the macaque corpus luteum during the menstrual cycle. *Molecular Human Reproduction*, 6, 993-998.
- HERLANDS, R. L. & SCHULTZ, R. M. 1984. Regulation of mouse oocyte growth: probable nutritional role for intercellular communication between follicle cells and oocytes in oocyte growth. *J Exp Zool*, 229, 317-25.
- HERNANDEZ-BARRANTES, S., TOTH, M., BERNARDO, M. M., YURKOVA, M., GERVASI, D. C., RAZ, Y., SANG, Q. A. & FRIDMAN, R. 2000. Binding of active (57 kDa) membrane type 1-matrix metalloproteinase (MT1-MMP) to tissue inhibitor of metalloproteinase (TIMP)-2 regulates MT1-MMP processing and pro-MMP-2 activation. *Journal of Biological Chemistry*, 275, 12080-12089.
- HILLIER, S. G. 1994. Current concepts of the roles of follicle stimulating hormone and luteinizing hormone in folliculogenesis. *Human Reproduction*, 9, 188-191.
- HIROI, H., CHRISTENSON, L. K., CHANG, L., SAMMEL, M. D., BERGER, S. L. & STRAUSS, I. I. I. J. F. 2004. Temporal and Spatial Changes in Transcription Factor Binding and Histone Modifications at the Steroidogenic Acute Regulatory Protein (StAR) Locus Associated with StAR Transcription. *Molecular Endocrinology*, 18, 791-806.
- HISANO, M., ERKEK, S., DESSUS-BABUS, S., RAMOS, L., STADLER, M. B. & PETERS, A. H. 2013a. Genome-wide chromatin analysis in mature mouse and human spermatozoa. *Nat Protoc*, 8, 2449-70.
- HISANO, M., ERKEK, S., DESSUS-BABUS, S., RAMOS, L., STADLER, M. B. & PETERS, A. H. F. M. 2013b. Genome-wide chromatin analysis in mature mouse and human spermatozoa. *Nat. Protocols*, 8, 2449-2470.
- HUNZICKER-DUNN, M. & MAIZELS, E. T. 2006. FSH signaling pathways in immature granulosa cells that regulate target gene expression: branching out from protein kinase A. *Cellular signalling*, 18, 1351-1359.

- IRELAND, J. J. & ROCHE, J. F. 1983. Growth and differentiation of large antral follicles after spontaneous luteolysis in heifers: changes in concentration of hormones in follicular fluid and specific binding of gonadotropins to follicles. *J Anim Sci*, 57, 157-67.
- IRVING-RODGERS, H. F., HARLAND, M. L. & RODGERS, R. J. 2004. A novel basal lamina matrix of the stratified epithelium of the ovarian follicle. *Matrix biology : journal of the International Society for Matrix Biology*, 23, 207-217.
- IRVING-RODGERS, H. F., HARLAND, M. L., SULLIVAN, T. R. & RODGERS, R. J. 2009. Studies of granulosa cell maturation in dominant and subordinate bovine follicles: novel extracellular matrix focimatrix is co-ordinately regulated with cholesterol side-chain cleavage CYP11A1. 137, 825.
- JENUWEIN, T. & ALLIS, C. D. 2001. Translating the histone code. *Science*, 293, 1074-80.
- JEZIEWSKA, A. & MOTYL, T. 2009. Matrix metalloproteinase-2 involvement in breast cancer progression: a mini-review. *Medical science monitor : international medical journal of experimental and clinical research*, 15, RA32-RA40.
- KIM, J., BAGCHI, I. C. & BAGCHI, M. K. 2009. Signaling by hypoxia-inducible factors is critical for ovulation in mice. *Endocrinology*, 150, 3392-3400.
- KIM, M., LEE, J. H., KOH, H., LEE, S. Y., JANG, C., CHUNG, C. J., SUNG, J. H., BLENIS, J. & CHUNG, J. 2006. Inhibition of ERK-MAP kinase signaling by RSK during Drosophila development. *EMBO J*, 25, 3056-67.
- KING, S. R. & LAVOIE, H. A. 2012. Gonadal transactivation of STARD1, CYP11A1 and HSD3B. *Frontiers in bioscience (Landmark edition)*, 17, 824-846.
- KO, C., GIESKE, M. C., AL-ALEM, L., HAHN, Y., SU, W., GONG, M. C., IGLARZ, M. & KOO, Y. 2006. Endothelin-2 in ovarian follicle rupture. *Endocrinology*, 147, 1770-1779.
- KOOS, R. D. 1995. Increased expression of vascular endothelial growth/permeability factor in the rat ovary following an ovulatory gonadotropin stimulus: potential roles in follicle rupture. *Biology of reproduction*, 52, 1426-1435.
- KUMAR, T. R., WANG, Y., LU, N. & MATZUK, M. M. 1997. Follicle stimulating hormone is required for ovarian follicle maturation but not male fertility. *Nat Genet*, 15, 201-4.
- KUO, M. H. & ALLIS, C. D. 1998. Roles of histone acetyltransferases and deacetylases in gene regulation. *Bioessays*, 20, 615-26.
- KUO, M. H. & ALLIS, C. D. 1999. In vivo cross-linking and immunoprecipitation for studying dynamic Protein:DNA associations in a chromatin environment. *Methods*, 19, 425-33.
- LANGMEAD, B. & SALZBERG, S. L. 2012. Fast gapped-read alignment with Bowtie 2. *Nat Methods*, 9, 357-9.
- LEE, L., ASADA, H., KIZUKA, F., TAMURA, I., MAEKAWA, R., TAKETANI, T., SATO, S., YAMAGATA, Y., TAMURA, H. & SUGINO, N. 2013. Changes in Histone Modification and DNA Methylation of the StAR and Cyp19a1 Promoter Regions in Granulosa Cells Undergoing Luteinization during Ovulation In Rats. *Endocrinology*, 154, 458-470.
- LEI, Z. M., MISHRA, S., ZOU, W., XU, B., FOLTZ, M., LI, X. & RAO, C. V. 2001. Targeted disruption of luteinizing hormone/human chorionic gonadotropin receptor gene. *Mol Endocrinol*, 15, 184-200.
- LI, B., CAREY, M. & WORKMAN, J. L. 2007. The role of chromatin during transcription. *Cell*, 128, 707-19.

- LI, J., KRITZER, M. D., MICHEL, J. J., LE, A., THAKUR, H., GAYANILO, M., PASSARIELLO, C. L., NEGRO, A., DANIAL, J. B., OSKOU EI, B., SANDERS, M., HARE, J. M., HANAUER, A., DODGE-KAFKA, K. & KAPILOFF, M. S. 2013. Anchored p90 ribosomal S6 kinase 3 is required for cardiac myocyte hypertrophy. *Circ Res*, 112, 128-39.
- LI, Y., CHENG, H. S., CHNG, W. J. & TERGAONKAR, V. 2016. Activation of mutant TERT promoter by RAS-ERK signaling is a key step in malignant progression of BRAF-mutant human melanomas. *Proceedings of the National Academy of Sciences of the United States of America*, 113, 14402-14407.
- LIU, D. T., BREWER, M. S., CHEN, S., HONG, W. & ZHU, Y. 2017. Transcriptomic signatures for ovulation in vertebrates. *General and Comparative Endocrinology*, 247, 74-86.
- LIU, Y. X., ZHANG, Y., LI, Y. Y., LIU, X. M., WANG, X. X., ZHANG, C. L., HAO, C. F. & DENG, S. L. 2019. Regulation of follicular development and differentiation by intra-ovarian factors and endocrine hormones. *Front Biosci (Landmark Ed)*, 24, 983-993.
- LUGER, K., MADER, A. W., RICHMOND, R. K., SARGENT, D. F. & RICHMOND, T. J. 1997. Crystal structure of the nucleosome core particle at 2.8[thinsp]Å resolution. *Nature*, 389, 251-260.
- LUSSIER, J. G., DIOUF, M. N., LÉVESQUE, V., SIROIS, J. & NDIAYE, K. 2017. Gene expression profiling of upregulated mRNAs in granulosa cells of bovine ovulatory follicles following stimulation with hCG. *Reproductive biology and endocrinology : RB&E*, 15, 88-88.
- LYDON, J. P., DEMAYO, F. J., FUNK, C. R., MANI, S. K., HUGHES, A. R., MONTGOMERY, C. A., JR., SHYAMALA, G., CONNEELY, O. M. & O'MALLEY, B. W. 1995. Mice lacking progesterone receptor exhibit pleiotropic reproductive abnormalities. *Genes Dev*, 9, 2266-78.
- MA, X., DONG, Y., MATZUK, M. M. & KUMAR, T. R. 2004. Targeted disruption of luteinizing hormone β -subunit leads to hypogonadism, defects in gonadal steroidogenesis, and infertility. *Proceedings of the National Academy of Sciences of the United States of America*, 101, 17294-17299.
- MAEKAWA, R., LEE, L., OKADA, M., ASADA, H., SHINAGAWA, M., TAMURA, I., SATO, S., TAMURA, H. & SUGINO, N. 2016. Changes in gene expression of histone modification enzymes in rat granulosa cells undergoing luteinization during ovulation. *Journal of Ovarian Research*, 9, 15.
- MARMORSTEIN, R. & TRIEVEL, R. C. 2009. Histone modifying enzymes: structures, mechanisms, and specificities. *Biochim Biophys Acta*, 1789, 58-68.
- MATSUMURA, Y., NAKAKI, R., INAGAKI, T., YOSHIDA, A., KANO, Y., KIMURA, H., TANAKA, T., TSUTSUMI, S., NAKAO, M., DOI, T., FUKAMI, K., OSBORNE, TIMOTHY F., KODAMA, T., ABURATANI, H. & SAKAI, J. 2015. H3K4/H3K9me3 Bivalent Chromatin Domains Targeted by Lineage-Specific DNA Methylation Pauses Adipocyte Differentiation. *Molecular Cell*, 60, 584-596.
- MCINTUSH, E. W. & SMITH, M. F. 1998. Matrix metalloproteinases and tissue inhibitors of metalloproteinases in ovarian function. *Reviews of Reproduction*, 3, 23-30.
- MCRAE, R. S., JOHNSTON, H. M., MIHM, M. & O'SHAUGHNESSY, P. J. 2005. Changes in Mouse Granulosa Cell Gene Expression during Early Luteinization. *Endocrinology*, 146, 309-317.
- MEHTA, A., RAVINDER, ONTERU, S. K. & SINGH, D. 2015. HDAC inhibitor prevents LPS mediated inhibition of CYP19A1 expression and 17 β -estradiol production in granulosa cells. *Mol Cell Endocrinol*, 414, 73-81.

- MEINSOHN, M. C., MORIN, F., BERTOLIN, K., DUGGAVATHI, R., SCHOONJANS, K. & MURPHY, B. D. 2018. The Orphan Nuclear Receptor Liver Homolog Receptor-1 (Nr5a2) Regulates Ovarian Granulosa Cell Proliferation. *J Endocr Soc*, 2, 24-41.
- MIHM, M. & AUSTIN, E. J. 2002. The final stages of dominant follicle selection in cattle. *Domestic Animal Endocrinology*, 23, 155-166.
- MIHM, M., AUSTIN, E. J., GOOD, T. E., IRELAND, J. L., KNIGHT, P. G., ROCHE, J. F. & IRELAND, J. J. 2000. Identification of potential intrafollicular factors involved in selection of dominant follicles in heifers. *Biol Reprod*, 63, 811-9.
- MO, R., RAO, S. M. & ZHU, Y. J. 2006. Identification of the MLL2 complex as a coactivator for estrogen receptor alpha. *J Biol Chem*, 281, 15714-20.
- MONNIAUX, D., MONGET, P., BESNARD, N., HUET, C. & PISSELET, C. 1997. Growth factors and antral follicular development in domestic ruminants. *Theriogenology*, 47, 3-12.
- MOORE, L. D., LE, T. & FAN, G. 2013. DNA methylation and its basic function. *Neuropsychopharmacology*, 38, 23-38.
- MOZZETTA, C., BOYARCHUK, E., PONTIS, J. & AIT-SI-ALI, S. 2015. Sound of silence: the properties and functions of repressive Lys methyltransferases. *Nat Rev Mol Cell Biol*, 16, 499-513.
- MURPHY, B. D. 2000. Models of luteinization. *Biology of reproduction*, 63, 2-11.
- NIMZ, M., SPITSCHAK, M., FURBASS, R. & VANSELOW, J. 2010. The pre-ovulatory luteinizing hormone surge is followed by down-regulation of CYP19A1, HSD3B1, and CYP17A1 and chromatin condensation of the corresponding promoters in bovine follicles. *Mol Reprod Dev*, 77, 1040-8.
- NIVET, A.-L., DUFORT, I., GILBERT, I. & SIRARD, M.-A. 2018. Short-term effect of FSH on gene expression in bovine granulosa cells *in vitro*. *Reproduction, Fertility and Development*, 30, 1154-1160.
- NORRIS, R. P., FREUDZON, M., MEHLMANN, L. M., COWAN, A. E., SIMON, A. M., PAUL, D. L., LAMPE, P. D. & JAFFE, L. A. 2008. Luteinizing hormone causes MAP kinase-dependent phosphorylation and closure of connexin 43 gap junctions in mouse ovarian follicles: one of two paths to meiotic resumption. *Development (Cambridge, England)*, 135, 3229-3238.
- OAKLEY, O. R., KIM, H., EL-AMOURI, I., LIN, P.-C. P., CHO, J., BANI-AHMAD, M. & KO, C. 2010. Periovarian leukocyte infiltration in the rat ovary. *Endocrinology*, 151, 4551-4559.
- OHNISHI, J., OHNISHI, E., SHIBUYA, H. & TAKAHASHI, T. 2005. Functions for proteinases in the ovulatory process. *Biochimica et Biophysica Acta (BBA)-Proteins and Proteomics*, 1751, 95-109.
- PALANISAMY, G. S., CHEON, Y.-P., KIM, J., KANNAN, A., LI, Q., SATO, M., MANTENA, S. R., SITRUK-WARE, R. L., BAGCHI, M. K. & BAGCHI, I. C. 2006. A novel pathway involving progesterone receptor, endothelin-2, and endothelin receptor B controls ovulation in mice. *Molecular endocrinology (Baltimore, Md.)*, 20, 2784-2795.
- PAN, Q., SHAI, O., LEE, L. J., FREY, B. J. & BLENCOWE, B. J. 2008. Deep surveying of alternative splicing complexity in the human transcriptome by high-throughput sequencing. *Nat Genet*, 40, 1413-5.
- PARAKH, T. N., HERNANDEZ, J. A., GRAMMER, J. C., WECK, J., HUNZICKER-DUNN, M., ZELEZNIK, A. J. & NILSON, J. H. 2006. Follicle-stimulating hormone/cAMP regulation of aromatase

- gene expression requires β -catenin. *Proceedings of the National Academy of Sciences*, 103, 12435-12440.
- PARK, J. Y., SU, Y. Q., ARIGA, M., LAW, E., JIN, S. L. & CONTI, M. 2004. EGF-like growth factors as mediators of LH action in the ovulatory follicle. *Science*, 303, 682-4.
- PETERS, A. H., MERMOUD, J. E., O'CARROLL, D., PAGANI, M., SCHWEIZER, D., BROCKDORFF, N. & JENUWEIN, T. 2002. Histone H3 lysine 9 methylation is an epigenetic imprint of facultative heterochromatin. *Nat Genet*, 30, 77-80.
- PIMENTEL, H., BRAY, N. L., PUENTE, S., MELSTED, P. & PACTER, L. 2017. Differential analysis of RNA-seq incorporating quantification uncertainty. *Nature Methods*, 14, 687.
- RAJU, G. A. R., CHAVAN, R., DEENADAYAL, M., GUNASHEELA, D., GUTGUTIA, R., HARIPRIYA, G., GOVINDARAJAN, M., PATEL, N. H. & PATKI, A. S. 2013. Luteinizing hormone and follicle stimulating hormone synergy: A review of role in controlled ovarian hyper-stimulation. *Journal of human reproductive sciences*, 6, 227-234.
- RAO, J. U., SHAH, K. B., PUTTAIAH, J. & RUDRAIAH, M. 2011. Gene Expression Profiling of Preovulatory Follicle in the Buffalo Cow: Effects of Increased IGF-I Concentration on Perioovulatory Events. *PLoS ONE*, 6, e20754.
- REDMER, D. A. & REYNOLDS, L. P. 1996. Angiogenesis in the ovary. *Reviews of reproduction*, 1, 182-192.
- REDON, C., PILCH, D., ROGAKOU, E., SEDELNIKOVA, O., NEWROCK, K. & BONNER, W. 2002. Histone H2A variants H2AX and H2AZ. *Curr Opin Genet Dev*, 12, 162-9.
- RICHARDS, J. A. S., RUSSELL, D. L., OCHSNER, S. & ESPEY, L. L. 2002a. Ovulation: new dimensions and new regulators of the inflammatory-like response. *Annual review of physiology*, 64, 69-92.
- RICHARDS, J. S. 1979. Hormonal Control of Ovarian Follicular Development: A 1978 Perspective. In: GREEP, R. O. (ed.) *Proceedings of the 1978 Laurentian Hormone Conference*. Boston: Academic Press.
- RICHARDS, J. S. 1994. Hormonal control of gene expression in the ovary. *Endocr Rev*, 15, 725-51.
- RICHARDS, J. S. 2001. Perspective: The Ovarian Follicle—A Perspective in 2001*. *Endocrinology*, 142, 2184-2193.
- RICHARDS, J. S. 2005. Ovulation: new factors that prepare the oocyte for fertilization. *Molecular and cellular endocrinology*, 234, 75-79.
- RICHARDS, J. S., RUSSELL, D. L., OCHSNER, S. & ESPEY, L. L. 2002b. Ovulation: new dimensions and new regulators of the inflammatory-like response. *Annu Rev Physiol*, 64, 69-92.
- RIVERA, G. M., CHANDRASEKHER, Y. A., EVANS, A. C., GIUDICE, L. C. & FORTUNE, J. E. 2001. A potential role for insulin-like growth factor binding protein-4 proteolysis in the establishment of ovarian follicular dominance in cattle. *Biol Reprod*, 65, 102-11.
- ROBERTSON, G., HIRST, M., BAINBRIDGE, M., BILENKY, M., ZHAO, Y., ZENG, T., EUSKIRCHEN, G., BERNIER, B., VARHOL, R., DELANEY, A., THIESSEN, N., GRIFFITH, O. L., HE, A., MARRA, M., SNYDER, M. & JONES, S. 2007. Genome-wide profiles of STAT1 DNA association using chromatin immunoprecipitation and massively parallel sequencing. *Nat Meth*, 4, 651-657.
- ROBINSON, J. T., THORVALDSDÓTTIR, H., WINCKLER, W., GUTTMAN, M., LANDER, E. S., GETZ, G. & MESIROV, J. P. 2011. Integrative genomics viewer. *Nature Biotechnology*, 29, 24.

- ROBKER, R. L., HENNEBOLD, J. D. & RUSSELL, D. L. 2018. Coordination of Ovulation and Oocyte Maturation: A Good Egg at the Right Time. *Endocrinology*, 159, 3209-3218.
- ROBKER, R. L., RUSSELL, D. L., ESPEY, L. L., LYDON, J. P., O'MALLEY, B. W. & RICHARDS, J. S. 2000a. Progesterone-regulated genes in the ovulation process: ADAMTS-1 and cathepsin L proteases. *Proc Natl Acad Sci U S A*, 97, 4689-94.
- ROBKER, R. L., RUSSELL, D. L., YOSHIOKA, S., SHARMA, S. C., LYDON, J. P., O'MALLEY, B. W., ESPEY, L. L. & RICHARDS, J. S. 2000b. Ovulation: a multi-gene, multi-step process. *Steroids*, 65, 559-70.
- ROUX, P. P. & BLENIS, J. 2004. ERK and p38 MAPK-activated protein kinases: a family of protein kinases with diverse biological functions. *Microbiol Mol Biol Rev*, 68, 320-44.
- RUSSELL, D. L. & ROBKER, R. L. 2007. Molecular mechanisms of ovulation: co-ordination through the cumulus complex. *Human reproduction update*, 13, 289-312.
- SALILEW-WONDIM, D., AHMAD, I., GEBREMEDHN, S., SAHADEVAN, S., HOSSAIN, M. D. M., RINGS, F., HOELKER, M., THOLEN, E., NEUHOFF, C., LOOFT, C., SCHELLANDER, K. & TESFAYE, D. 2014. The Expression Pattern of microRNAs in Granulosa Cells of Subordinate and Dominant Follicles during the Early Luteal Phase of the Bovine Estrous Cycle. *PLoS ONE*, 9, e106795.
- SANTOS-ROSA, H., SCHNEIDER, R., BANNISTER, A. J., SHERRIFF, J., BERNSTEIN, B. E., EMRE, N. C. T., SCHREIBER, S. L., MELLOR, J. & KOUZARIDES, T. 2002. Active genes are tri-methylated at K4 of histone H3. *Nature*, 419, 407-411.
- SAYASITH, K. & SIROIS, J. 2014. Expression and regulation of stromal cell-derived factor-1 (SDF1) and chemokine CXC motif receptor 4 (CXCR4) in equine and bovine preovulatory follicles. *Molecular and cellular endocrinology*, 391, 10-21.
- SCHUERMANN, Y., ROVANI, M. T., GASPERIN, B., FERREIRA, R., FERST, J., MADOGWE, E., GONCALVES, P. B., BORDIGNON, V. & DUGGAVATHI, R. 2018. ERK1/2-dependent gene expression in the bovine ovulating follicle. *Sci Rep*, 8, 16170.
- SCHULTZ, R. M., MONTGOMERY, R. R. & BELANOFF, J. R. 1983. Regulation of mouse oocyte meiotic maturation: implication of a decrease in oocyte cAMP and protein dephosphorylation in commitment to resume meiosis. *Dev Biol*, 97, 264-73.
- SEGERS, I., ADRIAENSSENS, T., WATHLET, S. & SMITZ, J. 2012. Gene expression differences induced by equimolar low doses of LH or hCG in combination with FSH in cultured mouse antral follicles. 215, 269.
- SHIMADA, M. & YAMASHITA, Y. 2011. The Key Signaling Cascades in Granulosa Cells During Follicular Development and Ovulation Process. *Journal of Mammalian Ova Research*, 28, 25-31.
- SIDDAPPA, D., BEAULIEU, E., GEVRY, N., ROUX, P. P., BORDIGNON, V. & DUGGAVATHI, R. 2015. Effect of the transient pharmacological inhibition of mapk3/1 pathway on ovulation in mice. *PLoS One*, 10, e0119387.
- SIMON, A. M., GOODENOUGH, D. A., LI, E. & PAUL, D. L. 1997. Female infertility in mice lacking connexin 37. *Nature*, 385, 525-9.
- SKINNER, M. K., SCHMIDT, M., SAVENKOVA, M. I., SADLER-RIGGLEMAN, I. & NILSSON, E. E. 2008. Regulation of granulosa and theca cell transcriptomes during ovarian antral follicle development. *Molecular Reproduction and Development*, 75, 1457-1472.

- STERNECK, E., TESSAROLLO, L. & JOHNSON, P. F. 1997. An essential role for C/EBPbeta in female reproduction. *Genes & development*, 11, 2153-2162.
- STOCCO, C. 2008. Aromatase expression in the ovary: hormonal and molecular regulation. *Steroids*, 73, 473-87.
- SVOTELIS, A., GEVRY, N. & GAUDREAU, L. 2009. Chromatin immunoprecipitation in mammalian cells. *Methods Mol Biol*, 543, 243-51.
- TAKAHASHI, Y. H., WESTFIELD, G. H., OLESKIE, A. N., TRIEVEL, R. C., SHILATIFARD, A. & SKINIOTIS, G. 2011. Structural analysis of the core COMPASS family of histone H3K4 methylases from yeast to human. *Proc Natl Acad Sci U S A*, 108, 20526-31.
- TEE, W. W., SHEN, S. S., OKSUZ, O., NARENDRA, V. & REINBERG, D. 2014. Erk1/2 activity promotes chromatin features and RNAPII phosphorylation at developmental promoters in mouse ESCs. *Cell*, 156, 678-90.
- TEINO, I., MATVERE, A., KUUSE, S., INGERPUU, S., MAIMETS, T., KRISTJUHAN, A. & TIIDO, T. 2014. Transcriptional repression of the Ahr gene by LHCGR signaling in preovulatory granulosa cells is controlled by chromatin accessibility. *Mol Cell Endocrinol*, 382, 292-301.
- UGARTE, F., SOUSAE, R., CINQUIN, B., MARTIN, E. W., KRIETSCH, J., SANCHEZ, G., INMAN, M., TSANG, H., WARR, M., PASSEGUE, E., LARABELL, C. A. & FORSBERG, E. C. 2015. Progressive Chromatin Condensation and H3K9 Methylation Regulate the Differentiation of Embryonic and Hematopoietic Stem Cells. *Stem Cell Reports*, 5, 728-40.
- VENKATESH, S. & WORKMAN, J. L. 2015. Histone exchange, chromatin structure and the regulation of transcription. *Nat Rev Mol Cell Biol*, 16, 178-89.
- VERBRAAK, E. J. C., VAN 'T VELD, E. M., GROOT KOERKAMP, M., ROELEN, B. A. J., VAN HAEFTEN, T., STOORVOGEL, W. & ZIJLSTRA, C. 2011. Identification of genes targeted by FSH and oocytes in porcine granulosa cells. *Theriogenology*, 75, 362-376.
- WANG, Z., JUTTERMANN, R. & SOLOWAY, P. D. 2000. TIMP-2 is required for efficient activation of proMMP-2 in vivo. *The Journal of biological chemistry*, 275, 26411-26415.
- WEN, Z., PAN, T., YANG, S., LIU, J., TAO, H., ZHAO, Y., XU, D., SHAO, W., WU, J., LIU, X., WANG, Y., MAO, J. & ZHU, Y. 2017. Up-regulated NRIP2 in colorectal cancer initiating cells modulates the Wnt pathway by targeting ROR β . *Molecular cancer*, 16, 20-20.
- WIGGLESWORTH, K., EPPIG, J. J., LEE, K.-B., EMORI, C. & SUGIURA, K. 2015. Transcriptomic Diversification of Developing Cumulus and Mural Granulosa Cells in Mouse Ovarian Follicles1. *Biology of Reproduction*, 92.
- WISSING, M. L., KRISTENSEN, S. G., ANDERSEN, C. Y., MIKKELSEN, A. L., HØST, T., BORUP, R. & GRØNDAHL, M. L. 2014. Identification of new ovulation-related genes in humans by comparing the transcriptome of granulosa cells before and after ovulation triggering in the same controlled ovarian stimulation cycle. *Human Reproduction*, 29, 997-1010.
- WOZNIAK, G. G. & STRAHL, B. D. 2014. Hitting the 'mark': Interpreting lysine methylation in the context of active transcription. *Biochim Biophys Acta*.
- WU, C. 1997. Chromatin remodeling and the control of gene expression. *J Biol Chem*, 272, 28171-4.

- XIA, J., BENNER, M. J. & HANCOCK, R. E. W. 2014. NetworkAnalyst - integrative approaches for protein-protein interaction network analysis and visual exploration. *Nucleic Acids Research*, 42, W167-W174.
- XIA, J., GILL, E. E. & HANCOCK, R. E. W. 2015. NetworkAnalyst for statistical, visual and network-based meta-analysis of gene expression data. *Nature Protocols*, 10, 823.
- XIA, J., LYLE, N. H., MAYER, M. L., PENA, O. M. & HANCOCK, R. E. 2013. INVEX--a web-based tool for integrative visualization of expression data. *Bioinformatics*, 29, 3232-4.
- XU, F., STOUFFER, R. L., MÜLLER, J., HENNEBOLD, J. D., WRIGHT, J. W., BAHAR, A., LEDER, G., PETERS, M., THORNE, M., SIMS, M., WINTERMANTEL, T. & LINDENTHAL, B. 2011. Dynamics of the transcriptome in the primate ovulatory follicle. *Molecular Human Reproduction*, 17, 152-165.
- XU, Z., GARVERICK, H. A., SMITH, G. W., SMITH, M. F., HAMILTON, S. A. & YOUNGQUIST, R. S. 1995. Expression of follicle-stimulating hormone and luteinizing hormone receptor messenger ribonucleic acids in bovine follicles during the first follicular wave. *Biol Reprod*, 53, 951-7.
- YADAV, V. & MEDHAMURTHY, R. 2006. Dynamic changes in mitogen-activated protein kinase (MAPK) activities in the corpus luteum of the bonnet monkey (*Macaca radiata*) during development, induced luteolysis, and simulated early pregnancy: a role for p38 MAPK in the regulation of luteal function. *Endocrinology*, 147, 2018-2027.
- YOON, S. & SEGER, R. 2006. The extracellular signal-regulated kinase: multiple substrates regulate diverse cellular functions. *Growth factors (Chur, Switzerland)*, 24, 21-44.
- YU, G., WANG, L.-G. & HE, Q.-Y. 2015. ChIPseeker: an R/Bioconductor package for ChIP peak annotation, comparison and visualization. *Bioinformatics*, 31, 2382-2383.
- YUAN, W., BAO, B., GARVERICK, H. A., YOUNGQUIST, R. S. & LUCY, M. C. 1998. Follicular Dominance in Cattle Is Associated With Divergent Patterns of Ovarian Gene Expression for Insulin-Like Growth Factor (IGF)-I, IGF-II, and IGF Binding Protein-2 in Dominant and Subordinate Follicles. *Domestic Animal Endocrinology*, 15, 55-63.
- ZENIOU, M., DING, T., TRIVIER, E. & HANAUER, A. 2002. Expression analysis of RSK gene family members: the RSK2 gene, mutated in Coffin-Lowry syndrome, is prominently expressed in brain structures essential for cognitive function and learning. *Hum Mol Genet*, 11, 2929-40.
- ZHANG, F. P., POUTANEN, M., WILBERTZ, J. & HUHTANIEMI, I. 2001. Normal prenatal but arrested postnatal sexual development of luteinizing hormone receptor knockout (LuRKO) mice. *Mol Endocrinol*, 15, 172-83.
- ZHANG, X., NOVERA, W., ZHANG, Y. & DENG, L. W. 2017. MLL5 (KMT2E): structure, function, and clinical relevance. *Cell Mol Life Sci*, 74, 2333-2344.
- ZHANG, Y., LIU, T., MEYER, C. A., EECKHOUTE, J., JOHNSON, D. S., BERNSTEIN, B. E., NUSBAUM, C., MYERS, R. M., BROWN, M., LI, W. & LIU, X. S. 2008. Model-based analysis of ChIP-Seq (MACS). *Genome biology*, 9, R137-R137.
- ZHANG, Y. L., XIA, Y., YU, C., RICHARDS, J. S., LIU, J. & FAN, H. Y. 2014. CBP-CITED4 is required for luteinizing hormone-triggered target gene expression during ovulation. *Mol Hum Reprod*, 20, 850-60.
- ZHAO, S., FUNG-LEUNG, W. P., BITTNER, A., NGO, K. & LIU, X. 2014. Comparison of RNA-Seq and microarray in transcriptome profiling of activated T cells. *PLoS One*, 9, e78644.

- ZHAO, Y., BJORBAEK, C., WEREMOWICZ, S., MORTON, C. C. & MOLLER, D. E. 1995. RSK3 encodes a novel pp90^{rsk} isoform with a unique N-terminal sequence: growth factor-stimulated kinase function and nuclear translocation. *Mol Cell Biol*, 15, 4353-63.
- ZIELAK-STECIWKO, A. E., BROWNE, J. A., MCGETTIGAN, P. A., GAJEWSKA, M., DZIĘCIOŁ, M., SZULC, T. & EVANS, A. C. O. 2014. Expression of microRNAs and their target genes and pathways associated with ovarian follicle development in cattle. *Physiological Genomics*, 46, 735-745.
- ZIELAK-STECIWKO, A. E. & EVANS, A. C. 2016. Genomic portrait of ovarian follicle growth regulation in cattle. *Reprod Biol*, 16, 197-202.
- ZUBEK, J., STITZEL, M. L., UCAR, D. & PLEWCZYNSKI, D. M. 2016. Computational inference of H3K4me3 and H3K27ac domain length. *PeerJ*, 4, e1750.